CLONING AND CHARACTERIZATION OF PHIP, A NOVEL PROTEIN LIGAND OF THE PH DOMAIN OF IRS-1

By

Janet Farhang-Fallah, B.Sc.

A Thesis

Submitted to the School of Graduate Studies

In Partial Fulfillment of the Requirements

For the Degree

Doctor of Philosophy

McMaster University

CLONING AND CHARACTERIZATION OF PHIP, A NOVEL PROTEIN LIGAND OF THE PH DOMAIN OF IRS-1

DOCTOR OF PHILOSOPHY (2002) McMaster University

(Biology) Hamilton, Ontario

TITLE: Cloning and characterization of PHIP, a novel protein ligand of the PH domain of IRS-1

AUTHOR: Janet Farhang-Fallah, B.Sc. (McMaster University)

SUPERVISOR: Maria Rozakis-Adcock Ph.D.

NUMBER OF PAGES: xxii, 205

COPYRIGHT PERMISSION NOTE

Part of the study presented in this thesis has previously been published in two journals; "**Farhang-Fallah, J., Yin, X., Trentin, G., Cheng, A.M., and Rozakis-Adcock, M.** (2000). Cloning and characterization of PHIP, a novel insulin receptor substrate-1 pleckstrin homology domain interacting protein. *J. Biol. Chem. 275*, 40492-40497." and "**Farhang-Fallah, J., Randhawa, V., Nimnual, A., Klip, A., Bar-Sagi, D., Maria Rozakis-Adcock, M.,** (2002) PHIP couples the IRS-1 PH domain to insulin signaling pathways leading to mitogenesis and GLUT4 translocation. *Mol. Cell. Biol.* **in press.**"

This material is republished with permissions from American Society for Microbiology, and The American Society for biochemistry and Molecular Biology for the above works; permission conveyed through Copyright clearance center, Inc.

ABSTRACT

Insulin receptor substrate- 1 (IRS-1) protein is a major substrate of the insulin receptor tyrosine kinase and is essential for transducing many of the biological effects of insulin including mitogenesis, gene expression and glucose transport. The N-terminus of IRS-1 contains a pleckstrin homology (PH) domain, followed by a phosphotyrosine-binding (PTB) domain that have been shown to co-operatively contribute in mediating productive receptor/substrate interactions. The PH domain is critical for recognition and subsequent phosphorylation of IRS-1 by the activated insulin receptor. In this thesis, the cloning and biochemical characterization of a novel protein, named PHIP (**PH**-interacting **p**rotein), has been described. PHIP binds selectively to the PH domain of IRS-1 *in vitro*, and stably associates with IRS-1 *in vivo*. Importantly, mutants of the IRS-1 PH domain that disrupt the PH fold fail to bind to PHIP. Anti-phosphotyrosine immunoblots of PHIP revealed no discernible insulin receptor-regulated phosphorylation, suggesting that PHIP is not itself a substrate of the insulin receptor. By contrast to full-length PHIP, overexpression of the PH-binding region of PHIP has a pronounced inhibitory effect on insulin-induced IRS-1 tyrosine phosphorylation levels. Moreover, expression of this dominant-negative PHIP mutant (DN/PHIP) leads to a marked attenuation of insulin-stimulated mitogen activated protein (MAP) kinase activity. Furthermore, overexpression of PHIP enhances insulin-induced transcriptional responses in a MAP Kinase-dependent manner. By contrast, DN/PHIP mutants specifically block mitogenic signals elicited by insulin and not serum. In addition, DN/PHIP mutant proteins also inhibit insulin-triggered GLUT4 translocation to the cell surface as well as actin assembly. It is therefore concluded that PHIP represents a physiological ligand of the IRS-1 PH domain which plays a critical role in insulin-stimulated biological responses mediated by IRS-1.

ACKNOWLEDGMENTS

I extend my sincere thanks to my supervisor Maria Rozakis-Adcock for her support, guidance and enthusiasm throughout my Ph.D. program. I am also grateful to Maria for sharing her experiences as a young successful scientist and showing me the skills required to thrive in science. I would like to thank my transfer and supervisory committee members for their input and advise. I am thankful to Roger Jacobs and Rick Austin for taking time to critically read this thesis. I extend my gratitude to the members of the William Muller and Amira Klip's labs who made my temporary work in their lab convenient and joyful. I also thank the following scientists for lending their support by providing me with reagents used in this study: Philip Billan (University of Toronto), Anjaruwee Nimnual (New York State University), Varinder Randhawa (University of Toronto), Peter Siegel (McMaster University), Nishi Singh, Sudesh Sood (Henderson, Hamilton Civic Hospital), Sarka Lhotak, Grace Trentin, Dixon Ho and Xianhua Yin. My thanks to Karen Dougherty and Pat Hayward for their administrative assistance. I am also thankful for the financial support and student fellowships provided by my Supervisor, Department of Biology, McMaster University, Cancer Research Society Inc. (CRS), and National Cancer Institute of Canada (NCIC).

Special thanks to my parents for their love and endless moral support. To Jinoos, Behzad and Pejman for their love and encouragement during my studies. I am deeply grateful and indebted to my husband, Mehdi for his beautiful love, friendship, and selflessness and for always being there for me.

CONTRIBUTIONS BY OTHERS

I like to acknowledge the efforts of my collaborators who performed the following experiments or provided me with reagents critical for some of these studies.

Figure 3.10 PHIP interaction with IRS-1 requires an intact PH domain.
The constructs used in the *in-vitro* mixes were generated by Xianhua Yin and the binding assay was performed by Grace Trentin.

Figure 4.4 Effect of DN-PHIP on insulin-mediated transcriptional activation of the SRE-fos promoter.

Figure 4.5 Effect of DN-PHIP on insulin-mediated mitogenesis.
The microinjections and staining were performed by Anjaruwee Nimnual from Dafna Bar-Sagi's group. The statistical analysis and the graphs were also done by Nimnual A.

Figure 4.6. Effect of PHIP and IRS-1 mutants on insulin-induced GLUT4 translocation.

Figure 4.7 Effect of DN/PHIP on insulin-induced actin remodeling.
Transient transfections and staining were performed by Varinder Randhawa in Amira Klip's lab. The statistical analysis and the graphs were also done by Randhawa V.

Section 2.1.1 BTM116 yeast two-hybrid constructs.

Section 2.2 Yeast Two-hybrid analysis

The constructs described are generated by Maria Rozakis-Adcock. The yeast two hybrid screen was performed by Maria Rozakis-Adcock.

Section 2.1.3 pCGN constructs.

Section 2.1.4 pBlueScript/PHIP vector.

The pCGN/IRS-1ΔPH, pCGN/HA-PHIP, and pBlueScript/PHIP plasmid constructs have been generated by Xianhua Yin.

Section 2.1.6 Adenoviral vectors.

All the constructs used for HA-PHIP encoding viral protein have been generated by Nishi Singh.

TABLE OF CONTENTS

CHAPTER TWO: MATERIALS AND METHODS

LIST OF FIGURES

LIST OF ABBREVIATIONS

ATP	Adenosine Triphosphate
β-ARK	β-Adrenergic Receptor Kinase
BTK	Bruton's Tyrosine Kinase
C	Carboxyl
cAMP	Cyclic Adenosine Monophosphate
CAP	Cbl Associated Protein
CBP	CREB binding protein
cDNA	Complementary Deoxyribonucleic Acid
CHO	Chinese Hamster Ovary
CREB	cAMP Response Element Binding
DAPI	DiAmidino Phenylindole Dihydrochloride
Dbs	Dbl's Big Sister
DEPC	DiEthyl PyroCarbonate
DH	Dbl Homology
DNA	Deoxyribonucleic Acid
EVH	Enabled/VASP Homology
FRET	Fluorescent Resonance Energy Transfer
GAP	GTPase Activating Protein
GEF	Guanine Nucleotide Exchange Factor
GLUT4	Glucose Transporter 4
Grb-2	Growth Factor Receptor Binding –2

GTP	Guanosine Triphosphate
HA	Hemagglutinin Antigen
HAT	Histone Acetyl Transferase
IGF-1	Insulin-like Growth Factor –1
IR	Insulin receptor
IRS	Insulin Receptor Substrate
KDa	Kilo Dalton
LDM	Low Density Microsome
LUC	Luciferase
MAP	Mitogen Activated Protein
N	Amino
NDRP	Neuronal Differentiation Related Protein
NMR	Nuclear Magnetic Resonance
PBR	PH binding Region
PCR	Polymerase Chain Reaction
PDGF	Platelet Derived Growth Factor
PH	Pleckstrin Homology
PHIP	PH Interacting Protein
PI	Phosphatidylinositol
PKB	Protein Kinase B
PKC	Protein Kinase C
PLC	Phospholipase C
PTB	Phosphotyrosine Binding

PTP	Protein Tyrosine Phosphatase
RACE	Rapid Amplification of cDNA Ends
RanBD	Ran Binding Domain
RT-PCR	Reverse Transcriptase-Polymerase Chain Reaction
SDS-PAGE	Sodium Dodecyl Sulfate – Polyacrylamide Gel Electrophoresis
Ser	Serine
SH2	Src-Homology 2
SHP	SH2-containing Phosphatase
Sos	Son-of-Sevenless
SRE	Serum Response Element
Thr	Threonine
TLC	Thin Layer Chromatography
Tyr	Tyrosine
UTR	Untranslated Region
WASP	Wiskott-Aldrich Syndrome Protein

CHAPTER ONE

INSULIN RECEPTOR SIGNAL TRANSDUCTION

1.1 INTRODUCTION

Insulin is an essential anabolic hormone secreted by the pancreatic β-cells in response to increased circulatory glucose levels. In order to regulate the glucose concentration in the blood, insulin augments glucose uptake by the muscle and fat tissue and inhibits glucose production by the liver (Saltiel and Kahn, 2001). In muscle and fat cells, insulin stimulates glucose uptake by increasing the concentration of the facilitative glucose transporter, GLUT4, at the cell surface (Pessin et al., 1999; Simpson et al., 2001). While glucose is stored primarily as lipid in adipocytes, it is either used to generate ATP or stored as glycogen in muscle cells. Insulin on the other hand, impedes glucose production by the liver by blocking gluconeogenesis and glycogenolysis and by stimulating glycogen synthesis (Kulkarni et al., 1999; Saltiel and Kahn, 2001; Spiegelman and Flier, 2001). Moreover, whereas the crucial role of insulin target tissues such as muscle, fat and liver in glucose regulation and metabolism is well recognized, recent data also provide evidence for the function of tissues such as pancreatic β-cells and brain, not commonly considered as insulin sensitive, in glucose homeostasis (Bruning et al., 2000; Kulkarni et al., 1999).

The breakdown or dysfunction of insulin signaling initiates a state of pathophysiological disorder known as insulin resistance, in which the peripheral target tissues become

unresponsive to the insulin actions (Hunter and Garvey, 1998; Mauvais-Jarvis and Kahn, 2000). Progressively, diabetes ensues when the pancreatic β-cells cannot meet the demands for higher insulin secretion to compensate for high blood glucose levels and insulin resistance (White, 2002).

1.2 INSULIN RECEPTOR

1.2.1 Basic structure and physical characteristics

The physiological actions of insulin are mediated through insulin receptor, a transmembrane glycoprotein belonging to the receptor tyrosine kinase superfamily. The insulin receptor consists of two α and two β subunits, which are covalently linked through disulfide bonds to form heterotetrameric $\alpha_2\beta_2$ insulin receptor (Perz and Torlinska, 2001). While the two α-subunits with molecular weight of 135 KDa are located exclusively at the cell surface and mediate insulin binding, the 95 KDa β-subunits consist of an extracellular, a membrane spanning and an intracellular domain containing tyrosine kinase activity. Binding of insulin to the extracellular α-subunit of the insulin receptor results in conformational changes leading to the activation of the tyrosine kinase of the β-subunit, which in turn promotes autophosphorylation on specific tyrosine residues. Several of the known phosphorylated tyrosine residues located at the intracellular segment of the β-subunit include Tyr^{960} in the juxtamembrane region, Tyr^{1146}, Tyr^{1150}, Tyr^{1151}, Tyr^{1158}, Tyr^{1162} and Tyr^{1163} in the regulatory loop of the kinase domain, and Tyr^{1316} and Tyr^{1322} in the carboxy-terminus (Hunter and Garvey, 1998; Myers and White, 1996). While autophosphorylation of the tyrosine residues in the

regulatory loop is required for full activation of the kinase activity of the insulin receptor, other tyrosines are often involved in association with the downstream substrate molecules. Unlike the majority of the growth factor receptors where downstream effectors are directly activated through binding to phosphotyrosine residues on the receptor, insulin receptor is unique in that it phosphorylates adaptor substrates such as Shc, Cbl and insulin receptor substrate (IRS), which function as scaffolds for the recruitment of signaling molecules containing Src homology 2 (SH2) domains (Ogawa et al., 1998; Van Obberghen et al., 2001)(Figure 1.1). These signaling intermediates in turn activate a complex network of intracellular biological cascades that cooperatively serve to maintain cellular functions such as growth and metabolism.

1.2.2 Insulin receptor signaling specificity

Insulin among other growth factors regulates cellular processes such as proliferation, differentiation and metabolism through activation of overlapping intermediate signaling molecules (Conejo and Lorenzo, 2001; Saltiel and Kahn, 2001). Yet it promotes unique metabolic responses in accordance with the physiological requirements of the cell, raising the important question of how biological specificity is maintained considering this apparent signaling redundancy.

A commonly held view supports a mechanism in which specificity is achieved by alternate utilization of homologous molecules differentially expressed in different tissues. For instance, different levels of the insulin and insulin-like growth factor receptors have been detected in various tissues of brain, liver, β-cell, adipose and muscle with the insulin sensitive tissues expressing the highest levels of the insulin receptor (Myers and White,

Figure 1.1. Activation of insulin receptor tyrosine kinase induces multiple signaling pathways. Interaction of insulin with the insulin receptors, located in different microdomains such as clathrin-coated pits (blue invaginations) and caveolae (gray flask-shaped invaginations) triggers tyrosine kinase activity of the insulin receptor. Recruitment and phosphorylation of insulin receptor substrates including IRS-1, Shc, and Cbl promotes activation of various signaling pathways leading to cellular growth, survival, differentiation and glucose metabolism. IRS-1 is shown to be mainly localized to the LDM compartments and is proposed to move to the proximity of the insulin receptor upon insulin stimulation. LDM-associated IRS-1/PI 3-kinase and CAP/Cbl/CrkII/C3G/TC10 complexes are thought to cooperatively regulate GLUT4 translocation to the cell surface, which leads to glucose uptake and metabolism. PI 3-kinase activated AKT is also thought to regulate cell survival. Both IRS-1 and Shc have been shown to activate MAP kinase (MAPK), hence regulate cellular growth. Actin cytoskeleton is shown with pink filaments, longitudinally aligned within the cell and aggregate upon insulin stimulation.

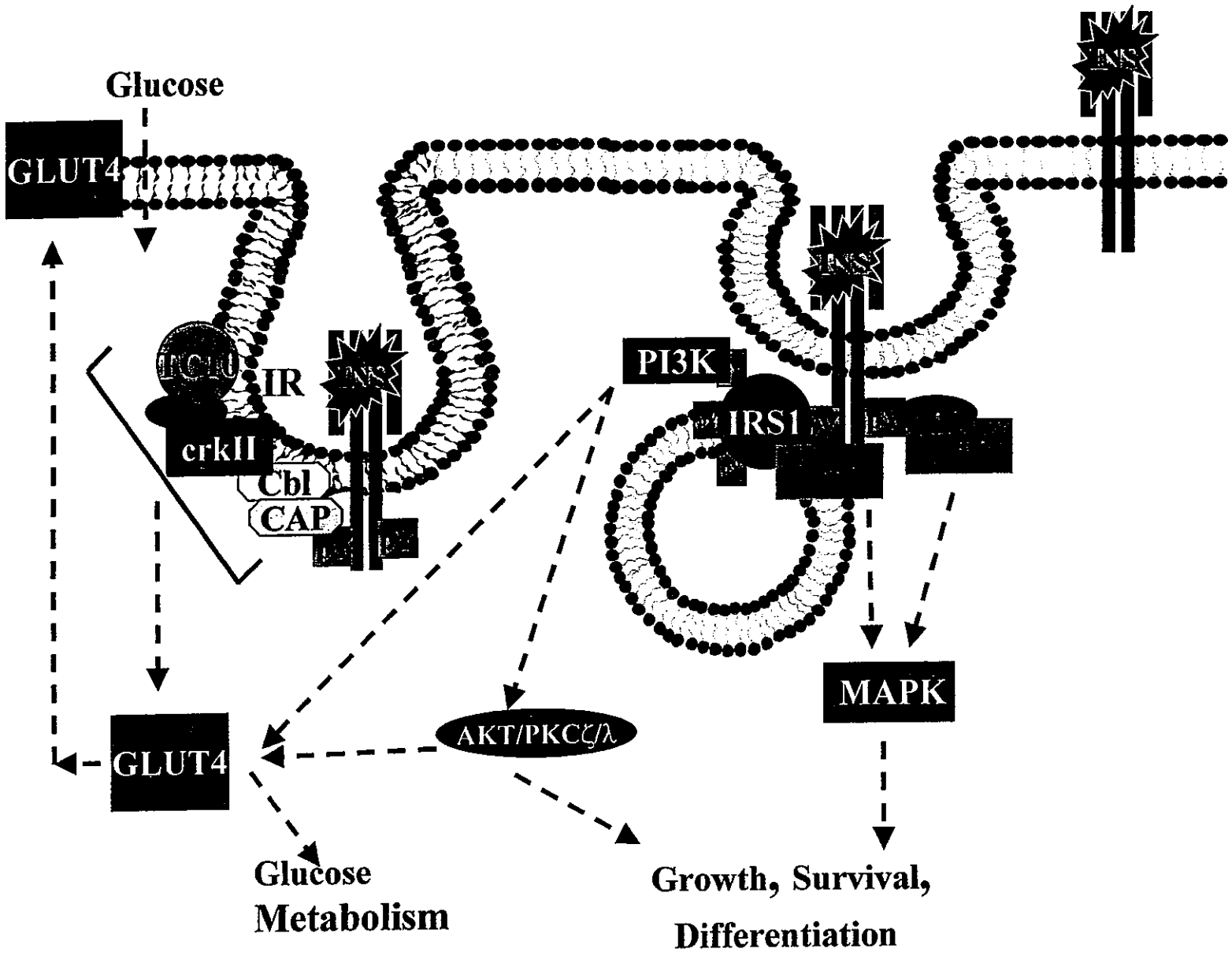
Glucose
GLUT4
IR
crkII
Cbl
CAP
PI3K
IRS1
MAPK
GLUT4
AKT/PKCζ/λ
Glucose
Metabolism
Growth, Survival,
Differentiation

1996). This differential expression often controls the duration and the strength of the signal generated, by establishing certain kinetic thresholds for activation of specific signaling molecules. As obvious as it may seem, this argument only provides a partial explanation to some fundamental questions with regards to specificity. As in the case of IRS family of proteins, IRS-3 is mainly expressed in adipocytes while IRS-4 in kidney, spleen, heart and brain (Lavan et al., 1997a; Lavan et al., 1997b; Ogawa et al., 1998). On the other hand, despite their extensive homology, IRS-1 and IRS-2 are ubiquitously expressed often to the same levels and yet are not functionally interchangeable (Giovannone et al., 2000). In the latter case, functional pleiotropism may be accomplished by differential phosphorylation of tyrosine residues in canonical consensus motifs for nucleating downstream signaling intermediates. In support of this contention, IRS-2 is larger and contains some unique putative phosphorylation sites potentially contributing to signaling specificity (Shpakov and Pertseva, 2000). Moreover, IRS-2 contains a central region, which interacts with the kinase domain of the activated insulin receptor, authenticating additional regulation of IRS-2 tyrosine phosphorylation (White and Yenush, 1998). However, existence of multiple tyrosine phosphorylation residues in the conserved binding motifs for SH2 containing proteins such as PI 3-kinase, Grb2 and protein tyrosine phosphatase 1B (PTP 1B) argues against differential phosphorylation as the sole factor causative in the observed signaling specificity between IRS-1 and IRS-2.

An emerging view to account for the specificity of insulin signaling on glucose transport is that biological specificity is conferred at the level of subcellular compartmentalization of signaling intermediates. Indeed, subcellular fractionation studies in 3T3-L1 adipocytes and insulin receptor overexpressing CHO cells, revealed that activated PI 3-kinase

complexes are found predominantly in the low-density microsomes (LDM) following insulin treatment, whereas activation of PI 3-kinase in response to platelet derived growth factor (PDGF) in the same cells, occurs at the plasma membrane (Clark et al., 1998; Clark et al., 2000). Analogously, differences in the pattern of intracellular distribution have been documented among four members of the IRS protein family and may account for differences in their ability to engage downstream signaling elements, which may ultimately contribute to their functional specificity *in vivo* (Anai et al., 1998; Giovannone et al., 2000; Inoue et al., 1998). For example, while the majority of IRS-1 is found in the LDM compartment, IRS-2 seems to be more concentrated in the cytosol (Inoue et al., 1998). IRS-3, on the other hand, is mainly localized at the plasma membrane and some expression is observed in the nucleus, suggesting its distinct function in accordance with its intracellular localization (Anai et al., 1998; Kabuta et al., 2002).

1.2.3 Insulin receptor subcellular distribution and trafficking

Traditionally, it is believed that under basal conditions insulin receptors are preferentially associated with microvilli in the plasma membrane. Concomitant with insulin binding, the insulin receptor is redistributed in the plane of the membrane and progressively accumulates in the clathrin-coated pits, which is eventually pinched off and internalized into acidic endosomal compartments through a complex set of intermediary steps (Carpentier et al., 1996; Ceresa et al., 1998). The acidic environment of the endosomal apparatus causes insulin dissociation and degradation followed by the recycling of the receptors back to the cell surface (Di Guglielmo et al., 1998; Wiley and Burke, 2001). The exact molecular mechanisms governing the coordination of this multi-step process is

yet to be defined. Recent studies have demonstrated that insulin-dependent receptor endocytosis requires both the kinase activity and tyrosine containing motifs in the juxtamembrane region (Backer et al., 1990; Backer et al., 1992; Carpentier et al., 1993). Several studies have demonstrated that endosomal-localized activated insulin receptor exhibits increased autophosphorylation and substrate tyrosine phosphorylation compared to plasma membrane-associated insulin receptor (Backer et al., 1989; Khan et al., 1989). Based on this hypothesis, internalized endosomal-bound insulin receptors are thought to be responsible for the tyrosine phosphorylation of IRS-1 localized mainly in the LDM compartments and subsequent activation of PI 3-kinase among other intracellular signaling pathways. However, other studies have reported that under conditions where receptor endocytosis is blocked either at low temperature (4°C) or by employing dominant-inhibiting mutant proteins such as dynamin K44A, insulin signaling remains intact (Ceresa et al., 1998; Heller-Harrison et al., 1995). Thus, by contrast, these studies suggest that activation of plasma membrane-associated insulin receptor is sufficient for insulin-specific signaling. A proposed hypothesis commensurate with both of these observations suggests that localization of IRS-1 to the cytoskeleton closely positioned underneath the plasma membrane may allow an efficient coupling of IRS-1 with the activated insulin receptor in the clathrin-coated pits (Clark et al., 2000).

Recent evidence has also shown that some insulin receptors are localized in highly specialized lipid microdomains called rafts, also known as caveolae (Gustavsson et al., 1999; Watson et al., 2001; Wu et al., 1997). The main components of these rafts include lipids such as sphingolipids, glycosphingolipids and cholesterol as well as proteins such as caveolin (Bickel, 2002). Interestingly, treatment of 3T3-L1 adipocytes with β-

cyclodextrin, which disrupts lipid raft structures by extracting cholesterol from the plasma membrane, mitigates IRS-1 tyrosine phosphorylation and Akt activation by the activated insulin receptor, suggesting that the integrity of raft organization is imperative for IRS-1-mediated insulin action and signaling (Gustavsson et al., 1996; Parpal et al., 2001). These lipid raft-localized insulin receptors have also been demonstrated to activate TC10, a member of the Rho family of exchange factors, and regulate GLUT4 translocation to the cell surface in response to insulin stimulation (Chiang et al., 2001). Interestingly, TC10 mutations causing its mislocalization to regions of the plasma membrane other than the lipid rafts disrupt insulin-mediated activation of TC10 and GLUT4 membrane translocation in 3T3-L1 adipocytes, suggesting that spatial compartmentalization of this molecule allows its access to both upstream activators and downstream effectors required for its function (Watson et al., 2001).

In summary, activation of the insulin receptor located in two distinct membrane compartments, namely clathrin-coated pits and caveolae seems to initiate signaling pathways required for ensuing metabolic responses of insulin.

1.3 INSULIN RECEPTOR SUBSTRATE PROTEINS

1.3.1 IRS family

IRS proteins play a central role in propagating and transducing insulin-instigated signals by providing multiple docking sites for the recruitment of downstream effectors. To date, four immediate members (IRS-1, IRS-2, IRS-3, and IRS-4) of this family have been discovered, which despite their highly conserved sequence and topology, differ in their

subcellular and tissue distribution and function (Giovannone et al., 2000). They all share two highly organized structural determinants, namely pleckstrin homology (PH) and phosphotyrosine binding (PTB) modules in their amino(N)-terminus, in addition to several conserved tyrosine phosphorylation sites in their carboxy(C)-terminus (Figure 1.2). The degree of homology is most prominent in the N-terminal domains with less conservation of the C-terminal region, both in size and sequence, among IRS members.

IRS-1 is the major and best characterized of the IRS proteins. IRS-1 is a hydrophilic protein with a calculated molecular mass of 131 KDa. It contains over 30 putative serine/threonine phosphorylation sites, which when phosphorylated results in retarded electrophoretic migration of the protein displaying an apparent molecular mass of 165-185 KDa in SDS-PAGE (Sun et al., 1992). Moreover, IRS-1 contains more than 20 putative tyrosine phosphorylation sites some of which are rapidly phosphorylated upon insulin stimulation and in turn allow recruitment of downstream effectors and subsequent activation of signal transduction pathways. Mice deficient in IRS-1 gene display insulin resistance in muscle and adipose tissues associated with hypertriglyceridemia and hypertension, supporting the physiological role of IRS-1 in insulin sensitivity for glucose homeostasis (Araki et al., 1994; Tamemoto et al., 1994). Surprisingly however, IRS-1 knock out mice do not develop diabetes leading to the idea of alternative mechanisms such as other IRS family members that may compensate for the lack of IRS-1 in these mice (Abe et al., 1998; Tamemoto et al., 1994).

Cloning of IRS-2 cDNA revealed the predicted structural moieties of the PH and PTB domains, which share extensive sequence homology to IRS-1 (Sun et al., 1995). Despite the highly similar N-terminal region and several putative conserved tyrosine

Figure 1.2. Schematic representation of four insulin receptor substrate (IRS) family members. Human (h) IRS-1 (GenBank™ accession number S62539), hIRS-2 (GenBank™ accession number AF073310), hIRS-4 (GenBank™ accession number NM003604) and rat (r) IRS-3 (GenBank™ accession number U93880) schematic structures are depicted. Human IRS-3 has not yet been found. Pleckstrin homology and phosphotyrosine domains are shown by black boxes labeled as PH and PTB, respectively, at the IRS N-terminus. Various phosphorylation sites including tyrosine, serine and threonine are represented by "P". Same colour phosphorylation sites represent conserved motifs among IRS family members, while different colours show distinct motifs.

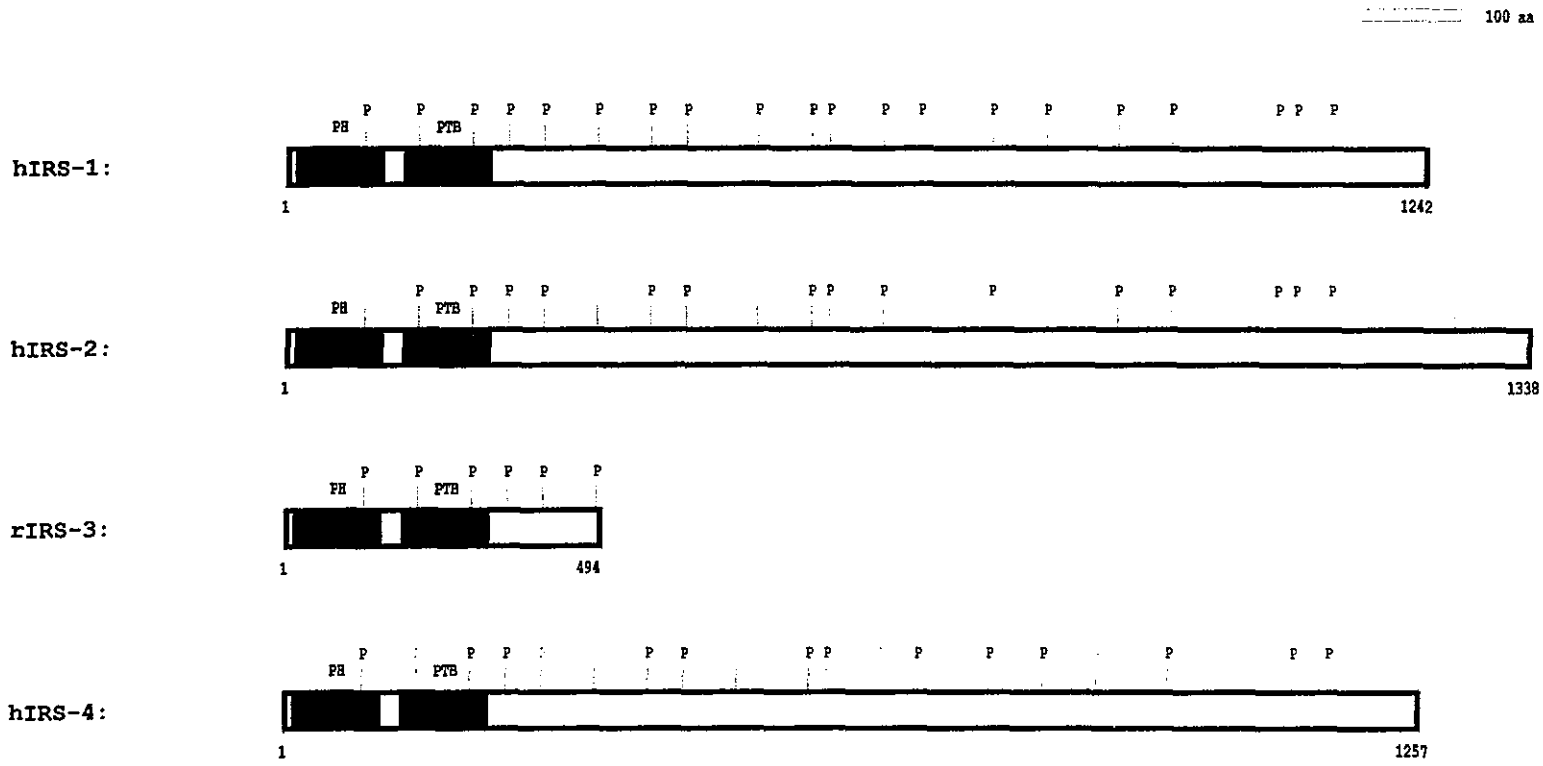
100 aa
hIRS-1:
PH
PTB
1
1242
hIRS-2:
PH
PTB
1
1338
rIRS-3:
PH
PTB
1
494
hIRS-4:
PH
PTB
1
1257

phosphorylation sites in the C-terminus, the central region of IRS-2 possesses a unique domain that interacts with the kinase domain of the insulin receptor. Moreover, IRS-2 also contains distinct tyrosine phosphorylation motifs at its carboxy-terminus, which potentially distinguishes some aspects of its function from that of IRS-1. Indeed, mice with targeted disruption of IRS-2 gene are born with insulin resistance and progressively develop diabetes accompanied with reduced pancreatic β-cell mass (Withers et al., 1998). Unlike the mice lacking IRS-1, in which prolonged hyperglycemia promotes skeletal muscle insulin resistance, IRS-2 knockout mice exhibit normal insulin-induced glucose uptake in muscle cells isolated from animals with normal glucose levels. Accordingly, studies on cells isolated from IRS-1 knockout mice demonstrate that IRS-2 can compensate for lack of IRS-1 function in liver and β-cells but not in muscle or adipocytes (Bruning et al., 1998; Tamemoto et al., 1994; Withers et al., 1998; Yamauchi et al., 1996). Collectively, these data indicate that whereas IRS-1 plays a major role in skeletal muscle and fat tissues, IRS-2 appears to be important in liver and β-cells. Thus, IRS-1 and IRS-2 are not functionally interchangeable.

Whilst the role of IRS-1 and IRS-2 in regulating insulin action has been well established, the function of IRS-3 and IRS-4 is less clear. The latter two proteins possess similar structural architecture as IRS-1 and IRS-2. IRS-3 is found to be the smallest member of the IRS family identified to date with a very short C-terminal region (Lavan et al., 1997b). Previous studies have illustrated that IRS-3 and not IRS-2 provides 50% compensation for insulin-instigated glucose transport in adipocytes lacking IRS-1, intimating some regulatory role of IRS-3 in glucose homeostasis (Kaburagi et al., 1997). Accordingly, overexpression of IRS-3 in rat adipocytes has been reported to increase

GLUT4 translocation to the plasma membrane (Zhou et al., 1999). Conversely, mice with targeted disruption of either IRS-3 or IRS-4 exhibit no detectable abnormalities, overshadowing the earlier *in vitro* data on a role of these proteins in insulin-mediated biological responses *in vivo* (Fantin et al., 2000; Liu et al., 1999). Interestingly, human IRS-3 has not yet been found, suggesting that IRS-3 function may not be required for insulin action in humans (Giovannone et al., 2000).

1.3.2 IRS-1 downstream effectors

As mentioned above, IRS-1 contains about 20 potential tyrosine phosphorylation consensus sites recognizable by several SH2 containing proteins such as phosphotidylinositol (PI) 3-kinase, Grb-2, Nck, Crk, Fyn kinase, and PTP phosphatase (Giovannone et al., 2000; White and Yenush, 1998). Recruitment of these molecules results in their activation and galvanizes multiple downstream signaling pathways leading to biological insulin responses.

PI 3-kinase is a heterodimeric complex composed of a 110 KDa catalytic subunit (p110) associated with an 85 KDa regulatory subunit (p85). While, the regulatory subunit of PI 3-kinase contains an SH2 domain, which recognizes and interacts with multiple YXXM motifs within IRS-1, the catalytic subunit carries dual specificity enzymatic function (Myers et al., 1994a; Myers and White, 1996). On the one hand, it phosphorylates the D3 position of the inositol ring of phosphotidylinositol derivatives generating second messenger PI 3P, PI $3,4P_2$ or PI $3,4,5P_3$ lipid molecules in the cytosolic leaflet of cellular membranes (Shepherd et al., 1998). On the other hand, PI 3-kinase bears serine kinase activity and has been known to phosphorylate IRS-1 among other molecules (Elbashir et

al., 2001). IRS-1, through direct activation of PI 3-kinase is primarily involved in regulation of glucose metabolism (Shpakov and Pertseva, 2000). Inhibition of PI 3-kinase catalytic activity by pharmacological inhibitors such as wortmanin and dominant-negative mutants attenuate GLUT4 membrane translocation and glucose transport, corroborating the role of PI 3-kinase as a central component of insulin-dependent metabolic responses (Okada et al., 1994).

Growth factor receptor binding –2 (Grb-2) is a small cytosolic adaptor protein, which contains SH2 and SH3 domains and has been reported to bind to phosphotyrosine within the context of YVNI motif in IRS-1 (Valverde et al., 2001). Grb-2 via its SH3 domains binds to mSos-1, a p21Ras exchange factor. mSos-1 in turn stimulates p21Ras GTP-binding and ultimately results in mitogen-activated protein (MAP) kinase activation leading to gene transcription and DNA synthesis (Ito et al., 1996; Myers et al., 1994b; Rose et al., 1994; Sun et al., 1993).

Nck and Crk, adaptor proteins comprising exclusively of SH2 and SH3 domains, also associate with IRS-1 in response to insulin stimulation. Although, their functional role in IRS-1-mediated signaling is less clear, some data have indicated the involvement of Nck in NIH 3T3 cellular transformation (Chou et al., 1992). Nck has also been implicated in receptor-mediated cytoskeletal organization via its interaction with N-WASP proteins in response to external stimuli, providing a potential mechanism through which insulin might regulate actin polymerization (Miki et al., 2000; Moreau et al., 2001; Takenawa and Miki, 2001). Analogously, CrkII, an alternative splice variant of Crk adaptor proteins has also been shown to be involved in actin cytoskeleton rearrangements and DNA synthesis in response to insulin and IGF-1 stimulation (Beitner-Johnson et al., 1996;

Nakashima et al., 1999). Moreover, through its interaction with C3G, a guanyl nucleotide exchange factor, CrkII recruits TC10 GTP-binding protein to lipid rafts upon insulin stimulation of adipocytes and regulate intracellular GLUT4 localization to the cell surface, supporting a PI 3-kinase independent glucose transport mechanism (Burkhard et al., 2001; Chiang et al., 2001) (Figure 1.1).

Fyn is a Src-related tyrosine kinase that binds to phosphorylated tyrosine residue Y^{895}, in the context of YXX(L/I) motif within IRS-1 (Sun et al., 1996). Interestingly, it has been shown that Fyn might compete with Grb-2 for binding to phosphotyrosine Y^{895} thereby regulating IRS-1-mediated mitogenic effects of insulin (Sun et al., 1996; Valverde et al., 2001).

Protein tyrosine phosphatase (PTP) family whose members include SHP1 and 2, are SH2 containing tyrosine phosphatases, which are thought to negatively regulate insulin and IRS-1-mediated signaling by dephosphorylating tyrosine residues of both the insulin receptor and IRS-1 (Egawa et al., 2001; Goldstein et al., 2000; Ouwens et al., 2001). Previous data have shown that SHP2, also known as PTP 1D, functions as an adaptor protein which promotes insulin receptor and IRS-1 interactions (Kharitonenkov et al., 1995). The correlation between the two apparently distinct functions is yet to be elucidated. Two major binding sites of PTPs have been mapped to $NYIDLD^{1171-1176}$ and $NYASIS^{1221-1226}$ in the C-terminus of IRS-1 (Shpakov and Pertseva, 2000). Interestingly, the PTP's consensus binding motif, specifically Y^{1172} is also shared by Fyn kinase, supporting a remarkable phosphorylation/dephosphorylation regulation of IRS-1 by the competition between its binding partners (Sun et al., 1996).

1.3.3 Role of IRS-1 in insulin-mediated mitogenic responses

One of the early signaling events instigated downstream of the insulin receptor is activation of p21Ras/MAP kinase pathway leading to gene transcription and mitogenesis (Burgering et al., 1991). Studies in mice with a targeted disruption of the IRS-1 gene demonstrate severe retardation in embryonic and postnatal growth, suggesting a pivotal role of IRS-1 in cellular growth and proliferation (Araki et al., 1994; Tamemoto et al., 1994). Recent biochemical studies on fetal brown adipocytes isolated from these mice demonstrated a severe impairment of insulin-elicited DNA synthesis (Valverde et al., 2001). Moreover, unlike wild-type IRS-1, expression of an IRS-1 mutant carrying a mutation at Grb-2 binding site, Y^{895}, could not rescue MAP kinase activation and subsequent mitogenesis in response to insulin in these cells, substantiating the essential role of IRS-1/Grb-2/MAP kinase pathway in insulin-stimulated DNA synthesis (Valverde et al., 2001). The specific role of IRS-1 in insulin-mediated DNA synthesis is further supported by studies on IGF-1 receptor-deficient brown adipocytes, where an increased insulin sensitivity for MAP kinase activation and mitogenesis is observed due to enhanced insulin-promoted IRS-1 tyrosine phosphorylation (Mur et al., 2002). Additionally, *in vitro* experiments in which IRS-1 proteins were overexpressed in 32D hematopoietic cells devoid of IRS-1, revealed enhanced mitogenesis induced by insulin, suggesting that IRS-1 expression is sufficient in mediating the cellular growth effects of insulin in these cells (Chen et al., 1995; Wang et al., 1993). Likewise, IRS-1 overexpression in NIH3T3 fibroblasts promotes neoplastic transformation as a result of activation of p21Ras signaling pathway leading to MAP kianse activation (Tanaka et al., 1996). By contrast, microinjection of anti-IRS-1 antibodies or expression of dominant

inhibitory mutants of IRS-1 abolishes insulin-stimulated mitogenic responses in adipocytes (Morris et al., 1996; Rose et al., 1994; Sharma et al., 1997). Collectively, these data provide strong evidence for the indispensable function of IRS-1 in insulin-induced DNA synthesis and cellular proliferation.

1.3.4 Role of IRS-1 in insulin-mediated metabolic responses

One of the major metabolic functions of insulin is to maintain a tight balance between the amount of glucose produced by the pancreatic β-cells and its utilization by the peripheral target tissues (Saltiel, 2001). Considerable evidence supports the importance of IRS-1 function in transducing metabolic signals of insulin mediated by the activated insulin receptor. *In vitro* studies have illustrated that IRS-1 overexpression in L6 myoblasts results in enhanced insulin sensitivity and responsiveness for both glucose uptake and glycogen synthesis (Hribal et al., 2000). Moreover, recent *in vivo* studies have reported a direct positive correlation between low levels of IRS-1 and insulin resistance associated with low glucose transporter 4 (GLUT4) translocation and impaired cellular glucose uptake (Carvalho et al., 2001). Similarly, reducing IRS-1 protein levels by expressing antisense ribozyme generated against IRS-1 leads to a significant attenuation of insulin-induced GLUT4 translocation to the plasma membrane in rat adipose cells (Quon et al., 1994). Given that GLUT4 membrane translocation is required for glucose uptake upon insulin stimulation of target cells, IRS-1 regulation of this process, as demonstrated by these studies corroborates the crucial role of IRS-1 in galvanizing components of the signaling pathways necessary for metabolic responses of insulin.

1.3.5 IRS-1 subcellular distribution and trafficking

Several cell fractionation studies have documented that IRS-1 is localized in two distinct pools within the cells, the cytoskeletal fraction associated with the LDM and the cytosolic compartment (Heller-Harrison et al., 1995; Kublaoui et al., 1995). In support of the idea that subcellular compartmentalization is central to IRS signal transduction, it has been demonstrated that altered trafficking and tight membrane association of CAAX-modified IRS-1 dramatically impairs insulin signaling (Kriauciunas et al., 2000). In particular, spatial arrangement of IRS-1 in the LDM compartment is thought to provide a unique platform in proximity of the insulin receptor for efficient generation of specific signals required for insulin action. Consistent with this notion, IRS-1 enriched in the LDM compartment is maximally phosphorylated by the activated insulin receptor in adipocytes (Kelly and Ruderman, 1993; Kelly et al., 1992). Furthermore, it has been reported that LDM and not cytosolic-associated IRS-1/PI 3-kinase complexes are mainly responsible for GLUT4 transporter translocation to the plasma membrane in response to insulin (Kelly and Ruderman, 1993). By contrast, previous reports have shown that activation of PI 3-kinase in the plasma membrane by PDGF has no significant effect on glucose transport and glycogen synthesis (Nave et al., 1996; Ricort et al., 1996). Taken together, these data emphasize the importance of compartmentalization of IRS-1 as one of the mechanisms that confers biological specificity in response to insulin.

Relatively short-term insulin treatment triggers a progressive release of IRS-1 from the microsomal compartment into the cytosol (Clark et al., 2000; Heller-Harrison et al., 1995; Inoue et al., 1998). This redistribution is postulated to promote attenuation of IRS-1 signaling, presumably due to the inaccessibility of IRS-1 to the activated insulin receptor.

The mechanisms of IRS-1 disengagement from the LDM remain elusive. One observation that may shed some light on this conundrum is that the release of IRS-1 is always accompanied by a significant decrease in its electrophoretic mobility apparently due to an increase in serine/threonine phosphorylation (Heller-Harrison et al., 1995). IRS-1 contains more than 30 serine/threonine residues in consensus phosphorylation motifs for kinases such as casein kinase II, cAMP-dependent protein kinase, protein kinase C, cdc2 kinase, Map kinase, PI 3-kinase, and Akt (del Peso et al., 1997; Sun et al., 1991; Sun et al., 1995). Enhanced IRS-1 serine/threonine phosphorylation has been shown to result in a decrease in IRS-1 association with the insulin receptor and impairment of IRS-1 tyrosine phosphorylation concomitant with IRS-1 accumulation in the cytosol, and attenuation of insulin signaling (Paz et al., 1997). Consistent with the notion that serine/threonine phosphorylation is implicated in IRS-1 cytosolic retention, it has recently been shown that 14-3-3, a specific phospho-serine binding protein, can promote displacement of IRS-1 from the LDM into the cytosol following insulin treatment of 3T3-L1 adipocytes (Xiang et al., 2002). Moreover, data from *in vitro* reconstitution assays have demonstrated the importance of an as yet unidentified serine/threonine phosphorylation event within LDM as the mechanism of IRS-1 dissociation (Inoue et al., 1998). Together, these studies suggest a potential cooperative mechanism in which serine/threonine phosphorylation of both IRS-1 and other microsomal components that might be required for an efficient export of IRS-1 from the LDM.

1.4 PLECKSTRIN HOMOLOGY DOMAIN

1.4.1 Basic structure and physical characteristics

The pleckstrin homology (PH) domains are small protein modules of roughly 120 amino acids found in various signaling molecules with diverse enzymatic and regulatory functions (Bottomley et al., 1998). Those include protein tyrosine and serine/threonine kinases such as β-adrenergic receptor kinase (β-ARK), protein kinase B (PKB/AKT), and phospholipase C isoforms (PLCβ, γ, δ) and guanine nucleotide exchange factors such as Cdc25, Sos, and Dbl, GTPase activating protein Ras-GAP as well as cytoskeletal proteins (Blomberg et al., 1999; Haslam et al., 1993; Musacchio et al., 1993). In general, PH domains are poorly conserved at the amino acid level. The most noticeable characteristic of PH domain sequences is an invariant single tryptophan residue in the distal C-terminal region. Remarkably however, despite the low degree of sequence conservation, the nuclear magnetic resonance (NMR) and X-ray crystallography analysis of various PH domains demonstrate a highly conserved tertiary structure reminiscent of a family of compact protein modules (Harlan et al., 1995). The core structure of the PH domain features a β-sandwich composed of two closely packed orthogonal β-sheets consisting of seven strands and a C-terminal α-helix. All PH domains whose structure has been solved to date, display an electrostatically polarized surface with positively charged residues, located on the variable loops connecting the β-strands, which is thought to confer binding to the negatively charged headgroups of phosphoinositide ligands (Harlan et al., 1995). The α-helical region of PH domains is enriched in acidic residues and has been proposed to mediate protein-protein interactions in proteins such as β-ARK and Bruton's tyrosine

kinase (Btk) (Pitcher et al., 1995; Touhara et al., 1994; Touhara et al., 1995; Tsukada et al., 1994).

1.4.2 PH domain ligands

On the basis of the structural similarity of PH domains with lipid-binding molecules such as retinal binding protein, fatty acid binding proteins and bilin binding protein, it was originally suggested that PH domains may function as lipid-binding modules. Subsequent *in vitro* binding assays using isolated PH domains from pleckstrin, Ras-GAP, β-ARK and Tsk confirmed these predictions and demonstrated PH domain interactions with Phosphotidylinositol (PI) 4,5 phosphates (Harlan et al., 1994). PH-phospholipid ionic interactions were mapped to the positively charged region of the β-sandwich within the PH domain (Harlan et al., 1995). Recently, various PH domains were reported to bind to the phospholipid products of PI 3-kinase, including PI3P, $PI3,4P_2$ and $PI3,4,5P_3$, which act as lipid secondary messengers in ligand-mediated signaling (Blomberg et al., 1999; Isakoff et al., 1998; Lemmon and Ferguson, 2000). For example, the PH domain of Akt serine/threonine kinase specifically recognizes and interacts with $PI3,4P_2$ and $PI3,4,5P_3$ with high affinity (Franke et al., 1997; Frech et al., 1997). Moreover, binding of Akt to these phospholipids has been illustrated to be crucial for Akt localization to the plasma membrane and its subsequent activation by PDK1, highlighting the significance of high affinity PH-lipid interactions in promoting the physiological function of this protein (Franke et al., 1997). Despite the mounting evidence of *in vitro* lipid-binding ability of various PH domains, by far the majority of these interactions have proven to be of low affinity ($K_D \geq 4\mu M$) and weak stereospecificity. Whilst limited number of specific

and high-affinity PH-PI4,5P_2 interactions as those observed for proteins such as PLCδ ($K_D \cong 1.7\mu M$) might be sufficient for membrane tethering and function of these molecules, non-specific low affinity interactions may require additional support to stabilize their interactions with membrane components for productive signaling *in vivo* (Bottomley et al., 1998; Lemmon et al., 2002). Indeed, while the N-terminal region of β-ARK PH domain is required for binding to PIP_2, the C-terminal region has been demonstrated to associate with the βγ dimer subunits of trimeric G-proteins (Gβγ) for effective membrane association and subsequent activation of β-ARK (Pitcher et al., 1995).

Specific PH-protein interactions have been documented for various proteins. Structural and biochemical studies on the PH domains isolated from Dbl, β-ARK and Btk proteins have demonstrated their interactions with the βγ subunits of heteroterimeric G-proteins with different affinities (Mahadevan et al., 1995; Tsukada et al., 1994; Wang et al., 1994). In addition, the PH domains of Btk and Rac protein kinase also interact with protein kinase Cζ (Konishi et al., 1994; Yao et al., 1994). Similarly, the PH domain of Btk was shown to mediate its localization to the filamentous actin through direct interaction (Yao et al., 1999). The PH-protein interactions in the above examples has been shown to be critical for the function of these proteins *in vivo*. For instance, the importance of Btk PH domain interaction with the Gβγ subunits has been implicated in B lymphocytes development and function (Tsukada et al., 1994). Interestingly, based on crystal structure analysis of various guanine nucleotide exchange factors (GEFs) such as Vav, mSos and Tiam, intramolecular interactions between the PH and the neighboring Dbl homology (DH) domain has also been observed, suggesting a regulatory role of the PH on DH domain enzymatic function (Das et al., 2000; Qian et al., 1998; Stam et al.,

1997; Wang et al., 1997). The relevance of some these PH-protein interactions and their respective lipid association *in vivo* is discussed later in this chapter.

1.4.3 PH domain superfamily

Recent structural studies have indicated that despite the lack of sequence similarity, PH domains adopt the same core structure as those of several protein-binding modules such as the phosphotyrosine binding (PTB) domain, the Ran-binding domain (RanBD), and the Enabled/VASP homology 1 (EVH1) domain (Prehoda et al., 1999; van der Geer and Pawson, 1995; Vetter et al., 1999). Interestingly however, the modes of the interaction of these domains with their respective ligands differ tremendously, underlying the functional plasticity of the PH fold supporting a range of cellular activities. The PTB domain recognizes phosphotyrosine in the context of the amino acid sequence NPXY and participates in recruitment of host proteins to the activated receptors. Of note in this regard is that phosphorylation of the tyrosine residue within NPXY motif is not necessarily required for PTB binding. For example, while, IRS-1 and Shc PTB domains require tyrosine to be phosphorylated in the activated insulin receptor, the PTB domains from X11 and Numb do not require phosphorylation of the neuronal growth factor receptor (NGFR) for binding (Li et al., 1998; Zhang et al., 1997). Several studies have also reported binding of the PTB domains of IRS-1 and Shc to phosphoinositides, albeit weakly and non-specifically, the physiological implications of which have yet to be determined (Takeuchi et al., 1998; Zhou et al., 1995).

Crystal structure studies of Ran Binding Domain (RanBD) found in the Ran-binding protein, a component of the nuclear transport machinery, unexpectedly displayed a stable

PH fold, placing this domain in the PH domain superfamily category (Vetter et al., 1999). While phosphoinositide binding capacity of RanBD has yet to be investigated, recent studies demonstrate that the region of RanBD which confers binding to Ran GTPase corresponds to phosphoinositide binding region of PLCδ and Btk PH domain (Vetter et al., 1999).

Finally, the third class of protein modules reported to adopt a PH-domain fold is the Enabled/VASP Homology 1 (EVH1) domain. This domain is found in cytoskeletal proteins that function as adaptor proteins recruiting components of the actin assembly machinery in response to upstream signals. EVH1 domains have been illustrated to bind to polyproline rich peptides in FPPPP consensus motifs (Prehoda et al., 1999). Interestingly, the N-terminal region of Wiskott-Aldrich Syndrome Protein (WASP) containing the EVH1 domain has been implicated in PI4,5P_2 binding, raising the possibility that this domain maybe capable of binding to both protein and lipid ligands (Miki et al., 1996). This is analogous to the PH domain of β-ARK where simultaneous binding to PI4,5P_2 and Gβγ is required for productive activation of β-ARK (Pitcher et al., 1995).

Clearly, these data demonstrate the flexibility of the basic PH domain superfold in recognizing both phosphoinositides and protein ligands. This property might reflect the adaptability of the PH domain superfold by constructing a structural scaffold which confers multiple cellular functions.

1.4.4 PH domain functions

The functional requirement for membrane localization of the majority of PH domain-containing proteins in addition to their ability to associate with phospholipids have implicated a membrane-tethering role for PH domains. Indeed, PLCδ PH domain interaction with the $PI4,5P_2$ presumably targets the protein to the plasma membrane where it can react on its substrate, $PI4,5P_2$ (Lemmon et al., 1997). Analogously, binding of the PH domain of AKT to $PI3,4P_2$ and PI $3,4,5P_3$, has been proven to sequester AKT to the plasma membrane thereby allowing its phosphorylation and activation by PDK1 (Downward, 1998). Moreover, AKT activity is shown to directly correlate with the extent of its PH domain interaction with phospholipids in response to insulin (Klippel et al., 1997).

However, despite the ability of some PH domains in recruiting host proteins to the plasma membrane, non-specific membrane targeting sequences such as CAAX motifs and myristoylation sequences do not always functionally substitute for PH domains. As in the case of mSos1, a Ras-specific guanine nucleotide exchange factor, addition of a membrane targeting signal to full-length Sos renders the protein constitutively active which leads to Ras-dependent transformation of NIH 3T3 cells (Quilliam et al., 1994). However, a myristoylated derivative of mSos1 devoid of its PH domain lacks transforming activity, although the protein is stable and localizes to the plasma membrane, suggesting a specific regulatory role of the PH domain on the mSos1 function (Qian et al., 1998). Consistent with the latter hypothesis, nearly all known members of the Dbl family of guanine nucleotide exchange factors (GEFs) contain a PH domain invariably located in tandem with the catalytic Dbl homology (DH) domain, lending

support to a functional interdependence of these two domains (Das et al., 2000; Nimnual et al., 1998; Qian et al., 1998). Indeed, recent structural studies have verified an allosteric inhibitory regulation of the PH domain on mSos1 DH domain, which is presumably relieved upon PH domain interaction with phospholipids (Nimnual et al., 1998). As in the case of Vav, binding to PI 3-kinase phospholipid products relieves PH inhibition of DH association with the GTPase (Das et al., 2000). While, these studies seem to suggest that PH regulation of the exchange activity of the DH domain in Dbl-family proteins is ultimately controlled through PH/phospholipid interactions, more recent data demonstrate that in the case of Tiam1, a second PH domain is directing Tiam1 membrane localization independent of the DH neighboring PH domain (Han et al., 1998; Worthylake et al., 2000). Tiam1 is a Dbl-related GEF involved in controlling actin cytoskeletal remodeling through Rho-GTPases, whose exchange activity does not change in response to the levels or composition of phosphoinositides *in vitro* (Worthylake et al., 2000). Consistent with the notion of PH domain-mediated regulation of exchange activity independent of phosphoinositide binding, a DH-PH fragment of Trio displays enhanced nucleotide exchange activity on Rac1, as compared to the isolated DH domain, indicating that the PH domain in concert with the DH domain is necessary for full exchange activity (Liu et al., 1998). Moreover, a crystallographic analysis of Dbl's big sister (Dbs) interaction with Cdc42 GTPase illustrates a direct association of the Dbs PH domain with Cdc42 switch 2 domain, supporting a unique mechanism of PH domain-mediated regulation of Dbs exchange activity (Rossman et al., 2002). Collectively, these data suggest that PH-lipid or PH-protein interactions are highly context dependent and that the PH superfold forms a versatile scaffold to facilitate various cellular functions.

1.5 AIMS OF THIS STUDY

Extensive analysis of IRS-1 structural and biochemical characteristics has advanced our understanding of the signaling pathways emanating from IRS-1/insulin receptor interactions. What is in dispute however is the mechanism by which LDM-tethered IRS-1 recognizes and associates with plasma membrane-embedded insulin receptor. It is generally accepted that following insulin stimulation, the PTB domain of IRS-1 mediates direct binding to the phosphorylated tyrosine residue within the NPEY motif in the juxtamembrane region of the activated insulin receptor (Eck et al., 1996; Wolf et al., 1995). An important question that remains is the contribution of the IRS-1 PH domain in promoting accessibility of IRS-1 proteins to plasma membrane-bound insulin receptor. Deletional analysis of the PH domain, revealed that the PH domain plays a principal role in promoting IRS-1 tyrosine phosphorylation following insulin stimulation in intact cells (Myers et al., 1995). Furthermore, chimeric IRS-1 molecules containing heterologous PH domains from the β-ARK, phospholipase Cγ or spectrin with a similar phospholipid binding profile as IRS-1, fail to functionally restore IRS-1-phosphotyrosine-dependent signaling (Burks et al., 1997). Similarly, recent studies have shown that whilst mutations disrupting the lipid-binding properties in the IRS-1 PH domain impair plasma membrane association, these same mutations do not appear to have any effects on IRS-1 phosphorylation or IRS-1-associated PI 3-kinase activity, arguing against phospholipid-binding as an important component of IRS-1 interactions with the activated insulin receptor (Jacobs et al., 2001; Razzini et al., 2000). Together, these data are consistent with the idea that the IRS-1 PH may interact with a specific cellular ligand(s) to direct

IRS-1 to the plasma membrane-associated insulin receptor. This ligand does not appear to be the insulin receptor itself as *in vitro* binding studies and yeast two-hybrid analysis failed to detect a direct interaction between the IRS-1 PH domain and the insulin receptor (Gustafson et al., 1995; He et al., 1996; O'Neill et al., 1994; Sawka-Verhelle et al., 1996). In an attempt to identify functional partners of the IRS-1 PH domain, a yeast two hybrid system was set uo where the PH domain of IRS-1 was used as a bait to screen a mouse cDNA library (Farhang-Fallah et al., 2000). A clone that displayed the strongest signal coded for a novel protein termed PHIP, for **PH** Interacting **P**rotein, which selectively bound to the IRS-1 PH domain *in vitro*. The purpose of this study was to clone full length mammalian PHIP and explore the molecular mechanism of PHIP action in modulating insulin-stimulated IRS-1 pathways involved in cellular growth and metabolism. Specifically, I investigated the role of PHIP in mediating IRS-1 tyrosine and serine/threonine phosphorylation by the activated insulin receptor. Moreover, the physiological function of PHIP in IRS-1-mediated MAP kinase and PI 3-kinase pathways leading to gene transcription, DNA synthesis and GLUT4 translocation in response to insulin was dissected (Farhang-Fallah et al., 2002). Lastly, as studies from various groups have suggested the PH domain as a potential candidate in tethering IRS-1 to the cytoskeletal component of the low-density microsomes, I also explored the role of PHIP in IRS-1 subcellular distribution and trafficking.

CHAPTER TWO

MATERIALS AND METHODS

2.1 PLASMID CONSTRUCTS:

2.1.1 BTM116 yeast two-hybrid constructs – PH domains from rat IRS-1 (residues 3-133) (Sun et al., 1991), mouse SOS1 (residues 448-577)(Bowtell et al., 1992), human RasGAP (residues 464-603)(Trahey and McCormick, 1987), and mouse Ect-2 (residues 495-621) (Miki et al., 1993) were amplified by polymerase chain reaction (PCR) and fused in frame to the LexA DNA binding domain of the yeast expression plasmid BTM116.

2.1.2 pGEX-3X/PHIP$^{5\text{-}209}$ construct – the 612 base pair (bp) fragment spanning the IRS-1 PH binding region (PBR) of the PHIP complementary DNA (cDNA) isolated from the yeast two-hybrid screen was subcloned in frame into the BamH1/EcoRI sites of pGEX-3X (Invitrogen).

2.1.3 pCGN constructs – All of the following constructs were subcloned in frame with the hemagglutinin (HA)-epitope in the pCGN mammalian expression vector. To generate a construct encoding a mutant form of IRS-1 lacking the PH domain, pCGN/IRS-1$^{\Delta PH}$, a 216 bp SpeI/XmnI PCR generated fragment containing a portion of the IRS-1 PTB domain (residues 143-175), and a 4139 bp XmnI/KpnI fragment (residues

175-1236), cleaved from pBlueScript/IRS-1 (a gift from Dr. White), were together subcloned into the compatible XbaI/KpnI sites within the pCGN vector. The primers used to make the IRS-1 PTB domain containing PCR fragment were sense 5'-AAAAAAACTAGTGAGGACTTGAGCTATGACACG-3' and anti-sense 5'-GGAATTCGGCAGTGATGCTCTCAGTTCG-3'. SpeI restriction site (underlined) was added to facilitate subcloning into the pCGN vector. To prepare constructs encoding IRS-1 PH^{WT} a PCR generated fragment containing the IRS-1 PH domain (residues 3-133) was subcloned into SmaI and BamHI sites within the pCGN expression vector. To generate the IRS-1 PH domain mutant constructs designated IRS-1 PH^{W106A}, where the Trp106 residue conserved in all PH domains was changed to Ala, and either N-terminal (PH^{NT}, residues 3-67) or C-terminal (PH^{CT}, residues 55-133) PH domain regions, the following primers were used to amplify the corresponding regions. For PH^{W106A}, primer (1) 5'-AAAAACCCGGGAAGCCCTCCGGATACCGATG-3', and primer (2) 5'-AAAAAAGGATCCTCAATTATGCAGCTGCAGAAGAGCCTGGTA**CGC**GCTGTCT TGTTCAGCCTCG-3' (**CCA** is replaced with C**GC**); for PH^{NT}, primer (1) and primer (3) 5'-AAAAAAGGATCCTCACTCGAGGGGGATCGAGCG-3'; for PH^{CT}, primer (4) 5'-AAAAAATCTAGAAGCTGTTTCAACATCAACAAGC-3' and primer (5) 5'-AAAAAAGGATCCTCAGCTGCAGCTACCACCGCA-3' were used. SmaI, BamHI and XbaI restriction sites were added (underlined) to facilitate subcloning into pCGN, which had been digested with the same enzymes. To generate the pCGN/HA-DN-PHIP mutant construct, a PCR fragment of 639 bp encompassing the IRS-1 PH binding region of human PHIP (hPHIP; residues 4-217) was amplified using sense primer 5'-GGACTAGTGCGAGATTGGCTGTGGAAGAACTAAC-3' and anti-sense primer 5'-

CGGGATCCTCAGCAATATCTAGTGTCATCAACTGG-3'. The PCR fragment was digested with SpeI and Kpn-1 and subcloned into the compatible XbaI/KpnI sites of the pCGN vector. To generate the full-length pCGN/HA-PHIP construct, a 2271 bp BstEII/BamHI fragment comprising amino acids 150-902 of PHIP was excised from the cDNA clone 6b-26 isolated from a human fetal brain cDNA library, and subcloned into the pCGN/HA-DN-PHIP vector which had been cleaved at the BstEII site within PHIP and BamHI within the pCGN vector.

2.1.4 pBlueScript/PHIP vector - A 440 bp EcoRI/BstEII fragment comprising amino acids 5-150 of PHIP, excised from the cDNA clone 23b-28 isolated from a human fetal brain cDNA library, and a 2396 bp BstEII/EcoRV fragment comprising amino acids 150-902, excised from the 6b-26 cDNA clone were together subcloned into the compatible EcoRI/SmaI sites in pBlueScript-KS vector.

2.1.5 pCAN vectors - The following constructs were subcloned in frame with the HA-epitope in the pCAN mammalian expression vector. To create a vector encoding DN-PHIP (residues 5-209), a 612 bp BamHI/EcoRI fragment spanning the PBR region of PHIP cDNA was excised from pGEX-3X/PHIP$^{5-209}$ plasmid and subcloned into the corresponding sites within the pCAN vector. To craft a vector encoding full-length PHIP, a 2836 bp EcoRV/SpeI PHIP fragment was excised from pBlueScript/PHIP vector and subcloned into the compatible EcoRV/XbaI sites within the pCAN vector.

2.1.6 Adenoviral vectors - To construct a pAdTrack vector containing full hPHIP encoding sequences, it was necessary to first subclone HA-PHIP into pBlueScript plasmid vector. To accomplish the later, a fragment containing HA-epitope and a 621 bp fragment comprising amino acids 5-212 of PHIP was amplified from pCGN/HA-PHIP with sense 5'-ATGTCGACGCCACCATGGCTTCTAGCTATCC-3' and anti-sense 5'-CTATGACGTCAGGCATATCATGGTATTT-3' primers. A SalI/BstEII fragment excised from the PCR fragment was subcloned into pBlueScript/PHIP vector, which had been cleaved at the BstEII site within PHIP and SalI within the pBlueScript vector. To produce pAdTrack/HA-PHIP vector, a 2896 bp fragment comprising HA-PHIP was then excised from the pBlueScript/HA-PHIP by cleavage with SalI and NotI and subcloned into the corresponding sites within the pAdTrack vector.

To generate pAdEasy/HA-PHIP construct, recombinants were generated by co-electroporation of pAdTrack/HA-PHIP with PmeI-digested pAdEasy shuttle plasmid vector into BJ5183 bacterial cells.

2.1.7 Other constructs – The pcDNAI/HA-tagged p44 ^{MAPK} plasmid was a gift from Dr. J. Avruch. The pSG5p85SH2-N construct was a generous gift from Julian Downward (Imperial Cancer Research Fund, United Kingdom).

2.2 YEAST TWO-HYBRID ANALYSIS:

The PH domain from rat IRS-1 (residues 3-133) was fused to the LexA binding domain within the BTM116 vector and used as a 'bait' in a yeast two hybrid system to screen for interacting clones from a mouse 10.5 day embryonic cDNA library fused with the VP16-

activation domain of the yeast pVP16 vector. Transformation of the yeast strain L40 with yeast plasmids, and screening for positive colonies by β-galactosidase assays were done essentially as described by Sawka-Verhelle et al. (Sawka-Verhelle et al., 1996). A total of 89 positive clones were identified, most of which were represented at least twice, indicating that the screen was saturated. The clone, which displayed the strongest interaction with the IRS-1 PH domain, VP1.32 was representative of 18/89 positive clones.

2.3 MOUSE THYMUS AND HUMAN FETAL BRAIN cDNA LIBRARY SCREENING:

Lambda ZAP mouse thymus (a gift from Dr. Muller) and Stratagene fetal brain (a gift from Dr. Rommans) cDNA libraries were titered by making serial dilutions of the lambda phage in SM buffer (5.8 g NaCl, 2.0 g $MgSO_4$. $7H_2O$, 50 ml Tris-HCl PH 7.5, 5 ml of 2% gelatin per liter). One million recombinants were screened by plating 50,000 plaque forming units (pfu)/plate. Following plaque lifting onto Hybond N membranes (Amersham), the filters were placed in denaturation solution (1.5M NaCl, 0.5M NaOH) then neutralization solution (1.5M NaCl, 0.5M Tris-HCl PH 8) for 5-10 minutes each. Filters were then rinsed in 2X SSC and air-dried. UV light (auto cross-link at 1200 J/cm^2) was used to cross-link DNA to the filters.

The membranes were prehybridized in prewarmed 65°C Church's buffer (1% BSA, 7% SDS, 0.5M NaH_2PO_4 PH 7) containing 200 μg/ml Salmon Sperm DNA for 2 hours at 65°C. Hybridization to a ^{32}P-labeled PHIP probe (Roche Random Primer Labeling Kit) was allowed to take place over night at 65°C in the same Church buffer used for

prehybridization. The filters were washed two times in buffer A (0.5% BSA, 5% SDS, 40mM NaH_2PO_4, 1mM EDTA) and four times in Buffer B (1% BSA, 40mM NaH_2PO_4, 1 mM EDTA) for 20 minutes each at 65°C and exposed to film overnight at –80°C. Positive plaques were cored and eluted from the library over night at 4°C in 1 ml of SM buffer and 20 µl of chloroform. In order to get pure phage population, this screening procedure was repeated two more times.

The pBlueScript phagemids were excised from the Lambda vectors in vivo by the helper phage, R408. DNA was then prepared from single colonies and analysed by sequencing.

2.4 DNA ANAYSIS:

2.4.1 CsCl banding of plasmid DNA - To prepare large scale purified plasmid DNA, bacterial cells containing the plamsid were grown in 500 ml LB (5 grams NaCl, 20 grams yeast extract, 35 grams bactotryptone, pH 7, per one litre buffer) containing the appropriate antibiotics at 37°C for 16 hours with vigorous shaking. Bacterial cells were sedimented by spinning at 6,000 rpm at 4°C for 10 minutes. The pellet was resuspended in 7.5 ml of BDI (50 mM glucose, 25 mM Tris pH 8, 10 mM EDTA) and 2.5 ml of 20 mg/ml lysozyme in BDI. The mixture was vortexed and incubated for 5 minutes at room temperature (RT). To lyse the cells, 20 ml of freshly made BDII (0.2 N NaOH, 1% SDS) was added, gently mixed and incubated on ice for 10 minutes. Fifteen millilitres of ice-cold BDIII solution (3 M KOAc, 5 M OAc PH 4.8) was then added, gently mixed and incubated on ice for 10 minutes. To remove cellular debris, the lysate was centrifuged at 7,000 rpm for 45 minutes. Plasmid DNA was then precipitated from the supernatant by

adding 28 ml of isopropanol per 42 ml of lysate. After 5-minute incubation on ice, the lysate was spun at 4,200 rpm at 4°C for 15 minutes. Plasmid DNA pellet was washed with 70% ethanol, air-dried and dissolved in 10 ml of TE buffer (10 mM Tris-HCl PH 8, 1 mM EDTA). Ten grams of CsCl and 200 µl of ethidium bromide (10 mg/ml) were added and the sample was spun in sealed polyallomer tubes (Beckman) at 60,000 rpm for 20 hours. Purified DNA band was extracted and diluted with three volumes of TE buffer. To remove ethidium bromide from DNA, equal volumes of water-saturated butanol was added, vortexed and centrifuged at 2,000 rpm for 5 minutes. Top red layer containing ethidium bromide was removed and this butanol extraction was repeated till all traces of red ethidium bromide were removed. Pure DNA was reprecipitated by adding 2.5 volumes of 100% ethanol and 1/10 volume of 3 M NaOAc and sedimented by spinning at 3,000 rpm for 30 minutes. The DNA pellet was washed with 70% ethanol, air-dried, dissolved in 500 µl of 10 mM Tris PH 8, and stored at –20°C.

2.4.2 Generation of recombinant DNA - To generate recombinant pAdEasy/HA-PHIP plasmid DNA, one-fifth of a minipreped AdEasy shuttle plasmid was digested with PmeI restriction enzyme. After digestion, DNAs were phenol-chloroform extracted, ethanol precipitated, and resuspended in 6 µl of water. To allow recombination to occur, a mixture of 1 µl of pAdTrack/HA-PHIP (100 ng/ml) plasmid and the PmeI-digested AdEasy vector was co-transformed into 20 µl of electrocompetent *E-Coli* BJ5183 bacterial cells by electroporation. Electroporation was performed in 2 mm cuvettes at 2,500 V, 200 Ohms, and 25 µFD in a Bio-Rad Gene Pulser electroporator. The transformation mixture was resuspended in 500 µl of LB and

incubated at 37°C for 15-20 minutes. The mixture was plated on 5 LB plates containing 25 μg/ml Kanamycin and incubated at 37°C overnight. Ten of the smallest colonies were picked and expanded in 2 ml LB containing 25 μg/ml Kanamycin at 37°C for 15 hours with vigorous shaking. DNA was prepared and digested with PacI enzyme to identify the positive clones. Two of the positive clones (clones 3 and 4), which yielded a large fragment of near 30 kb and a smaller fragment of 3 or 4 kb were re-transformed into DH10B cells. Purified plasmid DNAs were generated by CsCl-banding method as described in section 2.4.2 and used for viral production.

2.5 RNA ANALYSIS:

2.5.1 RNA isolation - RNA was prepared from different adult mouse tissues by the TRIzol (Gibco BRL) method. 50-100 mg of tissue samples were homogenized in 1 ml of TRIzol reagent. The homogenized samples were incubated for 5 minutes at RT before 200 μl of chloroform was added. Tubes were capped and shaked vigorously for 15-30 seconds and incubated for 2-3 minutes at RT. The samples were centrifuged at 12,000 rpm for 15 minutes at 4°C. Following centrifugation, the upper aqueous phase was transferred to a fresh tube and RNA was precipitated by adding 0.5 ml of isopropyl alcohol per 1 ml of the TRIzol reagent used for the initial homogenization. The RNA pellet was washed with 75% ethanol, air-dried, dissolved in DEPC (diethyl pyrocarbonate)-water and stored at –80°C.

2.5.2 Northern blot analysis - Fifteen micrograms of total RNA from various adult mouse tissues were resuspended in 1X MOPS (20 mM MOPS, 5 mM NaOAc, 1 mM EDTA, PH 7), 6.5% formaldehyde and 50% deionized formamide. The mixture was incubated at 55°C for 15 minutes, followed by a quick chill on ice. Loading buffer (5% glycerol, 1 mM EDTA, 0.25% bromophenol blue) was then added and samples were separated on a 1.2% formaldehyde-agarose gel. The RNA was transferred from the gel onto a Zeta-probe blotting membrane (Amersham) in 10X SSC by overnight capillary action. The RNA was crosslinked to the membrane using UV Stratalinker (Gibco BRL). The membrane was hybridized with ^{32}P-labeled probes of interest as previously described in section 2.3.

2.5.3 RT-PCR analysis – To generate cDNA from various mouse tissues, 2.5 pmols of hexameric random primers (Promega) were added to 1 μg of total RNA and optimised to a volume of 15.5 μl with DEPC-H_2O. The mixture was incubated at 70°C for 10 minutes to denature RNA and quickly chilled on ice. Optimal amounts of 10X PCR buffer (200 mM Tris-HCl PH 8.4, 500 mM KCl), 25 mM $MgCl_2$, 10 mM dNTPs mix (dATP, dCTP, dGTP, dTTP) and 0.1 M DTT was then added to achieve final concentrations of 1X, 2.5 mM, 400 μM and 10 mM, respectively. The reaction tubes were pre-warmed to 42°C for 2 minutes prior to the addition of 1 μl Superscript II reverse transcriptase (Gibco BRL) and were subsequently allowed to proceed for 1 hour at 42°C. The reverse transcription reaction was terminated at 70°C for 15 minutes followed by addition of 1 μl of RNase mix and incubation at 37°C for 30 minutes. One microliter of the cDNA products was used as template in various polymerase chain reactions (PCR).

All PCRs described in this section and section 2.6 were performed in 1X PCR buffer, 200 μM dNTP mix, 1.5 mM $MgCl_2$, 50 pmol of each of the sense and anti-sense primers and 5 units of Taq DNA polymerise (Roche). Each PCR was conducted in a 50 μl reaction volume and maintained on ice prior to transfer to thermocycler (VWR), preheated at 95°C for two minutes. To allow cDNA template denaturation, reaction tubes were incubated at 95°C for five minutes. Thirty cycles of PCR amplification was then performed by incubation at 95°C for 1 minute, 45 seconds at the appropriate annealing temperature that varied between different primer sets, and extension at 72°C for 1.5 minutes. An additional incubation at 72°C for 7 minutes was included, followed by the storage at 4°C. The PCR reactions, which yielded the 450 bp PHIP, 500 bp 5'UTR or 610 bp NDRP fragments were performed with the following sets of primers. For PHIP, primer (1) 5'-GAAATACCATGATATGCCTGACGTCATAG-3' and primer (2) 5'-CGCAATATCTAGTGTCATCAGCTG-3'; for 5'UTR, primer (3) 5'-GGAAAAGCTGAATAACTTTCGTCACTT-3' and primer (4) 5'-GTCAGGCATATCATGGTATTTCATGGT-3'; for NDRP, primer (5) 5'-GGACAGCAGATGCTGGAATTAACTTG-3' and primer (4) were used to amplify the corresponding regions.

2.6 5' RACE (RAPID AMPLIFICATION OF cDNA ENDS):

5' RACE was performed as per manufacturer's instructions (Gibco BRL). First strand cDNA was synthesized using 1 μg of total RNA prepared from adult mouse thymus and two and half pmol of PHIP specific primer 5'-GTCAGGCATATCATGGTATTTCATGGT-3' as previously described in section 2.5.3. cDNA was purified using a GlassMax DNA isolation spin cartridge and dC-tailed with Terminal Deoxynucleotidyl Transferase

(TDT) enzyme. Subsequent PCR amplification of dC-tailed cDNA using an abridged anchor primer, 5'-GGCCACGCGTCGACTAGTACGGGIIGGGIIGGGIIG-3' (provided by the kit), which binds to poly dC tail and a PHIP specific nested primer, 5'-CCTTAGTTCCATCTTATGCCATGGCTG-3' allowed amplification of 5'end PHIP sequences. Another round of amplification was then performed with a universal primer, AUAP, 5'-GGCCACGCGTCGACTAGTAC-3' (provided by the kit), ant the third nested PHIP specific primer, 5'-CCAAGCTGAAGGCAACCACTC-3' to ensure amplification of PHIP specific products. The PCR products of the third amplification were subcloned into TA cloning vector followed by bacterial transformation into DH5α cells. DNA was prepared from random single transformed bacterial colonies and analysed by sequencing.

2.7 ANTIBODIES

2.7.1 Anti-PHIP antibody generation - GST-PHIP fusion proteins containing PHIP PH binding region (residues 5-209) were generated from the pGEX-3X/PHIP$^{5-209}$ plasmid previously described in section 2.1.2. The plasmid DNA was transformed into RR1 bacterial cells and a single ampicillin resistant colony was selected and expanded to log phase (A_{600}=0.9) in 500 ml LB containing 100 μg/ml ampicillin. Expression of the fusion protein was induced by incubation of the culture with 1 mM IPTG (Bioshop) for 4 hours at 37°C with vigorous shaking. The bacteria were then pelleted by centrifugation at 5000 rpm for 10 minutes at 4°C. The bacterial cells were resuspended in 10 ml of ice-cold PBS buffer (137 mM NaCl, 2.7 mM KCl, 8.2 mM Na_2HPO_4, 1.5 mM KH_2PO_4) containing 1% tween 20, 1% triton-X100, 10 μg/ml aprotinin, 10 μg/ml leupeptin, and 10

mM DTT and sonicated on ice with three strokes, 20 seconds at 40 mAmps each. To remove the bacterial debris, the lysate was subjected to centrifugation at 10,000 rpm at 4°C for 10 minutes. The GST-PHIP fusion protein was purified from the clear supernatant using 1 ml of 50% Glutathione Sepharose bead mixture (Sigma) for 30 minutes at 4°C. The GST-PHIP proteins bound to the beads were washed with 30 bed volumes of PBS and eluted with 2 mls of elution buffer (20 mM reduced glutathione, 50 mM Tris-HCl PH 8, 150 mM NaCl). The purity and the concentration of the purified fusion protein were assessed by Coomassie Blue stain. The expressed fusion protein was approximately 45 KDa, corresponding to GST and residues 5-209 of PHIP.

The fusion protein was injected into two SPF rabbits (A and B) to generate the rabbit polyclonal antisera. The rabbits were originally injected subcutaneously with 500 μg of fusion protein in Freund's complete adjuvant (Sigma) at a 1:1 volume. The animals were subsequently given three more injections, at monthly intervals, with 100-200 μg fusion protein in Freund's incomplete adjuvant (Sigma) at a 1:1 volume. The animals were bled after two weeks of every Freund's incomplete injection; serum was collected and stored in 1 ml aliquots at –80°C. Rabbit A anti-PHIP sera was used for all the experiments performed for this study. Prior to the use of every newly thawed serum vial, the crude serum was cleared of anti-GST antibodies by incubation with 500 μg of purified GST protein bound to the Glutathione Sepharose beads for two hours at 4°C. The serum containing the anti-PHIP antibodies was then used at a 1:200 dilution in immunoblots and 10 μl/mg total lysate in immunoprecipitations.

2.7.2 Other antibodies - Monoclonal anti-IRS-1 and polyclonal anti-IRS-1^{PCT} (generated against a 16 amino acid pre C-terminal polypeptide sequence) were purchased from Santa Cruz and Upstate Biotechnology Inc. (UBI), respectively. Anti-MAPK (p42/44) and anti-phosphotyrosine, PY20, antibodies were from New England Biolabs (NEB). Anti-HA antibodies were purchased from Babco.

Anti-IRS-1^{PH} (generated against the IRS-1 PH domain) and anti-IRS-2 antibodies were gifts from Dr. M. F. White, anti-IR and anti-Shc antibodies were generously provided by Dr. K. Siddle and Dr. J. McGlade, respectively.

Monoclonal anti-HA (12CA5) was from Babco and anti-Myc (9E10) and monoclonal IRS-1 (E-12) antibodies were from Santa Cruz Biotechnology. Anti-CAT antibodies and mouse antibody to BrdU were purchased from 5 prime-3 prime Inc. and Sigma, respectively. Rhodamine-conjugated phalloidin was obtained from Molecular Probes. Anti-transferrin receptor antibody is purchased from Zymed.

2.8 IN-VITRO TRANSCRIPTION/TRANSLATION ASSAY:

One microgram of purified EcoRI digested DNA fragment from pCAN/DN-PHIP was used in an in-vitro transcription/translation assay (Promega TNT T7 Coupled Reticulocyte Lysate System). The reaction mixture contained 25 µl TNT rabbit reticulocyte lysate, 2 µl TNT reaction buffer, 1 µl T7 RNA Polymerase, 1 µl amino acid mixture lacking methionine, 5 µl [^{35}S]Methionine (10 mCi/ml), 1 µl RNasin (40 units/µl), DNA template and Nuclease-free water to volume of 50 µl. The reaction mixture was incubated at 30°C for 90 minutes. The [^{35}S]Methionine labeled translation products were immunoprecipitated using preimmune serum or anti-PHIP antibodies and separated on a

10% SDS-polyacrylamide gel. The gel was fixed in a solution composed of isopropanol, water and acetic acid in 25:15:10 ratios for 30 minutes. The gel was then soaked in Amplify™ (Amersham Life Science) solution for 30 minutes and dried under vacuum at 60-80°C. The gel was later exposed to X-ray film at –80°C.

2.9 CELL CULTURE:

2.9.1 Cell lines – All cells were maintained in an incubator containing 5% CO_2 under 80% humidity at 37°C. Rat-1 fibroblasts, 293 human embryonic kidney cells, NIH/IR (NIH/3T3 mouse fibroblasts stably overexpressing the human insulin receptor), 3T3-L1 mouse preadipocytes and COS-1/7 monkey kidney epithelial cell lines were maintained in Dulbecco's Modified Eagle's Medium (DMEM) supplemented with 10% heat-inactivated fetal bovine serum (HI-FBS), 2 mM glutamine, 100 IU/ml penicillin-G and 100 μg of streptomycin (1% Pen/Strep). The human multiple myeloma cell line U266 was cultured in RPMI medium 1640 supplemented with the same reagents. L6GLUT4myc (L6 mouse myoblasts stably overexpressing myc-tagged GLUT4 glucose transporter in which myc-epitope is inserted into an exofacial GLUT4 domain (Kanai et al., 1993b; Randhawa et al., 2000)) were maintained in α-Minimum Essential Medium (α-MEM) supplemented with the same reagents. In cases of serum starvation, cells were cultured in DMEM alone for 16 to 18 hours and then stimulated with the indicated doses of insulin (Sigma) at 37°C. L6GLUT4myc cells were often starved in α-MEM alone for only 4 hours.

2.9.2 Differentiation of 3T3-L1 cells – $4x10^5$ 3T3-L1 fibroblasts were seeded in 6-cm^2 dishes containing DMEM medium supplemented with 10% HI-FBS and 1% Pen/Strep and incubated in a 37°C, 5% CO_2 humidified incubator to reach confluency (three days). At this point, the cell number had increased by a factor of 10 to $4x10^6$, which was considered as the standard for subsequent calculations. Two days after confluency, the cells media were changed to DMEM containing 10% HI-FBS, 1% Pen/Strep, 390 ng/ml Dexamethasone (Sigma), 100 µg/ml IBMX (Sigma) and 5 µg/ml insulin and incubated in the same environment for another two days. Next, the cells media were changed to DMEM supplemented with 10% HI-FBS, 1% Pen/Strep and 5 µg/ml insulin alone and continued to differentiate for another two days. Finally, the differentiation media was replaced by the regular growth media, DMEM containing 10% HI-FBS, 1% Pen/Strep, and incubated in the same environment until full differentiation was achieved (two-four days). Differentiation of 3T3-L1 fibroblasts into adipocytes was marked by the appearance of multiple fat droplets in the cells' cytoplasm around day 9, which often joined and formed bigger droplets by the end of the differentiation period (11-13 days).

2.9.3 Differentiation of L6GLUT4myc cells – $4x10^5$ cells were seeded in 6-cm^2 dishes containing α-MEM medium supplemented with 2% HI-FBS and 1% Pen/Strep and incubated in a 37°C, 5% CO_2 humidified incubator for nine days. Media were changed every two days for up to 9 days. The number of cells increased by a factor 8 to $3x10^6$ cells/plate, during this period and was considered as the standard for subsequent

calculations. Complete differentiation is detected by the formation of the multinuclear cells, which display long tube morphology packed against one another.

2.10 IMMUNOPRECIPITATION AND IMMUNOBLOTTING:

Cells were lysed in PLC lysis buffer containing 50 mM Hepes, pH 7.5, 150 mM NaCl, 10% glycerol, 1% NP-40, 1.5 mM $MgCl_2$, 1 mM EGTA, 10 mM sodium pyruvate, 10 mM sodium fluoride, 10 μM sodium orthophosphate, 1 mM PMSF, 10 μg/ml aprotinin, 10 μg/ml leupeptin. The extracts were clarified by centrifugation at 11,000 rpm for 10 minutes at 4°C. Lysates were immunoprecipitated with either the corresponding antibodies or immobilized beads for 2 hours at 4°C, separated on SDS polyacrylamide gels and transferred to polyvinylidene difluoride (PVDF) membranes and immunoblotted with the corresponding antibodies. Whole cell lysates (WCL) were prepared by harvesting cells 48 hours after transfection with hot 2X SDS sample buffer. Fifty to two hundred microgram of lysate was resolved by SDS-PAGE and probed with the corresponding antibodies as indicated. COS and 293 cell lines were transfected with the indicated expression plasmids using the calcium phosphate precipitation method as described in section 2.22.2 Rat-1 cells were transfected using GenePorter 2 (Gene Therapy Systems) as per manufacturer's instructions.

2.11 IN-VITRO BINDING ASSAYS:

L40 yeast cells expressing various HA-tagged PH domains (rat IRS-1, mouse SOS1, human RasGAP, and mouse Ect-2) were lysed with acid-washed beads in 1 ml of distilled water containing 0.1 mM PMSF as previously described (Rozakis-Adcock et al.,

1993). Clarified cell lysates were incubated with ~5 μg of GST-PHIP (PBR) proteins for 90 minutes at 4°C. For pull-down experiments with IRS-1 PH domain mutants, COS-1 cell lysates transiently transfected with plasmids expressing HA-tagged PH^{WT} , PH^{NT} , PH^{CT} , PH^{W106A} were mixed with either GST or GST-PHIP (PBR) proteins for 2 hours at 4°C. Proteins bound to GST or GST-PBR were resolved by SDS-PAGE and analyzed by immunoblotting with anti-HA antibodies.

2.12 IN-VITRO MAPK ASSAY:

COS cells transiently co-transfected by Calcium Phosphate precipitation method (Section 2.22.2) with HA-$p44^{MAPK}$ and either pCGN control vector or pCGN/DN-PHIP, were stimulated with or without insulin (100 nM) for 5 minutes and lysed in PLC lysis buffer. Anti-HA immunoprecipitates were incubated for 20 minutes at 30°C in a 30 μl reaction mixture containing 10 mM $MgCl_2$, 50 mM Tris pH 7.4, 2 mM EGTA, 1 mM DTT, 30 μM cold ATP, and 5 μCi of [γ-^{32}P]ATP. Twenty microgram of MBP (Sigma) was used as a substrate. The reaction was stopped by 6X SDS sample buffer and the supernatant was resolved by 12% SDS-PAGE. The top portion of the gel was transferred to a PVDF membrane for immunoblotting with anti-MAPK antibodies, and the bottom portion containing labeled MBP was detected by autoradiography.

2.13 PI 3-KINASE ASSAY:

COS cells growing in 6-cm^2 tissue culture dishes were transiently transfected by Calcium Phosphate precipitation method (Section 2.22.2) with either pCGN control vector,

pCGN/DN-PHIP, pCGN-PHIP or pCGN-IRS-1. Twenty-four hours after transfection, the cells were starved for 16 hours at 37°C incubator. Serum-starved cells were either left unstimulated or stimulated with insulin (100 nM) for 5 minutes and lysed in PLC lysis buffer. Untransfected NIH/IR cells were used as positive control for the kinase assay. Immobilized anti-IRS-1^{PCT} complexes, immunoprecipitated from the cell lysates were subjected to the kinase assay. The reaction was initiated by adding 80 µl of the reaction mixture containing 55 µl of Kinase Buffer (10 mM Tris PH 7.5, 100 mM NaCl, 1 mM $MgCl_2$, 0.1 mM Sodium Orthovanadate), 13.8 mM $MgCl_2$, 10 µl Phosphatidylinositol (20 mg/ml, Avanti Polar-Lipids Inc.), 0.156 mM ATP and 5 µCi [$^{32}\gamma$P]ATP, and incubated at 30°C for 15 minutes with gentle shaking. The reaction was terminated by adding 20 µl of 8 M HCl and 160 µl of $CHCl_3$:MeOH (1:1). Fifty microliter of the organic phase (Bottom portion) was spotted on a TLC plate and the lipid products were separated by incubation in the running solvent ($CHCl_3$: MeOH: H_2O: NH_4PH = 60: 47: 11.6: 2 (ml)) for 3-4 hours. The plate was dried in the fume hood and exposed in PhosphoImager cassette over night.

2.14 REPORTER GENE ASSAYS:

COS-1 cells growing in 6-cm^2 dishes were transiently transfected by Calcium Phosphate precipitation method (Section 2.22.2) in triplicate samples with 5X SRE-fos luciferase reporter gene (5X SRE-LUC) and the indicated plasmids. Twenty-four hours after transfection, the cells were serum starved for 16 hours at 37°C. Serum-starved cells were either left untreated or treated with Mek-1 inhibitor (50 µM, NEB) for 2 hours. Cells were incubated for 10 hours with or without insulin (0.2 µM, Sigma). Cells were then

rinsed with PBS and lysed in 200 µl of 25 mM Tricine PH 7.8 lysis buffer (Roche) containing Noniodet P-40, glycerol, DTT, and EDTA for 15 minutes at RT. To remove cellular debris, solubilized cells were spun for 10 seconds at maximum speed. To measure luciferase activity, 50 µg of cleared lysate was added to 360 µl of luciferase assay buffer (25 mM glycylglycine PH 7.8, 15 mM potassium phosphate PH 7.8, 15 mM $MgSO_4$, 4 mM EGTA, 2 mM ATP, 1 mM DTT) and placed in a luminometer cuvette. The cuvette was placed in luminometer chamber and 100 µl of diluted luciferin (Sigma) solution (1:5 in 25 mM glycylglycine PH 7.8) was added in dark and light output was immediately measured for 20 seconds at RT. Three separate measurements were taken for each lysate and the average was plotted on a graph.

2.15 MICROINJECTION ASSAYS:

NIH/IR or Rat-1 fibroblasts plated onto gridded glass cover slips and serum starved for 30 hours, were microinjected with the indicated plasmids with or without 5X serum response element - chroramphenicol acetyltransferase (SRE-CAT) reporter gene as previously described (Soisson et al., 1998). Briefly, the plasmids were resuspended in the microinjection buffer (20 mM Tris-acetate pH 7.4, 20 mM NaCl, 1 mM $MgCl_2$, 0.1 mM EDTA, 5 mM BME, and 150 mM KCl) and injected into a total of 50 cells for each condition. For the reporter assay, 2 hours after injection, cells were treated with 0.5 µM insulin or serum (20%) as indicated and incubated for 5 hours before fixation. For the mitogenesis assay, 3 hours after injection, cells were treated with 10 µM BrdU (Roche), followed by addition of either 0.5 µM insulin or 20% serum. Cells were incubated for 36 hours before fixation. Anti-HA and anti-CAT antibodies were utilised to detect ectopic

PHIP mutants and CAT expression, respectively. Anti-BrdU antibodies were used to monitor BrdU incorporation into the newly synthesized DNA. In DNA synthesis experiments, rabbit anti-rat IgG was coinjected with the indicated plasmids and was used to detect microinjected cells. The values represent average of 5 independent experiments. The results are plotted in graphs and are expressed as % of maximum, which represented the average number of cells either expressing SRE-CAT or incorporating BrdU upon serum stimulation.

2.16 GLUT4MYC TRANSLOCATION ASSAY:

L6GLUT4myc stable cell lines were generated as previously described (Kanai et al., 1993b; Kishi et al., 1998; Mitsumoto et al., 1991). Cells growing on cover slips were cotransfected with the indicated HA-epitope tagged protein encoding constructs (0.9 μg) and 0.3 μg of enhanced green fluorescent protein (EGFP, Clontech) expressing plasmid according to the Effectene protocol manual (Qiagen). Forty-three hours after transfection, cells were deprived of serum in culture medium for 3 hours and were left either untreated or treated with 100 nM insulin for 20 minutes. Transfected cells were monitored by GFP expression. Indirect immunofluorescence for expression of cDNA constructs and GLUT4myc translocation was carried out on intact cells as previously described (Randhawa et al., 2000). Briefly, transfected cells were rinsed three times with ice-cold PBS^M (100 mM NaCl, 1 mM $CaCl_2$, 1 mM $MgCl_2$, 50 mM NaH_2PO_4/Na_2HPO_4, pH 7.4) and fixed with 3% paraformaldehyde in PBS^M for 2 minutes, followed by incubation with 100 nM glycine in PBS^M for 10 minutes. Cells were then rinsed with

PBS^M three times and blocked with 5% goat serum in PBS^M for 10 minutes. The blocking serum was then completely removed and 50 µl of the primary antibody, namely, anti-HA (1:200) and anti-Myc (1:100) were added to detect the cDNA constructs and GLUT4myc expression, respectively, and incubated for 1 hour at RT. Cells were rinsed with PBS^M three times and incubated with the secondary antibody (FITC-conjugated goat anti-mouse 1:1000 for anti-HA and Cy3-conjugated goat anti-mouse IgG 1:1000 for anti-Myc) in PBS^M for 1 hour. Rinsed cover slips were mounted and analyzed with the Leica TCS 4D fluorescence microscope (Leica Mikroscoipe Systeme GmbH, Wetzlar, Germany). Several representative images of at least three separate experiments were quantified with the use of NIH (National Institute of Health) image software.

2.17 ACTIN LABELING:

Growing L6GLUT4myc cells on cover slips were cotransfected with the indicated plasmids and EGFP expressing construct as described in section 2.16. The cells were either left untreated or treated with 100 nM of insulin for 10 minutes following serum deprivation. Cells were rinsed with ice-cold PBS^M before fixing with 3% paraformaldehyde in PBS^M for 30 minutes (initiated at 4°C for 5 minutes and shifted immediately to room temperature). The rest of the procedure was performed at room temperature. The cells were the rinsed once with PBS^M, and unreacted fixative was quenched with 100 nM glycine in PBS^M for 10 minutes. Permeabilized cells (0.1% Triton X-100 in PBS^M for 3 minutes) were washed quickly with PBS^M and blocked with 5% goat serum in PBS^M for 10 minutes. Transfected cells were monitored by GFP expression. To detect filamentous actin, cells were incubated in the dark with

Rhodamine-conjugated phalloidin for 1 hour. Rinsed cover slips were then mounted and analyzed with the Leica TCS 4D fluorescence microscope (Leica Mikroscoipe Systeme GmbH, Wetzlar, Germany).

2.18 INDIRECT IMMUNOFLURESCENCE ANALYSIS:

Cells growing on cover slips were rinsed with PBS twice and fixed with 4% paraformaldehyde in phosphate buffer PH 7.4 for 1 hr at RT. Cells were then rinsed with PBS three times and permeabilized with 0.2% triton X100 for 5 minutes. Following three PBS rinses cells were blocked with 1/20 normal goat serum in PBS for 30 minutes. The blocking serum was then completely removed and 50 µl of the primary antibody with appropriate dilution was added and incubated for 1 hr at RT. For polyclonal anti-PHIP serum and monoclonal anti-IRS-1, 1:10 and 1:100 dilutions were used, respectively. Cells were rinsed with PBS three times and incubated with the secondary antibody in 1/200 dilution in PBS for 30 minutes. The secondary antibodies used include Alexa 350 (blue), 488 (green) and 546 (red) nm anti-mouse and anti-rabbit antibodies. Rinsed cover slips were mounted and analyzed with the Leica TCS 4D fluorescence microscope (Leica Mikroscoipe Systeme GmbH, Wetzlar, Germany). For negative control, either rabbit pre-immune sera were used or no primary antibody was added.

2.19 SUBCELLULAR FRACTIONATION ASSAY:

L6GLUT4myc cells growing in 10-cm^2 dishes (three dishes/condition) were serum starved for 4-6 hours and left untreated or treated with 100 nM of insulin for 20 minutes. Cell fractions were then prepared as previously described (Heller-Harrison et al., 1995)

with slight modifications. All procedures were performed at 0-4°C. Briefly, cells were washed and homogenized in ice-cold buffer A containing 20 mM Tris-HCl pH 7.5, 1 mM EDTA, 255 mM sucrose, 1 mM PMSF, 10 mM NaF, 100 μM Na_3VO_4, 1 mM NaPPi, 10 μg/ml aprotinin, and 10 μg/ml leupeptin for twenty strokes with a motor-driven Teflon/glass homogenizer. The homogenate was centrifuged at 11,000 rpm for 20 minutes. The pellet was resuspended in ice-cold buffer A and homogenized as describe above. The homogenate was slowly layered onto a sucrose cushion (20 mM Tris-HCl pH 7.5, 1 mM EDTA, 1.12 M sucrose) and centrifuged at 48,000 rpm for 1 hour. The white plasma membrane band was then collected from the sucrose cushion interface and following dilution (1:5) in ice-cold buffer A was recentrifuged at 53,000 rpm for 1 hour. The plasma membrane pellet was dissolved in hot 2X SDS sample buffer. The supernatant from the original centrifugation step was centrifuged at 53,000 rpm to sediment the low-density membrane (LDM) pellet. The final LDM pellet was resuspended in hot 2X SDS sample buffer. The supernatant containing cytosolic fraction from the latter centrifugation step was concentrated using a UFV2BGC40 filter apparatus (Millipore Corp.). Fifty microgram of protein from each fraction was separated on a SDS-PAGE and immunoblotting with the corresponding antibody as previously described in section 2.10.

2.20 IN-VIVO ^{35}S METABOLIC LABELING OF CELLS:

L6GLUT4myc cells growing in 10-cm^2 dishes were incubated for 2 hours in DMEM lacking methionine amino acid (Gibco BRL) at in a 37°C, 5% CO_2 humidified incubator. Pro-Mix [^{35}S] Methionine (Amersham Pharmacia Biotech) was then added at 100 μCi/ml

and cells were incubated for 4 hours under the same environmental conditions. The cells were then treated with 100 nM of insulin for 10 minutes and lysed in ice-cold PLC lysis buffer. Immunoprecipitations with the indicated antibodies were performed as previously described in section 2.10. To confirm the authenticity of the anti-PHIP immunoprecipitated proteins, 10 µl of anti-PHIP serum diluted in 100 µl of PLC buffer was pre-cleared with 100 µg of purified GST-PHIP or control GST proteins. The resulting anti-PHIP pre-cleared serum was used in an immunoprecipitation assay as control. Preimmune serum from the same rabbit (A) was used as negative control in immunoprecipitation of labeled proteins. Immunoprecipitated proteins were separated on a 7.5% SDS-polyacrylamide gel and processed for diphenyloxazole (PPO) fluorography. The gel was first rinsed and then incubated in 5 volumes of dimethylsulfoxide (DMSO) for 45 minutes at RT. It was then incubated in 5 gel volumes of 22% (wt/vol) PPO in DMSO for another 45 minutes at RT. The PPO-impregnated gel was placed under a gentle flow of water for 1-2 hours and subsequently dried under vacuum at 60-80°C. Fluorographed gel was exposed on X-ray film for 16 hours at –80°C.

2.21 ADENOVIRUS ANALYSIS

2.21.1 Adenoviral production - Seventy-per-cent confluent 293 cells growing in 10-cm^2 dishes in a 37°C, 5% CO_2 humidified incubator, were transfected with 10 µg of purified PacI-digested AdEasy/HA-PHIP plasmid DNA from clone 3, by calcium phosphate precipitation method as described in section 2.22.2. Transfections and viral production, which was driven by CMV promoter in pAdEasy vector was monitored by

GFP expression. Seven to ten days following transfection, cells were scraped off the plates and transferred to 50 ml conical tubes. Cells were centrifuged at 2,000 rpm for 5 minutes and the pellet was resuspended in 2 ml PBS buffer. To release the viruses, the cells were repeatedly frozen in dry ice/methanol bath, thawed in a 37°C water bath and vortexed. The samples were briefly spun and the supernatants were subsequently used to infect 293 cells. To amplify the virus, 70% confluent 293 cells growing in 10-cm^2 dishes were infected with 1 ml of viral supernatant for 30 minutes followed by addition of 9 ml of DMEM containing the supplements. Three to five days post-infection, when 50% of the cells were detached, cells were scraped and viral supernatant was prepared as described above. The viral supernatant was stored at –20°C. Control viruses of empty pAdEasy vector were prepared in the same manner.

2.21.2 Preparation of high titre viral stocks - Twenty, 90% confluent plates of 293 cells were infected with 1 ml of control or HA-PHIP viral supernatant as previously described in section 2.21.1. After 4-5 days, when all the cells had rounded up and 50% were detached, cells were harvested and pelleted. Cell pellets were resuspended in 8 ml sterile PBS and four cycles of freeze/thaw/vortex were performed to release the viruses as previously described in section 2.21.1. Cell lysates were centrifuged at 6,000 rpm for 5 minutes to remove the cellular debris. Four grams of CsCl was added to the cleared lysate, mixed well and transferred to polyallomer tubes; sealed tubes were then centrifuged at 32,000 rpm at 10°C for 16-20 hours. The viral fraction was collected, mixed with equal volume of 2X storage buffer (10 mM Tris PH 8, 100 mM NaCl, 0.1% BSA, 50% glycerol, filter sterilized) and stored at –20°C. To measure the viral titre, 15

µl of virus solution was mixed with 15 µl of blank solution (1.35 g/ml CsCl mixed with equal volume of 2X storage buffer) plus 100 µl TE/0.1% SDS. The OD was measured at A_{260} nm. One A_{260} unit contains ~50 infectious viral particles. The titers obtained for control and HA-PHIP viruses were $6x10^{11}$ and $3.6x10^{11}$ pfu/ml, respectively.

2.22 EXOGENOUS DNA INTRODUCTION INTO CELLS:

2.22.1 Prokaryotic cell transformation - Fifty to hundred nanograms of DNA was added to 50 µl competent bacterial cells and incubated on ice for 20 minutes. Bacterial cells used in this series of studies included DH5α and RR1. The samples were heat-shocked for 45 seconds at 42°C and placed on ice immediately. After 1 minute, 150 µl of LB was added and the cells were spread on LB plates containing the appropriate antibiotics. The plates were incubated at 37°C overnight to allow growth of single bacterial colonies carrying the plasmid of interest.

2.22.2 Eukaryotic cell transfection - *Calcium Phosphate Precipitation Method -* Ten to twenty micrograms of purified DNA was mixed with 1 ml of 1X HBS (21 mM HEPES, 0.137 M NaCl, 5 mM KCl, 0.7 mM Na_2HPO_4, 5.5 mM glucose, PH 7) in polystyrene tubes. To this mixture, 50 µl of sterile 2.5 M $CaCl_2$ was added drop wise with gentle shaking and incubated for 30 minutes at RT. These amounts of reagents are

sufficient to transfect one 10-cm^2 or two 6-cm^2 plates of 70% confluent adherent mammalian cells. One hour prior to transfection, cells media were replaced by 9 ml and 4.5 ml of fresh medium on 10-cm^2 and 6-cm^2, respectively. The transfection mixture was then added to the cells and incubated in a 37°C, 5% CO_2 humidified incubator. In the case of 293 cells, transfection continued for 16 hours before the transfection medium was replaced by fresh DMEM medium. For Cos cells, 5 hours after transfection, cells were shocked with 10% of DMSO in DMEM medium. Following the transfection medium removal, 1 ml or 2 ml of 10% DMSO solution was added to 10-cm^2 or 6-cm^2, respectively and incubated for 3 minutes at RT. The cells were washed twice with PBS and fresh medium was added, followed by further incubation in a 37°C, 5% CO_2 humidified incubator.

Other methods of transfection used in this series experiments such as Effectene (Quigen), Geneporter (Gene Therapy Systems) or Lipofectamine (Gibco BRL) were performed as per manufacturer's instructions.

2.22.3 Eukaryotic cell transduction - One day prior to infections, $4x10^5$ L6GLUT4myc myoblasts were seeded in 6-cm^2 dishes containing 5 ml of media supplemented with 10% HI-FBS and 1% Pen/Strep and incubated in a 37°C, 5% CO_2 humidified incubator overnight. $4x10^9$ control or HA-PHIP encoding adenoviral particles were diluted in 1 ml of α-MEM containing 2% HI-FBS and 1% Pen/Strep to achieve an MOI of 5000. Growth media were removed and the viral mixtures were overlayed on the cells and incubated for 24 hours with gentle shaking in a 37°C, 5% CO_2 humidified incubator. Four milliliter of fresh medium was added following by 24 hours of

incubation under the same environmental conditions prior to assaying. In the case of L6GLUT4myc myotubes or 3T3-L1 adipocytes, $4x10^5$ undifferentiated cells were seeded and allowed to differentiate as previously described in section 2.9.2 and 2.9.3. To achieve an MOI of 5000, $1.5\text{-}2x10^{10}$ viral particles were added and infections were proceeded as described above. The efficiency of infectivity detected by monitoring the number of GFP positive cells was estimated over 80%. In experiments where serum starvation was required, 48 hours after infection of L6GLUT4myc cells or 3T3-L1 adipocytes, infection media were replaced with fresh media containing no supplements and incubated under the same environmental conditions for 3 or 16 hours, respectively, prior to assaying.

CHAPTER THREE

ISOLATION AND INITIAL BIOCHEMICAL CHARACTERIZATION OF PHIP

3.1 INTRODUCTION

Studies have shown that IRS-1 proteins are enriched in intracellular low-density microsomes (LDM) (Heller-Harrison et al., 1995). An important question that remains to be addressed is the mechanism by which LDM-associated IRS-1 interacts with the activated IR, an integral component of the plasma membrane. The PTB domain of IRS-1 can bind directly to phosphorylated Tyr^{960} within the NPEY motif in the juxtamembrane region of the activated IR, *in vitro* (Eck et al., 1996; Wolf et al., 1995). However, the exact molecular mechanism by which the IRS-1 PH domain promotes receptor coupling is not known. It is generally accepted that most PH domains bind to phosphoinositides (Lemmon and Ferguson, 1998). Given that the majority of PH domain-containing proteins have a functional requirement for membrane association, it has been postulated that the lipid-binding function of PH domains serves to recruit these signaling proteins to membrane compartments. However, non-specific membrane targeting sequences such as CAAX and myristoylation sequences cannot always substitute for PH domains. As in the case of IRS-1, constitutively membrane-bound IRS-1 (IRS-1-CAAX) disrupts insulin-induced IRS-1-mediated signaling such as PI 3-kinase and Mitogen-activated Protein (MAP) kinase signaling (Kriauciunas et al., 2000), suggesting that proper membrane localization of IRS-1 is essential for its function. Moreover, failure of heterologous PH

domains all known to promote plasma membrane targeting by binding to phosphoinositides to restore IRS-1 specific signaling suggests that the IRS-1 PH domain is not simply a membrane targeting device but may interact with specific cellular ligands (Burks et al., 1997). Although a recent report by Burks et al. (Burks et al., 1998) revealed that the IRS-1 PH domain binds to acidic motifs in the nucleolar protein, nucleolin, physiological ligands for the IRS-1 PH domain have yet to be defined. In order to identify proteins that bind to the PH domain of IRS-1, a yeast two-hybrid screen was initially used in which the PH domain from rat IRS-1 was used as a bait to screen a murine 10.5 day embryonic cDNA library (Farhang-Fallah et al., 2000). Sequence analysis of a cDNA clone, VP1.32, which displayed the strongest interaction with the IRS-1 PH domain, revealed an open reading frame (ORF) of 204 amino acids with no significant homology to any known proteins. This protein was designated as PHIP, for **PH** Interacting **P**rotein. *In vitro* binding studies in yeast have demonstrated that PHIP is associated with the PH domain of IRS-1 and not with PH domain derivatives from unrelated signaling proteins such as mSos1 (Ras nucleotide exchanger), Ect-2 (Rho/Rac exchanger) and RasGAP (GTPase activating protein) (Bowtell et al., 1992; Miki et al., 1993; Trahey and McCormick, 1987; Trahey and McCormick, 1987), suggesting that PHIP may function as a specific ligand of the IRS-1 PH domain (Farhang-Fallah et al., 2000).

This chapter reports the molecular cloning of the mouse and human PHIP cDNAs and preliminary biochemical characterization of the corresponding proteins. I have provided a detailed analysis of PHIP sequences and their relation to other family members. I have also examined the tissue and intracellular distribution pattern of PHIP expression as well as its ability to interact with IRS-1 both *in vitro* and *in vivo*.

3.2 RESULTS

3.2.1 Isolation of PHIP cDNA. The longest PHIP cDNA clone (VP1.32) from the yeast two-hybrid analysis spanned a nucleotide sequence of 629 base pairs (bp), which was devoid of in-frame termination codon and an N-terminal Kozak consensus (Kozak, 1986).

In order to obtain full-length mouse PHIP (mPHIP) cDNA sequences, a mouse thymus cDNA library was screened using the 629 bp VP1.32 as a probe. Eighteen positive clones were obtained; twelve of the clones displaying the strongest signals were subsequently sequenced. Sequence analysis of the overlapping clones shaped a large but incomplete open reading frame. In order to obtain clones containing the carboxy-terminal sequences, the mouse thymus library was subsequently re-screened with a p18F'5-T7 DNA fragment spanning a 570 bp nucleotide of the most C-terminal clone from the first screening attempt (p18). Twenty positive clones were obtained, several of which were subsequently sequenced. The largest clone (14A-18) extended the C-terminus by approximately 1.5 kilo-bases (kb) and found to contain a termination codon (TAA) and 903 bp 3'-untranslated region (UTR) followed by a 14 nt polyadenine (Poly (A)) tract. In order to locate the PHIP N-terminal initiating methionine, 5'RACE experiments were performed on total RNA isolated from adult mouse thymus tissue. Data obtained from these experiments identified a translational start codon (ATG) in the context of a Kozak consensus (Kozak, 1986), which was preceded by a series of stop codons. An additional

219 bp 5'-UTR was also obtained by 5' RACE. Collectively, these results demonstrated an open reading frame of 2706 bp encoding 902 amino acid (aa) residues (Figure 3.1A).

To obtain the human homologue of mouse PHIP cDNA, a human fetal brain cDNA library was screened using the 629 bp VP1.32 as a probe. Eighteen positive clones were obtained; eight of the clones displaying the strongest signal were subsequently sequenced. The largest clone (6b-26) contained an insert of 2784 bp, which contained 121 bp 3'-UTR followed by 16 bp poly(A) tract. The N-terminal initiation codon was never found for human PHIP (hPHIP) in either of the fetal brain cDNA library screen or 5'RACE analysis, leading to an open reading frame of 2694 bp encoding 898 aa residues (Figure 3.1B). Interestingly, one of the clones (19b-4) from the human fetal brain cDNA library screen identified a large insert of 2839 bp, which extended hPHIP N-terminus by 498 bp but was devoid of any initiation methionine (Figure 3.2). BLAST analysis using the latter sequence detected a second member of the PHIP family, encoding neuronal differentiation-related protein (NDRP) (Kato et al., 2000) (Figure 3.3). A full length NDRP cDNA contains an open reading frame of 3057 bp encoding a protein of 1019 aa residues. NDRP is an alternative splice variant from the hPHIP locus mapped to chromosome 6 and has been shown to be predominantly expressed in developing neurons and may be involved in neuronal regeneration and differentiation. The pre-carboxy terminal region of NDRP is identical to the amino-terminal region of PHIP (residues 5-80) (Figure 3.2). Genomic sequence analysis revealed that PHIP and NDRP share two exons; the penultimate two exons, 24^{th} and 25^{th}, of NDRP correspond to the 1^{st} and 2^{nd}

Figure 3.1. Nucelotide and deduced amino acid sequences of mouse and human PHIP. The entire mouse PHIP (A) human PHIP (B) nucleotide sequences. The mouse ATG encoding methionine shown in bold letter is likely the translation initiation codon as it matches well with the Kozak consensus and is preceded by multiple in frame stop codons (GenBank™ accession number AF310251). The corresponding initiation methionine in human PHIP sequences was never obtained (GenBank™ accession number AF310250). The complete amino acid open reading frames are also included beneath the nucleotide sequences. Underlined are amino acid sequences of the two bromodomains located centrally in tandem. The termination codons are depicted by asterisks in bold letters.

A.

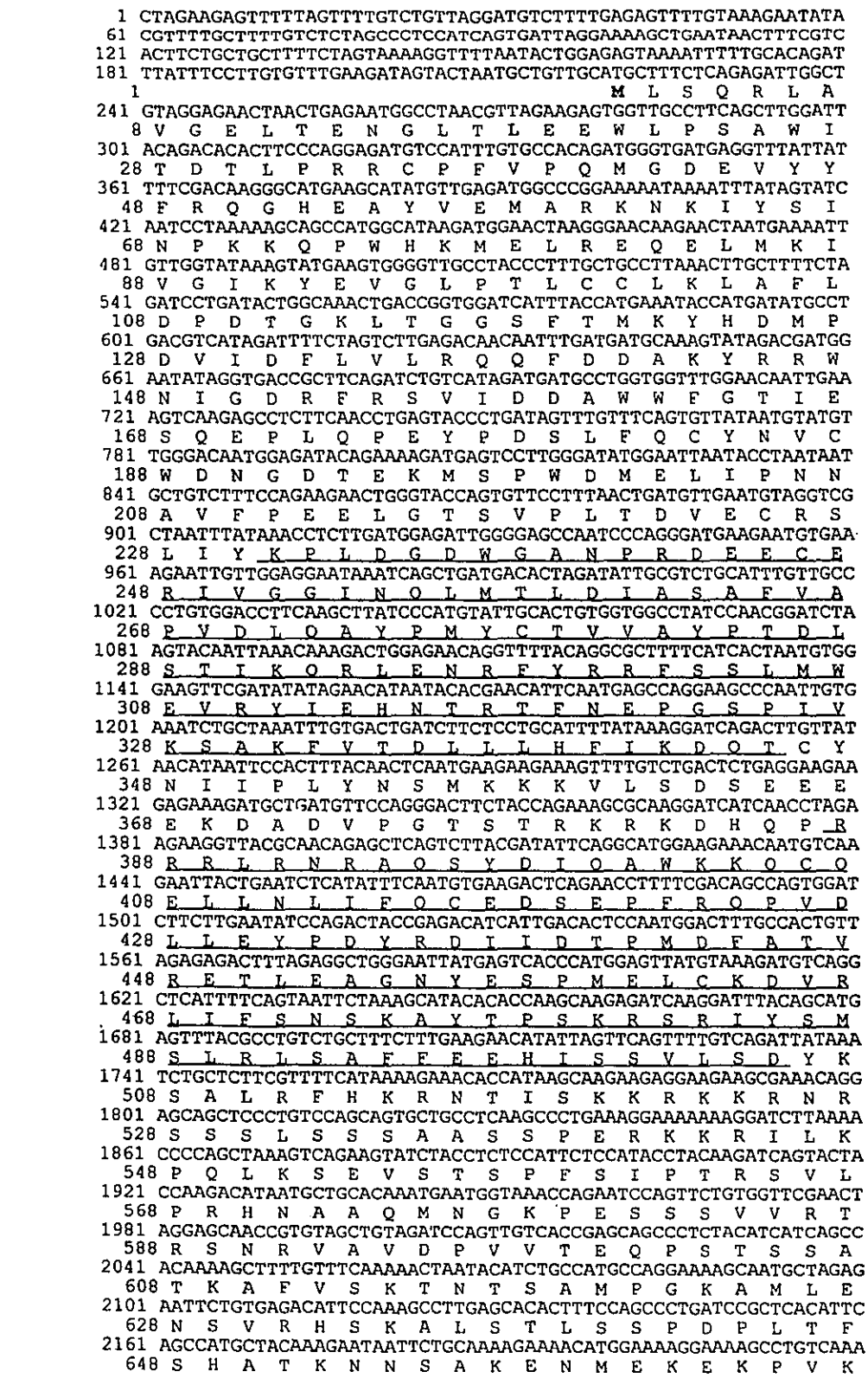
1 CTAGAAGAGTTTTTAGTTTTGTCTGTTAGGATGTCTTTTGAGAGTTTTGTAAAGAATATA
61 CGTTTTGCTTTTGTCTCTAGCCCTCCATCAGTGATTAGGAAAAGCTGAATAACTTTCGTC
121 ACTTCTGCTGCTTTTCTAGTAAAAGGTTTTAATACTGGAGAGTAAAATTTTTGCACAGAT
181 TTATTTCCTTGTGTTTGAAGATAGTACTAATGCTGTTGCATGCTTTCTCAGAGATTGGCT
1 M L S Q R L A
241 GTAGGAGAACTAACTGAGAATGGCCTAACGTTAGAAGAGTGGTTGCCTTCAGCTTGGATT
8 V G E L T E N G L T L E E W L P S A W I
301 ACAGACACACTTCCCAGGAGATGTCCATTTGTGCCACAGATGGGTGATGAGGTTTATTAT
28 T D T L P R R C P F V P Q M G D E V Y Y
361 TTTCGACAAGGGCATGAAGCATATGTTGAGATGGCCCGGAAAAATAAAATTTATAGTATC
48 F R Q G H E A Y V E M A R K N K I Y S I
421 AATCCTAAAAAGCAGCCATGGCATAAGATGGAACTAAGGGAACAAGAACTAATGAAAATT
68 N P K K Q P W H K M E L R E Q E L M K I
481 GTTGGTATAAAGTATGAAGTGGGGTTGCCTACCCTTTGCTGCCTTAAACTTGCTTTTCTA
88 V G I K Y E V G L P T L C C L K L A F L
541 GATCCTGATACTGGCAAACTGACCGGTGGATCATTTACCATGAAATACCATGATATGCCT
108 D P D T G K L T G G S F T M K Y H D M P
601 GACGTCATAGATTTTCTAGTCTTGAGACAACAATTTGATGATGCAAAGTATAGACGATGG
128 D V I D F L V L R Q Q F D D A K Y R R W
661 AATATAGGTGACCGCTTCAGATCTGTCATAGATGATGCCTGGTGGTTTGGAACAATTGAA
148 N I G D R F R S V I D D A W W F G T I E
721 AGTCAAGAGCCTCTTCAACCTGAGTACCCTGATAGTTTGTTTCAGTGTTATAATGTATGT
168 S Q E P L Q P E Y P D S L F Q C Y N V C
781 TGGGACAATGGAGATACAGAAAAGATGAGTCCTTGGGATATGGAATTAATACCTAATAAT
188 W D N G D T E K M S P W D M E L I P N N
841 GCTGTCTTTCCAGAAGAACTGGGTACCAGTGTTCCTTTAACTGATGTTGAATGTAGGTCG
208 A V F P E E L G T S V P L T D V E C R S
901 CTAATTTATAAACCTCTTGATGGAGATTGGGGAGCCAATCCCAGGGATGAAGAATGTGAA
228 L I Y K P L D G D W G A N P R D E E C E
961 AGAATTGTTGGAGGAATAAATCAGCTGATGACACTAGATATTGCGTCTGCATTTGTTGCC
248 R I V G G I N Q L M T L D I A S A F V A
1021 CCTGTGGACCTTCAAGCTTATCCCATGTATTGCACTGTGGTGGCCTATCCAACGGATCTA
268 P V D L Q A Y P M Y C T V V A Y P T D L
1081 AGTACAATTAAACAAAGACTGGAGAACAGGTTTTACAGGCGCTTTTCATCACTAATGTGG
288 S T I K Q R L E N R F Y R R F S S L M W
1141 GAAGTTCGATATATAGAACATAATACACGAACATTCAATGAGCCAGGAAGCCCAATTGTG
308 E V R Y I E H N T R T F N E P G S P I V
1201 AAATCTGCTAAATTTGTGACTGATCTTCTCCTGCATTTTATAAAGGATCAGACTTGTTAT
328 K S A K F V T D L L L H F I K D Q T C Y
1261 AACATAATTCCACTTTACAACTCAATGAAGAAGAAAGTTTTGTCTGACTCTGAGGAAGAA
348 N I I P L Y N S M K K K V L S D S E E E
1321 GAGAAAGATGCTGATGTTCCAGGGACTTCTACCAGAAAGCGCAAGGATCATCAACCTAGA
368 E K D A D V P G T S T R K R K D H Q P R
1381 AGAAGGTTACGCAACAGAGCTCAGTCTTACGATATTCAGGCATGGAAGAAACAATGTCAA
388 R R L R N R A Q S Y D I Q A W K K Q C Q
1441 GAATTACTGAATCTCATATTTCAATGTGAAGACTCAGAACCTTTTCGACAGCCAGTGGAT
408 E L L N L I F Q C E D S E P F R Q P V D
1501 CTTCTTGAATATCCAGACTACCGAGACATCATTGACACTCCAATGGACTTTGCCACTGTT
428 L L E Y P D Y R D I I D T P M D F A T V
1561 AGAGAGACTTTAGAGGCTGGGAATTATGAGTCACCCATGGAGTTATGTAAAGATGTCAGG
448 R E T L E A G N Y E S P M E L C K D V R
1621 CTCATTTTCAGTAATTCTAAAGCATACACACCAAGCAAGAGATCAAGGATTTACAGCATG
468 L I F S N S K A Y T P S K R S R I Y S M
1681 AGTTTACGCCTGTCTGCTTTCTTTGAAGAACATATTAGTTCAGTTTTGTCAGATTATAAA
488 S L R L S A F F E E H I S S V L S D Y K
1741 TCTGCTCTTCGTTTTCATAAAAGAAACACCATAAGCAAGAAGAGGAAGAAGCGAAACAGG
508 S A L R F H K R N T I S K K R K K R N R
1801 AGCAGCTCCCTGTCCAGCAGTGCTGCCTCAAGCCCTGAAAGGAAAAAAAGGATCTTAAAA
528 S S S L S S S A A S S P E R K K R I L K
1861 CCCCAGCTAAAGTCAGAAGTATCTACCTCTCCATTCTCCATACCTACAAGATCAGTACTA
548 P Q L K S E V S T S P F S I P T R S V L
1921 CCAAGACATAATGCTGCACAAATGAATGGTAAACCAGAATCCAGTTCTGTGGTTCGAACT
568 P R H N A A Q M N G K P E S S S V V R T
1981 AGGAGCAACCGTGTAGCTGTAGATCCAGTTGTCACCGAGCAGCCCTCTACATCATCAGCC
588 R S N R V A V D P V V T E Q P S T S S A
2041 ACAAAAGCTTTTGTTTCAAAAACTAATACATCTGCCATGCCAGGAAAAGCAATGCTAGAG
608 T K A F V S K T N T S A M P G K A M L E
2101 AATTCTGTGAGACATTCCAAAGCCTTGAGCACACTTTCCAGCCCTGATCCGCTCACATTC
628 N S V R H S K A L S T L S S P D P L T F
2161 AGCCATGCTACAAAGAATAATTCTGCAAAAGAAAACATGGAAAAGGAAAAGCCTGTCAAA
648 S H A T K N N S A K E N M E K E K P V K

```
2221 CGTAAAATGAAGTCTTCTGTGTTTTCAAAAGCATCTCCACTTCCAAAGTCAGCCGCAGTC
  668 R  K  M  K  S  S  V  F  S  K  A  S  P  L  P  K  S  A  A  V
2281 ATAGAGCAAGGAGAGTGTAAGAACAATGTTCTTATACCAGGAACCATTCAAGTAAATGGC
  688 I  E  Q  G  E  C  K  N  N  V  L  I  P  G  T  I  Q  V  N  G
2341 CATGGAGGACAACCATCAAAACTCGTGAAGAGAGGACCTGGGAGGAAGCCCAAGGTAGAA
  708 H  G  G  Q  P  S  K  L  V  K  R  G  P  G  R  K  P  K  V  E
2401 GTTAACACCAGCAGTGGTGAAGTGACACACAAGAAAAGAGGTAGAAAGCCCAAGAATCTG
  728 V  N  T  S  S  G  E  V  T  H  K  K  R  G  R  K  P  K  N  L
2461 CAGTGTGCAAAGCAGGAAAACTCTGAGCAAAATAACATGCATCCCATCAGGGCTGACGTG
  748 Q  C  A  K  Q  E  N  S  E  Q  N  N  M  H  P  I  R  A  D  V
2521 CTTCCTTCTTCAACATGCAACTTCCTTTCTGAAACTAATGCTGTCAAGGAGGATTTGTTA
  768 L  P  S  S  T  C  N  F  L  S  E  T  N  A  V  K  E  D  L  L
2581 CAGAAAAAGAGTCGTGGAGGCAGAAAACCCAAAAGGAAGATGAAAACTCACAACCTAGAT
  788 Q  K  K  S  R  G  G  R  K  P  K  R  K  M  K  T  H  N  L  D
2641 TCAGAACTCATAGTTCCTACAAATGTTAAAGTGTTAAGGAGAAGTAACCGGAAAAAAACA
  808 S  E  L  I  V  P  T  N  V  K  V  L  R  R  S  N  R  K  K  T
2701 GATGATCCTATAGATGAGGAAGAGGAGTTTGAAGAACTCAAAGGCTCTGAGCCTCACATG
  828 D  D  P  I  D  E  E  E  E  F  E  E  L  K  G  S  E  P  H  M
2761 AGAACTAGAAATCAGGGTCGAAGGACAACTTTCTATAATGAGGATGACTCCGAGGAAGAA
  848 R  T  R  N  Q  G  R  R  T  T  F  Y  N  E  D  D  S  E  E  E
2821 CAGAGACAGCTGTTGTTCGAGGACACCTCCTTGACATTTGGAACTTCTAGTAGAGGACGA
  868 Q  R  Q  L  L  F  E  D  T  S  L  T  F  G  T  S  S  R  G  R
2881 GTCCGAAAGTTGACTGAAAAAGCAAAGGCTAATTTAATTGGTTGGTAACTTGAAGCAAAA
  888 V  R  K  L  T  E  K  A  K  A  N  L  I  G  W  *
2941 TATTGCATTTTAAAAAATCTGTAACGCAGGTACAGTTAAGGAGTAAGTAGAACTAAGGTC
3001 TCTGCTTCCTTGCTGCTATGACGGATTAGGGAATGTTACAATTTGACTTGGGAAAATGGA
3061 CAAAAACACATTTAGAAGATAATTTACATCTTTGAATGAAAAAAATCTATATACATATAT
3121 ATTTCAAATGTTTGCTATTTATTGCCCTTAGGTAGGTTATTCGGTTCCACATTCATTTCA
3181 TTTGCTGTTTGAAATTGAGGACCTGTTATAAATTCTGGTTTATTTATGGAAGAGACAGCT
3241 CTGCTACACTATTAAGAAACATAGTATTCCTAGAGATAAAGTATGTTCCCTCTTAAATTG
3301 AGTTATTTTTGACCAAGTGAGGTACATTTTTACTGATAGCAGAAGGCATGCCCTAGGAAG
3361 AGAGATGTTACAAAGAGTAGCAGTACATTAAGAATGGCTTCCTCTAAAGATAACTTTCCA
3421 GTTCCCACCATTTGGTATCCTGAAAAGTGTTGTGAACTGTAGGTGTTCAATTACAGAATA
3481 TCTAGAGGAAGCTTTTGTTTTACTCCATTTCTGCCAAACTTAGGAGAAAAATGTATTGAT
3541 GCAAAGGAAACATATCCACATTGGAAAACATTTGACTGTCTAATTTTTCAGACCTTGATT
3601 CTTATATCAGTCACTCTATCTCTGTTTATTGTGCCAAAGACTGAGAATCAGTGCAGTGGA
3661 AAGCCTGTTTTTGACTGTCAGGACAGCATACACTTTTCAGTACTGGAAAAGCTATATATT
3721 CTAAAGAGCAAGTTATTACAAAATTATGCTGAGTTATATCCTTTTTTTGGTACTAAATGT
3781 AGGAAAATAATGCACTGGTGGGTCCTTTGACAGAGATATCTTAGAGAAAAAAAAAAAAA
```

B.

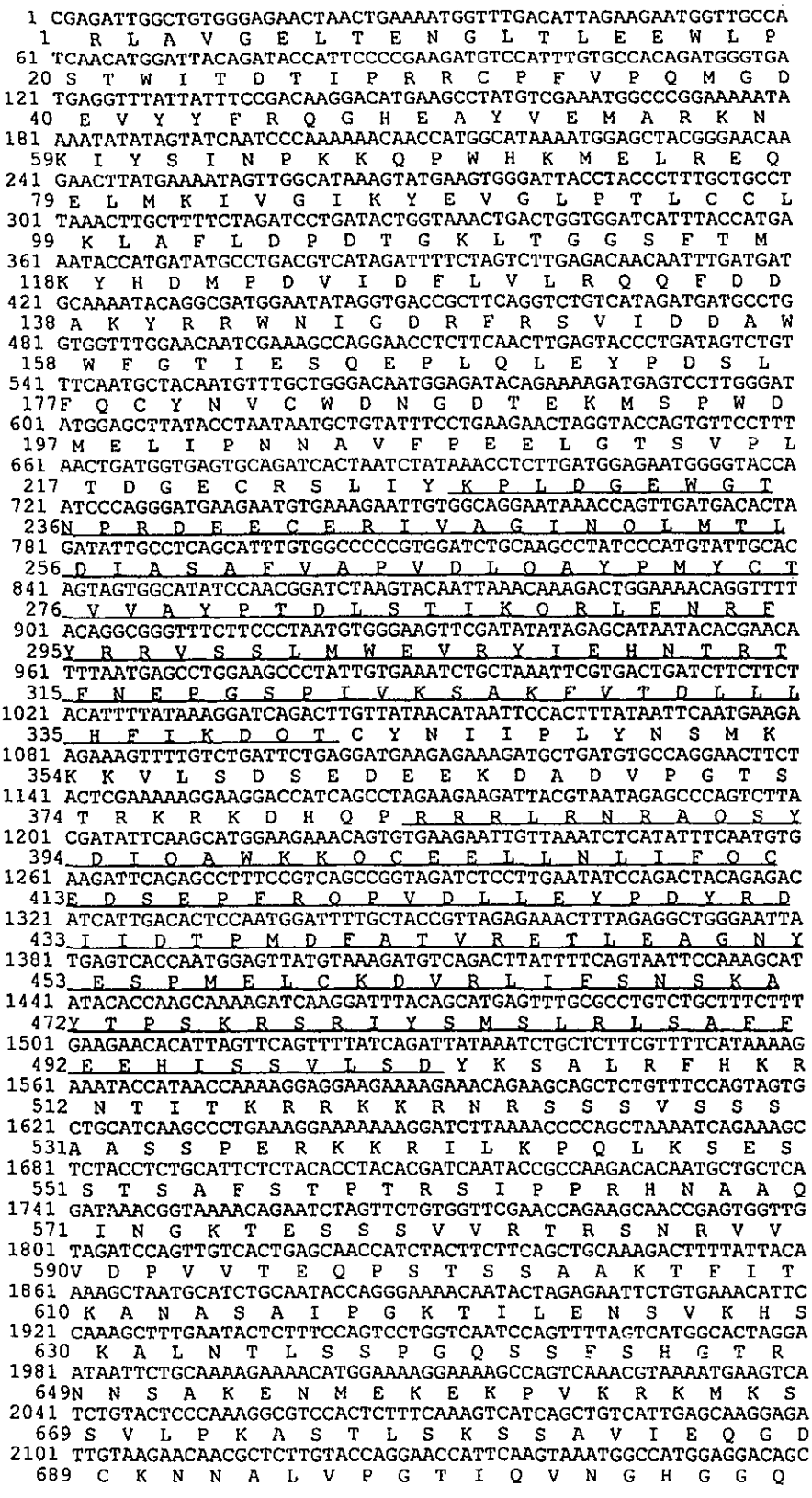
1 CGAGATTGGCTGTGGGAGAACTAACTGAAAATGGTTTGACATTAGAAGAATGGTTGCCA
1 R L A V G E L T E N G L T L E E W L P
61 TCAACATGGATTACAGATACCATTCCCCGAAGATGTCCATTTGTGCCACAGATGGGTGA
20 S T W I T D T I P R R C P F V P Q M G D
121 TGAGGTTTATTATTTCCGACAAGGACATGAAGCCTATGTCGAAATGGCCCGGAAAAATA
40 E V Y Y F R Q G H E A Y V E M A R K N
181 AAATATATAGTATCAATCCCAAAAAACAACCATGGCATAAAATGGAGCTACGGGAACAA
59K I Y S I N P K K Q P W H K M E L R E Q
241 GAACTTATGAAAATAGTTGGCATAAAGTATGAAGTGGGATTACCTACCCTTTGCTGCCT
79 E L M K I V G I K Y E V G L P T L C C L
301 TAAACTTGCTTTTCTAGATCCTGATACTGGTAAACTGACTGGTGGATCATTTACCATGA
99 K L A F L D P D T G K L T G G S F T M
361 AATACCATGATATGCCTGACGTCATAGATTTTCTAGTCTTGAGACAACAATTTGATGAT
118K Y H D M P D V I D F L V L R Q Q F D D
421 GCAAAATACAGGCGATGGAATATAGGTGACCGCTTCAGGTCTGTCATAGATGATGCCTG
138 A K Y R R W N I G D R F R S V I D D A W
481 GTGGTTTGGAACAATCGAAAGCCAGGAACCTCTTCAACTTGAGTACCCTGATAGTCTGT
158 W F G T I E S Q E P L Q L E Y P D S L
541 TTCAATGCTACAATGTTTGCTGGGACAATGGAGATACAGAAAAGATGAGTCCTTGGGAT
177F Q C Y N V C W D N G D T E K M S P W D
601 ATGGAGCTTATACCTAATAATGCTGTATTTCCTGAAGAACTAGGTACCAGTGTTCCTTT
197 M E L I P N N A V F P E E L G T S V P L
661 AACTGATGGTGAGTGCAGATCACTAATCTATAAACCTCTTGATGGAGAATGGGGTACCA
217 T D G E C R S L I Y K P L D G E W G T
721 ATCCCAGGGATGAAGAATGTGAAAGAATTGTGGCAGGAATAAACCAGTTGATGACACTA
236N P R D E E C E R I V A G I N Q L M T L
781 GATATTGCCTCAGCATTTGTGGCCCCCGTGGATCTGCAAGCCTATCCCATGTATTGCAC
256 D I A S A F V A P V D L Q A Y P M Y C T
841 AGTAGTGGCATATCCAACGGATCTAAGTACAATTAAACAAAGACTGGAAAACAGGTTTT
276 V V A Y P T D L S T I K Q R L E N R F
901 ACAGGCGGGTTTCTTCCCTAATGTGGGAAGTTCGATATATAGAGCATAATACACGAACA
295Y R R V S S L M W E V R Y I E H N T R T
961 TTTAATGAGCCTGGAAGCCCTATTGTGAAATCTGCTAAATTCGTGACTGATCTTCTTCT
315 F N E P G S P I V K S A K F V T D L L L
1021 ACATTTTATAAAGGATCAGACTTGTTATAACATAATTCCACTTTATAATTCAATGAAGA
335 H F I K D Q T C Y N I I P L Y N S M K
1081 AGAAAGTTTTGTCTGATTCTGAGGATGAAGAGAAAGATGCTGATGTGCCAGGAACTTCT
354K K V L S D S E D E E K D A D V P G T S
1141 ACTCGAAAAAGGAAGGACCATCAGCCTAGAAGAAGATTACGTAATAGAGCCCAGTCTTA
374 T R K R K D H Q P R R R L R N R A Q S Y
1201 CGATATTCAAGCATGGAAGAAACAGTGTGAAGAATTGTTAAATCTCATATTTCAATGTG
394 D I Q A W K K Q C E E L L N L I F Q C
1261 AAGATTCAGAGCCTTTCCGTCAGCCGGTAGATCTCCTTGAATATCCAGACTACAGAGAC
413E D S E P F R Q P V D L L E Y P D Y R D
1321 ATCATTGACACTCCAATGGATTTTGCTACCGTTAGAGAAACTTTAGAGGCTGGGAATTA
433 I I D T P M D F A T V R E T L E A G N Y
1381 TGAGTCACCAATGGAGTTATGTAAAGATGTCAGACTTATTTTCAGTAATTCCAAAGCAT
453 E S P M E L C K D V R L I F S N S K A
1441 ATACACCAAGCAAAAGATCAAGGATTTACAGCATGAGTTTGCGCCTGTCTGCTTTCTTT
472Y T P S K R S R I Y S M S L R L S A F F
1501 GAAGAACACATTAGTTCAGTTTTATCAGATTATAAATCTGCTCTTCGTTTTCATAAAAG
492 E E H I S S V L S D Y K S A L R F H K R
1561 AAATACCATAACCAAAAGGAGGAAGAAAAGAAACAGAAGCAGCTCTGTTTCCAGTAGTG
512 N T I T K R R K K R N R S S S V S S S
1621 CTGCATCAAGCCCTGAAAGGAAAAAAAGGATCTTAAAACCCCAGCTAAAATCAGAAAGC
531A A S S P E R K K R I L K P Q L K S E S
1681 TCTACCTCTGCATTCTCTACACCTACACGATCAATACCGCCAAGACACAATGCTGCTCA
551 S T S A F S T P T R S I P P R H N A A Q
1741 GATAAACGGTAAAACAGAATCTAGTTCTGTGGTTCGAACCAGAAGCAACCGAGTGGTTG
571 I N G K T E S S S V V R T R S N R V V
1801 TAGATCCAGTTGTCACTGAGCAACCATCTACTTCTTCAGCTGCAAAGACTTTTATTACA
590V D P V V T E Q P S T S S A A K T F I T
1861 AAAGCTAATGCATCTGCAATACCAGGGAAAACAATACTAGAGAATTCTGTGAAACATTC
610 K A N A S A I P G K T I L E N S V K H S
1921 CAAAGCTTTGAATACTCTTTCCAGTCCTGGTCAATCCAGTTTTAGTCATGGCACTAGGA
630 K A L N T L S S P G Q S S F S H G T R
1981 ATAATTCTGCAAAAGAAAACATGGAAAAGGAAAAGCCAGTCAAACGTAAAATGAAGTCA
649N N S A K E N M E K E K P V K R K M K S
2041 TCTGTACTCCCAAAGGCGTCCACTCTTTCAAAGTCATCAGCTGTCATTGAGCAAGGAGA
669 S V L P K A S T L S K S S A V I E Q G D
2101 TTGTAAGAACAACGCTCTTGTACCAGGAACCATTCAAGTAAATGGCCATGGAGGACAGC
689 C K N N A L V P G T I Q V N G H G G Q

```
2161 CATCAAAACTTGTGAAGAGGGGACCTGGAAGGAAACCTAAAGTAGAAGTTAATACCAAT
  708P  S  K  L  V  K  R  G  P  G  R  K  P  K  V  E  V  N  T  N
2221 AGTGGTGAAATTATACACAAGAAAAGGGGTAGAAAGCCCAAAAAGCTACAGTATGCAAA
  728 S  G  E  I  I  H  K  K  R  G  R  K  P  K  K  L  Q  Y  A  K
2281 GCCAGAAGATTTAGAGCAAAATAATGTGCATCCCATCAGAGATGAAGTACTTCCTTCTT
  748  P  E  D  L  E  Q  N  N  V  H  P  I  R  D  E  V  L  P  S
2341 CAACATGCAATTTTCTTTCTGAAACTAATAATGTAAAGGAAGATTTGTTACAGAAAAAG
  767S  T  C  N  F  L  S  E  T  N  N  V  K  E  D  L  L  Q  K  K
2401 AATCGTGGAGGTAGGAAGCCCAAAAGGAAGATGAAGACACAAAAATTAGATGCAGATCT
  787 N  R  G  G  R  K  P  K  R  K  M  K  T  Q  K  L  D  A  D  L
2461 CCTAGTCCCTGCAAGTGTCAAAGTGTTAAGGAGAAGTAACCGAAAAAAGATAGATGATC
  807  L  V  P  A  S  V  K  V  L  R  R  S  N  R  K  K  I  D  D
2521 CTATAGATGAGGAAGAAGAGTTTGAAGAACTCAAAGGCTCTGAACCCCACATGAGAACT
  826P  I  D  E  E  E  E  F  E  E  L  K  G  S  E  P  H  M  R  T
2581 AGAAATCAAGGTCGAAGGACAGCTTTCTATAATGAGGATGACTCTGAAGAGGAGCAAAG
  846 R  N  Q  G  R  R  T  A  F  Y  N  E  D  D  S  E  E  E  Q  R
2641 GCAGCTGTTGTTCGAAGACACCTCTTTAACTTTTGGAACTTCTAGTAGAGGACGAGTCC
  866  Q  L  L  F  E  D  T  S  L  T  F  G  T  S  S  R  G  R  V
2701 GAAAGTTGACTGAAAAAGCAAAAGCTAATTTAATTGGTTGGTAACTTGTACCAAAATAT
  885R  K  L  T  E  K  A  K  A  N  L  I  G  W  *
2761 TTTACTTCAAAATCTATAAAGCAGGTACAGTTAAGGAATAAGTAGGACTAAGGCTTCTG
2821 CTTCCTTGCTGCTGTGGTGGAGTAGGGAATGTTATGATTTGATTTGCAAAAAAAAAAAA
2881 AAAA
```

Figure 3.2. Schematic representation of PHIP, NDRP and WDR11. Schematic representation of PHIP illustrates the presence of two bromodomains located centrally in PHIP, BD1 (230-345) and BD2 (387-503). The PHIP PBR (5-209) isolated from the yeast clone VP1.32 is shown as a marked thin line. The pre-carboxy terminus of mouse NDRP (923-999) is identical to mouse (m) PHIP amino-terminus (5-80); the C-terminal NDRP sequences then completely diverge and terminate after 20 amino acids (999-1019), while PHIP continues for another 822 amino acids (80-902). A long human PHIP clone, 19b-4 isolated from the fetal brain cDNA library that extends into NDRP is also shown as a marked thin line. A putative NDRP-PHIP fusion (WDR11) diagram is also demonstrated.

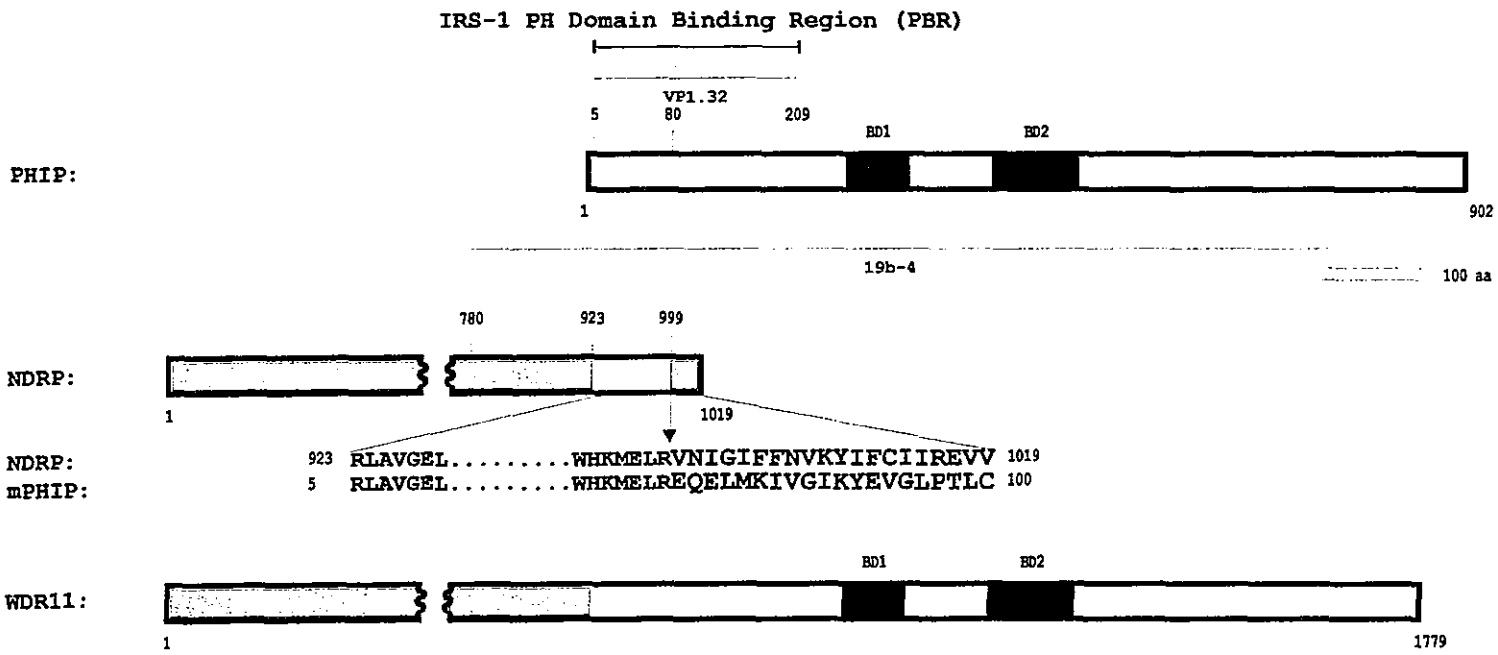
IRS-1 PH Domain Binding Region (PBR)
VP1.32
5
80
209
BD1
BD2
PHIP:
1
902
19b-4
100 aa
780
923
999
NDRP:
1
1019
NDRP:
923 RLAVGEL.....WHKMELRVNIGIFFNVKYIFCIIREVV 1019
mPHIP:
5 RLAVGEL.....WHKMELREQELMKIVGIKYEVGLPTLC 100
BD1
BD2
WDR11:
1
1779

Figure 3.3. Deduced amino acid sequence of NDRP. Alignment of mouse (m) and human (h) NDRP sequences represents a 94% identity. The carboxy-terminal sequences of human NDRP are yet to be defined. The GenBank™ accessions numbers for mouse and human NDRP are AB049460 and AK057039, respectively. The double dots (colon) represent identical amino acids, while single dots represent conserved residues.

```
hNDRP: 1    MSCERKGLSELRSELYFLIARFLEDGPCQQAAQVLIREVAEKELLPRRTDWTGKEHPRTY 60
mNDRP: 1    MSRERKGLSELRSELYFLIARFLEDGPCQQAAQVLIREVAEKELLPRRTDWTGKEHPRTY 60

hNDRP: 61   QNLVKYYRHLAPDHLLQICHRLGPLLEQEIPQSVPGVQTLLGAGRQSLLRTNKSCKHVVW 120
mNDRP: 61   QNLVKYYRHLAPDHLLQICHRLGPLLEQEIPQSVPGVQTLLGAGRQSLLRTNKSCKHVVW 120

hNDRP: 121  KGSALAALHCGRPPESPVNYGSPPSIADTLFSRKLNGKYRLERLVPTAVYQHMKMHKRIL 180
mNDRP: 121  KGSALAALHCGRPPESPVNYGSPPSIADTLFSRKLNGKYRLERLVPTAVYQHMKMHKRIL 180

hNDRP: 181  GHLSSVYCVTFDRTGRRIFTGSDDCLVKIWATDDGRLLATLRGHAAEISDMAVNYENTMI 240
mNDRP: 181  GHLSSVYCVTFDRTGRRIFTGSDDCLVKIWATDDGRLLATLRGHAAEISDMAVNYENTMI 240

hNDRP: 241  AAGSCDKMIRVWCLRTCAPLAVLQGHSASITSLQFSPLCSGSKRYLSSTGADGTICFWLW 300
mNDRP: 241  AAGSCDKMIRVWCLRTCAPLAVLQGHSASITSLQFSPLCSGSKRYLSSTGADGTICFWLW 300

hNDRP: 301  DAGTLKINPRPAKFTERPRPGVQMICSSFSAGGMFLATGSTDHIIRVYFFGSGQPEKISE 360
mNDRP: 301  DAGTLKINPRPTKFTERPRPGVQMICSSFSAGGMFLATGSTDHIIRVYFFGSGQPEKISE 360

hNDRP: 361  LEFHTDKVDSIQFSNTSNRFVSGSRDGTARIWQFKRREWKSILLDMATRPAGQNLQGIED 420
mNDRP: 361  LEFHTDKVDSIQFSNTSNRFVSGSRDGTARIWQFKRREWKSILLDMATRPAGQNLQGIED 420

hNDRP: 421  KITKMKVTMVAWDRHDNTVITAVNNMTLKVWNSYTGQLIHVLMGHEDEVFVLEPHPFDPR 480
mNDRP: 421  KITKMKVTMVAWDRHDNTVITAVNNMTLKVWNSYTGQLIHVLMGHEDEVFVLEPHPFDPR 480

hNDRP: 481  VLFSAGHDGNVIVWDLARGVKIRSYFNMIEGQGHGAVFDCKCSPDGQHFACTDSHGHLLI 540
mNDRP: 481  VLFSAGHDGNVIVWDLARGVKVRSYFNMIEGQGHGAVFDCKCSPDGQHFACTDSHGHLLI 540

hNDRP: 541  FGFGSSSKYDKIADQMFFHSDYRPLIRDANNFVLDEQTQQAPHLMPPPFLVDVDGNPHPS 600
mNDRP: 541  FGFGSSSKYDKIADQMFFHSDYRPLIRDANNFVLDEQTQQAPHLMPPPFLVDVDGNPHPS 600

hNDRP: 601  RYQRLVPGRENCREEQLIPQMGVTSSGLNQVLSQQANQEISPLDSMIQRLQQEQDLRRSG 660
mNDRP: 601  RYQRLVPGRENCREEQLIPQMGVTSSGLNQVLSQQANQDISPLDSMIQRLQQEQDLRRSG 660

hNDRP: 661  EAGISNTSRLSRGSISSTSEVHSPPNVGLRRSGQIEGVRQMHSNAPRSEIATERDLVAWS 720
mNDRP: 661  EAGVSNASRVNRGSVSSTSEVHSPPNIGLRRSGQIEGVRQMHSNAPRSEIATERDLVAWS 720

hNDRP: 721  RRVVVPELSAGVASRQEEWRTAKGEEEIKTYRSEEKRKHLTVPKENKIPIVSKNHAHEHF 780
mNDRP: 721  RRVVVPELSAGVASRQEEWRTAKGEEEIKSYRSEEKRKHLTVAKENKILTVSKNHAHEHF 780

hNDRP: 781  LDLGESKKQQTNQHNYRTRSALEETPRPSEEIENGSSSSDEGEVVAVSGGTSEEEERAWH 840
mNDRP: 781  LDLGDSKKQQANQHNYRTRSALEETPRPLEELENGTSSSDEGEVLAVSGGTSEEEERAWH 840

hNDRP: 841  SDGSSSDYSSDYSDWTADAGINLQPPKKVPKNKTKKAESSSDEEEESEKQKQKQIKKEKK 900
mNDRP: 841  SDGSSSDYSSDYSDWTADAGINLQPPKKVPKHKTKKPESSSDEEEESENQKQKHIKKERK 900

hNDRP: 901  KVNEEKDGPISP                                                  912
mNDRP: 901  KANEEKDGPTSPKKKKPKERKQKRLAVGELTENGLTLEEWLPSAWITDTLPRRCPFVPQM 960
       961  GDEVYYFRQGHEAYVEMARKNKIYSINPKKQPWHKMELRVNIGIFFNVKYIFCIIREVV 1019
```

exons of PHIP. However, the last exon of NDRP extends 3' into the intronic region flanking the second exon of PHIP and is followed by multiple stop codons (Lhotak V., personal communication). In addition, BLAST analysis of PHIP or NDRP identified a putative NDRP-PHIP fusion partial mRNA which is referred to as "WDR11" (Figure 3.4). Using RT-PCR analysis with NDRP and PHIP specific primers, I have also confirmed the existence of such transcript within various mouse tissues (Figure 3.5). Furthermore, metabolic labelling of L6 myoblasts has also revealed a large protein of approximately 250 KDa immunoprecipitated with anti-PHIP antibodies, which might correspond to the NDRP-PHIP fusion protein (data not shown). The functional significance and expression profile of the NDRP-PHIP fusion protein however is yet to be determined.

In addition, two alternatively splice variant orthologues of PHIP, termed WDR9 form A and B have also been identified on human Chromosome 21 (data not shown).

3.2.2 PHIP transcript is ubiquitously expressed in various adult mouse tissues. To determine the transcript size and the pattern of PHIP gene expression, northern blot analysis was performed on total RNA extracts isolated from adult mouse tissues. Although multiple PHIP transcripts might have been expected, only a single transcript of approximately 7.0 Kb was resolved by hybridization with both N-terminal and central ^{32}P-radiolabeled PHIP probes (data not shown). PHIP mRNA was ubiquitously expressed at low levels in all tissues assayed including brain, heart, liver, lung, kidney, large and small intestine, ovaries, skeletal muscle, spleen, stomach, and thymus. The full-length mPHIP cDNA was about 3.8 Kb representing a difference of about 3.2 Kb in

Figure 3.4. Alignment of human amino acid sequences from PHIP and NDRP with WDR11. As shown, the amino-terminal sequences of human WDR11 (GenBank™ accession number AJ303102) are 100% identical to NDRP (A), while the carboxy-terminal sequences are absolutely identical to PHIP (B). There is a very small gap between the end of hWDR11/hNDRP amino acid alignment and hWDR11/hPHIP alignment (912-924), potentially due to differential splicing events.

A.

```
hWDR11:1   MSCERKGLSELRSELYFLIARFLEDGPCQQAAQVLIREVAEKELLPRRTDWTGKEHPRTY 60
           ::::::::::::::::::::::::::::::::::::::::::::::::::::::::::::
hNDRP: 1   MSCERKGLSELRSELYFLIARFLEDGPCQQAAQVLIREVAEKELLPRRTDWTGKEHPRTY 60

hWDR11:61  QNLVKYYRHLAPDHLLQICHRLGPLLEQEIPQSVPGVQTLLGAGRQSLLRTNKSCKHVVW 120
           ::::::::::::::::::::::::::::::::::::::::::::::::::::::::::::
hNDRP: 61  QNLVKYYRHLAPDHLLQICHRLGPLLEQEIPQSVPGVQTLLGAGRQSLLRTNKSCKHVVW 120

hWDR11:121 KGSALAALHCGRPPESPVNYGSPPSIADTLFSRKLNGKYRLERLVPTAVYQHMKMHKRIL 180
           ::::::::::::::::::::::::::::::::::::::::::::::::::::::::::::
hNDRP: 121 KGSALAALHCGRPPESPVNYGSPPSIADTLFSRKLNGKYRLERLVPTAVYQHMKMHKRIL 180

hWDR11:181 GHLSSVYCVTFDRTGRRIFTGSDDCLVKIWATDDGRLLATLRGHAAEISDMAVNYENTMI 240
           ::::::::::::::::::::::::::::::::::::::::::::::::::::::::::::
hNDRP: 181 GHLSSVYCVTFDRTGRRIFTGSDDCLVKIWATDDGRLLATLRGHAAEISDMAVNYENTMI 240

hWDR11:241 AAGSCDKMIRVWCLRTCAPLAVLQGHSASITSLQFSPLCSGSKRYLSSTGADGTICFWLW 300
           ::::::::::::::::::::::::::::::::::::::::::::::::::::::::::::
hNDRP: 241 AAGSCDKMIRVWCLRTCAPLAVLQGHSASITSLQFSPLCSGSKRYLSSTGADGTICFWLW 300

hWDR11:301 DAGTLKINPRPAKFTERPRPGVQMICSSFSAGGMFLATGSTDHIIRVYFFGSGQPEKISE 360
           ::::::::::::::::::::::::::::::::::::::::::::::::::::::::::::
hNDRP: 301 DAGTLKINPRPAKFTERPRPGVQMICSSFSAGGMFLATGSTDHIIRVYFFGSGQPEKISE 360

hWDR11:361 LEFHTDKVDSIQFSNTSNRFVSGSRDGTARIWQFKRREWKSILLDMATRPAGQNLQGIED 420
           ::::::::::::::::::::::::::::::::::::::::::::::::::::::::::::
hNDRP: 361 LEFHTDKVDSIQFSNTSNRFVSGSRDGTARIWQFKRREWKSILLDMATRPAGQNLQGIED 420

hWDR11:421 KITKMKVTMVAWDRHDNTVITAVNNMTLKVWNSYTGQLIHVLMGHEDEVFVLEPHPFDPR 480
           ::::::::::::::::::::::::::::::::::::::::::::::::::::::::::::
hNDRP: 421 KITKMKVTMVAWDRHDNTVITAVNNMTLKVWNSYTGQLIHVLMGHEDEVFVLEPHPFDPR 480

hWDR11:481 VLFSAGHDGNVIVWDLARGVKIRSYFNMIEGQGHGAVFDCKCSPDGQHFACTDSHGHLLI 540
           ::::::::::::::::::::::::::::::::::::::::::::::::::::::::::::
hNDRP: 481 VLFSAGHDGNVIVWDLARGVKIRSYFNMIEGQGHGAVFDCKCSPDGQHFACTDSHGHLLI 540

hWDR11:541 FGFGSSSKYDKIADQMFFHSDYRPLIRDANNFVLDEQTQQAPHLMPPPFLVDVDGNPHPS 600
           ::::::::::::::::::::::::::::::::::::::::::::::::::::::::::::
hNDRP: 541 FGFGSSSKYDKIADQMFFHSDYRPLIRDANNFVLDEQTQQAPHLMPPPFLVDVDGNPHPS 600

hWDR11:601 RYQRLVPGRENCREEQLIPQMGVTSSGLNQVLSQQANQEISPLDSMIQRLQQEQDLRRSG 660
           ::::::::::::::::::::::::::::::::::::::::::::::::::::::::::::
hNDRP: 601 RYQRLVPGRENCREEQLIPQMGVTSSGLNQVLSQQANQEISPLDSMIQRLQQEQDLRRSG 660

hWDR11:661 EAGISNTSRLSRGSISSTSEVHSPPNVGLRRSGQIEGVRQMHSNAPRSEIATERDLVAWS 720
           ::::::::::::::::::::::::::::::::::::::::::::::::::::::::::::
hNDRP: 661 EAGISNTSRLSRGSISSTSEVHSPPNVGLRRSGQIEGVRQMHSNAPRSEIATERDLVAWS 720

hWDR11:721 RRVVVPELSAGVASRQEEWRTAKGEEEIKTYRSEEKRKHLTVPKENKIPTVSKNHAHEHF 780
           :::::::::::::::::::::::::::::::::::::::::::::::::: ::::::::::
hNDRP: 721 RRVVVPELSAGVASRQEEWRTAKGEEEIKTYRSEEKRKHLTVPKENKIPIVSKNHAHEHF 780

hWDR11:781 LDLGESKKQQTNQHNYRTRSALEETPRPSEEIENGSSSSDEGEVVAVSGGTSEEEERAWH 840
           ::::::::::::::::::::::::::::::::::::::::::::::::::::::::::::
hNDRP: 781 LDLGESKKQQTNQHNYRTRSALEETPRPSEEIENGSSSSDEGEVVAVSGGTSEEEERAWH 840

hWDR11:841 SDGSSSDYSSDYSDWTADAGINLQPPKKVPKNKTKKAESSSDEEEESEKQKQKQIKKEKK 900
           ::::::::::::::::::::::::::::::::::::::::::::::::::::::::::::
hNDRP: 841 SDGSSSDYSSDYSDWTADAGINLQPPKKVPKNKTKKAESSSDEEEESEKQKQKQIKKEKK 900

hWDR11:901 KVNEEKDGPISP 912
           ::::::::::::
hNDRP: 901 KVNEEKDGPISP 912
```

B.

```
hWDR11:924   RLAVEELTENGLTLEEWLPSTWITDTIPRRCPFVPQMGDEVYYFRQGHEAYVEMARKNKI 983
             ::::::::::::::::::::::::::::::::::::::::::::::::::::::::::::
hPHIP: 1     RLAVEELTENGLTLEEWLPSTWITDTIPRRCPFVPQMGDEVYYFRQGHEAYVEMARKNKI 60

hWDR11:984   YSINPKKQPWHKMELREQELMKIVGIKYEVGLPTLCCLKLAFLDPDTGKLTGGSFTMKYH 1043
             ::::::::::::::::::::::::::::::::::::::::::::::::::::::::::::
hPHIP: 61    YSINPKKQPWHKMELREQELMKIVGIKYEVGLPTLCCLKLAFLDPDTGKLTGGSFTMKYH 120

hWDR11:1044  DMPDVIDFLVLRQQFDDAKYRRWNIGDRFRSVIDDAWWFGTIESQEPLQLEYPDSLFQCY 1103
             ::::::::::::::::::::::::::::::::::::::::::::::::::::::::::::
hPHIP: 121   DMPDVIDFLVLRQQFDDAKYRRWNIGDRFRSVIDDAWWFGTIESQEPLQLEYPDSLFQCY 180

hWDR11:1104  NVCWDNGDTEKMSPWDMELIPNNAVFPEELGTSVPLTDGECRSLIYKPLDGEWGTNPRDE 1163
             ::::::::::::::::::::::::::::::::::::::::::::::::::::::::::::
hPHIP: 181   NVCWDNGDTEKMSPWDMELIPNNAVFPEELGTSVPLTDGECRSLIYKPLDGEWGTNPRDE 240

hWDR11:1164  ECERIVAGINQLMTLDIASAFVAPVDLQAYPMYCTVVAYPTDLSTIKQRLENRFYRRVSS 1223
             ::::::::::::::::::::::::::::::::::::::::::::::::::::::::::::
hPHIP: 241   ECERIVAGINQLMTLDIASAFVAPVDLQAYPMYCTVVAYPTDLSTIKQRLENRFYRRVSS 300

hWDR11:1224  LMWEVRYIEHNTRTFNEPGSPIVKSAKFVTDLLLHFIKDQTCYNIIPLYNSMKKKVLSDS 1283
             ::::::::::::::::::::::::::::::::::::::::::::::::::::::::::::
hPHIP: 301   LMWEVRYIEHNTRTFNEPGSPIVKSAKFVTDLLLHFIKDQTCYNIIPLYNSMKKKVLSDS 360

hWDR11:1284  EDEEKDADVPGTSTRKRKDHQPRRRLRNRAQSYDIQAWKKQCEELLNLIFQCEDSEPFRQ 1343
             ::::::::::::::::::::::::::::::::::::::::::::::::::::::::::::
hPHIP: 361   EDEEKDADVPGTSTRKRKDHQPRRRLRNRAQSYDIQAWKKQCEELLNLIFQCEDSEPFRQ 420

hWDR11:1344  PVDLLEYPDYRDIIDTPMDFATVRETLEAGNYESPMELCKDVRLIFSNSKAYTPSKRSRI 1403
             ::::::::::::::::::::::::::::::::::::::::::::::::::::::::::::
hPHIP: 421   PVDLLEYPDYRDIIDTPMDFATVRETLEAGNYESPMELCKDVRLIFSNSKAYTPSKRSRI 480

hWDR11:1404  YSMSLRLSAFFEEHISSVLSDYKSALRFHKRNTITKRRKKRNRSSSVSSSAASSPERKKR 1463
             ::::::::::::::::::::::::::::::::::::::::::::::::::::::::::::
hPHIP: 481   YSMSLRLSAFFEEHISSVLSDYKSALRFHKRNTITKRRKKRNRSSSVSSSAASSPERKKR 540

hWDR11:1464  ILKPQLKSESSTSAFSTPTRSIPPRHNAAQINGKTESSSVVRTRSNRVVVDPVVTEQPST 1523
             ::::::::::::::::::::::::::::::::::::::::::::::::::::::::::::
hPHIP: 541   ILKPQLKSESSTSAFSTPTRSIPPRHNAAQINGKTESSSVVRTRSNRVVVDPVVTEQPST 600

hWDR11:1524  SSAAKTFITKANASAIPGKTILENSVKHSKALNTLSSPGQSSFSHGTRNNSAKENMEKEK 1583
             ::::::::::::::::::::::::::::::::::::::::::::::::::::::::::::
hPHIP: 601   SSAAKTFITKANASAIPGKTILENSVKHSKALNTLSSPGQSSFSHGTRNNSAKENMEKEK 660

hWDR11:1584  PVKRKMKSSVLPKASTLSKSSAVIEQGDCKNNALVPGTIQVNGHGGQPSKLVKRGPGRKP 1643
             ::::::::::::::::::::::::::::::::::::::::::::::::::::::::::::
hPHIP: 661   PVKRKMKSSVLPKASTLSKSSAVIEQGDCKNNALVPGTIQVNGHGGQPSKLVKRGPGRKP 720

hWDR11:1644  KVEVNTNSGEIIHKKRGRKPKKLQYAKPEDLEQNNVHPIRDEVLPSSTCNFLSETNNVKE 1703
             ::::::::::::::::::::::::::::::::::::::::::::::::::::::::::::
hPHIP: 721   KVEVNTNSGEIIHKKRGRKPKKLQYAKPEDLEQNNVHPIRDEVLPSSTCNFLSETNNVKE 780

hWDR11:1704  DLLQKKNRGGRKPKRKMKTQKLDADLLVPASVKVLRRSNRKKIDDPIDEEEEFEELKGSE 1763
             ::::::::::::::::::::::::::::::::::::::::::::::::::::::::::::
hPHIP: 781   DLLQKKNRGGRKPKRKMKTQKLDADLLVPASVKVLRRSNRKKIDDPIDEEEEFEELKGSE 840

hWDR11:1764  PHMRTRNQGRRTAFYNEDDSEEEQRQLLFEDTSLTFGTSSRGRVRKLTEKAKANLIGW 1821
             ::::::::::::::::::::::::::::::::::::::::::::::::::::::::::
hPHIP: 841   PHMRTRNQGRRTAFYNEDDSEEEQRQLLFEDTSLTFGTSSRGRVRKLTEKAKANLIGW 898
```

Figure 3.5. RT-PCR analysis of PHIP splice forms. Multiple alternatively spliced variants of PHIP exist in mouse tissues. PHIP and NDRP specific primers were used in reverse transcription-polymerase chain reactions (RT-PCR) with RNA isolated from various mouse tissues such as brain, heart, kidney, large intestine (Large Int.), liver, lung, skeletal muscle (SK Muscle), ovary, thymus, spleen and stomach. Lanes labeled with PHIP show an RT-PCR product of 423 bp produced by two specific internal PHIP primers. The forward and reverse primers are located at nucleotides 582-610 and 982-1005, respectively (See Figure 3.1A). Lanes labeled with 5'UTR illustrate an RT-PCR product of 505 bp created by a forward primer in the 5'UTR region of PHIP (nucleotides 98-124) and a nested PHIP reverse primer (nucleotides 577-603). Laslty, lanes labeled with NDRP demonstrate a fusion NDRP-PHIP fusion RT-PCR product of 610 bp generated by a forward NDRP primer and the same reverse PHIP primer as employed for 5'UTR.

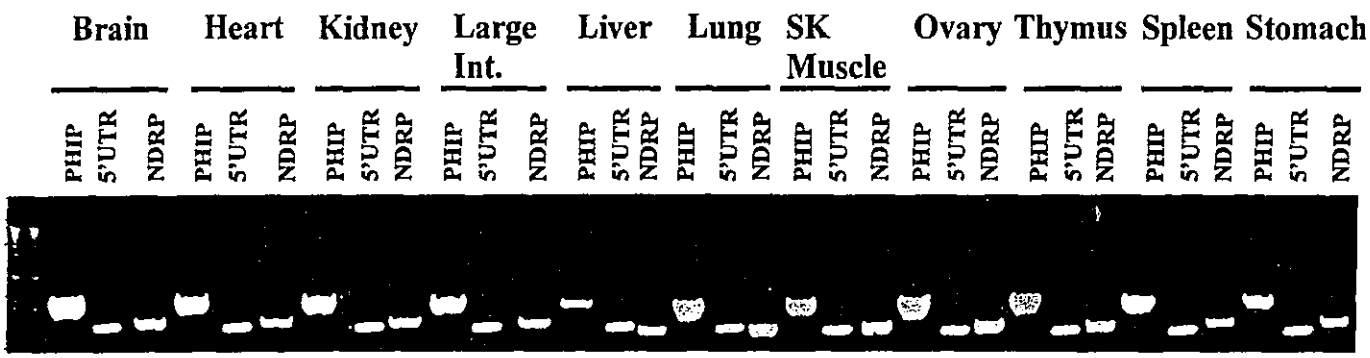
Brain
Heart
Kidney
Large Int.
Liver
Lung
SK Muscle
Ovary
Thymus
Spleen
Stomach
PHIP
5'UTR
NDRP

comparison to the transcript size. This might either be due to a large 5'-UTR or that an NDRP-PHIP fusion (WDR11) transcript was actually detected in the northern blot analysis and post-transcriptional regulation may give rise to PHIP, NDRP, or NDRP-PHIP. To further confirm the northern blot data, PHIP or NDRP specific primers were used in a reverse-transcription-polymerase chain (RT-PCR) with RNA isolated from various mouse tissues. The resulting PCR products verified existence of both PHIP and NDRP-PHIP transcript fragments (Figure 3.5).

3.2.3 PHIP sequences are evolutionary conserved from *Drosophila* to *Human*. Multiple alignment of PHIP protein sequences from Drosophila, Mouse and Human species shows that homology between them extends along their entire sequence with several regions in the sequence being strongly conserved, suggesting that they are essential for PHIP function (Figure 3.6). The IRS-1 PH binding region (PBR) of PHIP is the most conserved, suggesting an evolutionary conserved function. Interestingly, the Drosophila homologue of PHIP starts with a region highly similar to NDRP which extends into the PHIP homologous region encompassing the PBR region, suggesting the expression of a Drosophila homologue of NDRP-PHIP fusion protein or WDR11 (dWDR11). The Drosophila PHIP (dPHIP or dWDR11) carboxy-terminus diverges completely as compared to Mouse or Human PHIP, suggesting a distinct function of this region in mammalian organisms.

3.2.4 Sequence analysis of PHIP family of proteins. PHIP proteins do not share sequence homology with any known proteins. As shown in Figure 3.2, the IRS-1 PH

Figure 3.6. Alignment of PHIP amino acid sequences. **(A)** Alignment of human and mouse PHIP sequences. The initiation methionine of human (h) PHIP is yet to be found, thus amino acid alignment shown started from the 5th amino acid of mPHIP. The amino-terminal and central region of PHIP encompassing the PHIP PBR and the two bromodomains are highly conserved, while the carboxy-terminus hosts less conserved residues. **(B), (C)** Alignment of mouse and Drosophila PHIP and NDRP sequences, respectively. The Drosophila PHIP seqences is depicted as dWR11. The double dots (colon) represent identical amino acids, while single dots represent conserved residues.

A.

```
mPHIP: 5    RLAVGELTENGLTLEEWLPSAWITDTLPRRCPFVPQMGDEVYYFRQGHEAYVEMARKNKI 64
            :::::::::::::::::::.::::.:::::::::::::::::::::::::::::::::::
hPHIP: 1    RLAVGELTENGLTLEEWLPSTWITDTIPRRCPFVPQMGDEVYYFRQGHEAYVEMARKNKI 60

mPHIP: 65   YSINPKKQPWHKMELREQELMKIVGIKYEVGLPTLCCLKLAFLDPDTGKLTGGSFTMKYH 124
            :::::::::::::::::::::::::::::::::::::::::::::::::::::::::::::
hPHIP: 61   YSINPKKQPWHKMELREQELMKIVGIKYEVGLPTLCCLKLAFLDPDTGKLTGGSFTMKYH 120

mPHIP: 125  DMPDVIDFLVLRQQFDDAKYRRWNIGDRFRSVIDDAWWFGTIESQEPLQPEYPDSLFQCY 184
            :::::::::::::::::::::::::::::::::::::::::::: ::::::::::::
hPHIP: 121  DMPDVIDFLVLRQQFDDAKYRRWNIGDRFRSVIDDAWWFGTIESQEPLQLEYPDSLFQCY 180

mPHIP: 185  NVCWDNGDTEKMSPWDMELIPNNAVFPEELGTSVPLTDVECRSLIYKPLDGDWGANPRDE 244
            :::::::::::::::::::::::::::::::::::: :::::::::::.:: :::::
hPHIP: 181  NVCWDNGDTEKMSPWDMELIPNNAVFPEELGTSVPLTDGECRSLIYKPLDGEWGTNPRDE 240

mPHIP: 245  ECERIVGGINQLMTLDIASAFVAPVDLQAYPMYCTVVAYPTDLSTIKQRLENRFYRRFSS 304
            ::::::.:::::::::::::::::::::::::::::::::::::::::::::::: ::
hPHIP: 241  ECERIVAGINQLMTLDIASAFVAPVDLQAYPMYCTVVAYPTDLSTIKQRLENRFYRRVSS 300

mPHIP: 305  LMWEVRYIEHNTRTFNEPGSPIVKSAKFVTDLLLHFIKDQTCYNIIPLYNSMKKKVLSDS 364
            ::::::::::::::::::::::::::::::::::::::::::::::::::::::::::::
hPHIP: 301  LMWEVRYIEHNTRTFNEPGSPIVKSAKFVTDLLLHFIKDQTCYNIIPLYNSMKKKVLSDS 360

mPHIP: 365  EEEEKDADVPGTSTRKRKDHQPRRRLRNRAQSYDIQAWKKQCQELLNLIFQCEDSEPFRQ 424
            :.::::::::::::::::::::::::::::::::::::::::::.::::::::::::::::
hPHIP: 361  EDEEKDADVPGTSTRKRKDHQPRRRLRNRAQSYDIQAWKKQCEELLNLIFQCEDSEPFRQ 420

mPHIP: 425  PVDLLKYPDYRDIIDTPMDFATVRETLEAGNYESPMELCKDVRLIFSNSKAYTPSKRSRI 484
            :::::.::::::::::::::::::::::::::::::::::::::::::::::::::::::
hPHIP: 421  PVDLLEYPDYRDIIDTPMDFATVRETLEAGNYESPMELCKDVRLIFSNSKAYTPSKRSRI 480

mPHIP: 485  YSMSLRLSAFFEEHISSVLSDYKSALRFHKRNTISKKRKKRNRSSSLSSSAASSPERKKR 544
            ::::::::::::::::::::::::::::::::.:.:::::::::.::::::::::::::
hPHIP: 481  YSMSLRLSAFFEEHISSVLSDYKSALRFHKRNTITKRRKKRNRSSSVSSSAASSPERKKR 540

mPHIP: 545  ILKPQLKSEVSTSPFSIPTRSVLPRHNAAQMNGKPESSSVVRTRSNRVAVDPVVTEQPST 604
            ::::::::: ::: :: :::::. ::::::::.::: ::::::::::::.::::::::::
hPHIP: 541  ILKPQLKSESSTSAFSTPTRSIPPRHNAAQINGKTESSSVVRTRSNRVVVDPVVTEQPST 600

mPHIP: 605  SSATKAFVSKTNTSAMPGKAMLENSVRHSKALSTLSSPDPLTFSHATKNNSAKENMEKEK 664
            :::.:.:..:.:.::.:::..:::::.:::::.::::: ...::::.:.::::::::::::
hPHIP: 601  SSAAKTFITKANASAIPGKTILENSVKHSKALNTLSSPGQSSFSHGTRNNSAKENMEKEK 660

mPHIP: 665  PVKRKMKSSVFSKASPLPKSAAVIEQGECKNNVLIPGTIQVNGHGGQPSKLVKRGPGRKP 724
            ::::::::::. ::: : ::.:::::::.::::.:.:::::::::::::::::::::::
hPHIP: 661  PVKRKMKSSVLPKASTLSKSSAVIEQGDCKNNALVPGTIQVNGHGGQPSKLVKRGPGRKP 720

mPHIP: 725  KVEVNTSSGEVTHKKRGRKPKNLQCAKQENSEQNNMHPIRADVLPSSTCNFLSETNAVKE 784
            :::::::.::::. ::::::::::.:: :: :. ::::.:::: .:::::::::::::.:::
hPHIP: 721  KVEVNTNSGEIIHKKRGRKPKKLQYAKPEDLEQNNVHPIRDEVLPSSTCNFLSETNNVKE 780

mPHIP: 785  DLLQKKSRGGRKPKRKMKTHNLDSELIVPTNVKVLRRSNRKKTDDPIDEEEEFEELKGSE 844
            ::::::.:::::::::::::..::..:.::..:::::::::::.::::::::::::::::
hPHIP: 781  DLLQKKNRGGRKPKRKMKTQKLDADLLVPASVKVLRRSNRKKIDDPIDEEEEFEELKGSE 840

mPHIP: 845  PHMRTRNQGRRTTFYNEDDSEEEQRQLLFEDTSLTFGTSSRGRVRKLTEKAKANLIGW 902
            ::::::::::::.::::::::::::::::::::::::::::::::::::::::::::::
hPHIP: 841  PHMRTRNQGRRTAFYNEDDSEEEQRQLLFEDTSLTFGTSSRGRVRKLTEKAKANLIGW 898
```

B.

```
mPHIP: 14   NGLTLEEWLPSAWITDTLPRRCPFVPQMGDEVYYFRQGHEAYVEMARKNKIYSINPKKQP 73
dWR11: 983  NGEIPELYRPAEWLSEVIPRKAPYYPQMGDEVVYFRQGHAKYLDAVRLKKVYKLSHSSEP 1042

mPHIP: 74   WHKMELREQELMKIVGIKYEVGLPTLCCLKLAFLDPDTGKLTGGSFTMKYHDMPDVIDFL 133
dWR11: 1043 WNFHTLRDHELVRVIGIKYEIRPPRLCCLKLAIIDEE-GNMTGTTFKIKYHDMPDVLDFL 1101

mPHIP: 134  VLRQQFDDAKYRRWNIGDRFRSVIDDAWWFGTIESQEPLQPEYPDSLFQCYNVCWDNGDT 193
dWR11: 1102 VLRQTFDLAVQRNWSIGDRFRCMIVDGWWMGQIESRHALSADFPDSSFMCFRVRWDNGEY 1161

mPHIP: 194  EKMSPWDMELIPNNAVFPEELGTSVPLTDVECRSLIYKPLDGDWGANPRDEECERIVGGI 253
dWR11: 1162 EFMSPWDMEPIDQQRV-PDEVGGAVPVLPEEIRATLYQPKSEEWHRGDRDGTCRRIINGL 1220

mPHIP: 254  NQL 256
dWR11: 1221 EQV 1223
```

C.

```
dWR11: 3    TRQPSSGDDLKPELYFLISKFLAAGPLEETAKVLIRELEEKKVLPRRLDWQGNEHEQTFE 62
mNDRP: 2    SRERKGLSELRSELYFLIARFLEDGPCQQAAQVLIREVAEKELLPRRTDWTGKEHPRTYQ 61

dWR11: 63   ELERKYKHIGANHLLEICSRLGPLVDRELPPSVPGINSLLGTGRQNLLRT----KETVYC 118
mNDRP: 62   NLVKYYRHLAPDHLLQICHRLGPLLEQEIPQSVPGVQTLLGAGRQSLLRTNKSCKHVVWK 121

dWR11: 119  HRSLRD-YCTRLNGVSLPDSVLTKPTH-NLDRVLTGREHGGEVRRKLLVPTDLYRRTKLL 176
mNDRP: 122  GSALAALHCGRP-----PESPVNYGSPPSIADTLFSRKLNGKYRLERLVPTAVYQHMKMH 176

dWR11: 177  RRTVGHLSSVYCVLFDRTGRYIITGADDLLIKIWSAADGRLLATLRGASSEITDIAINLD 236
mNDRP: 177  KRILGHLSSVYCVTFDRTGRRIFTGSDDCLVKIWATDDGRLLATLRGHAAEISDMAVNYE 236

dWR11: 237  NTMLAAGSLDHILRVWDMQTTSPIAVLSAHTGMITSVNFCPSPRSDLKYLVTTSTDGSIA 296
mNDRP: 237  NTMIAAGSCDKMIRVWCLRTCAPLAVLQGHSASITSLQFSPLCSGSKRYLSSTGADGTIC 296

dWR11: 297  FWQYSTPRGQKITFAPKPTQYHEKLRPGQAQMMCTTFSPGGIFLAAGSADHHVRVYMMGE 356
mNDRP: 297  FWLWD---AGTLKINPRPTKFTERPRPG-VQMICSSFSAGGMFLATGSTDHIIRVYFFGS 352

dWR11: 357  DGPKRILETEAYTDAVDSVQWSHRGLRFISGSKDGTAHIWTFESQQWKSSKLCMTERLAS 416
mNDRP: 353  GQPEKISELEFHTDKVDSIQFSNTSNRFVSGSRDGTARIWQFKRREWKSILLDMATRPAG 412

dWR11: 417  CP-EPEEGK--RLKVTMVAWDASDRYVITAVNDFTIKIWDSKSAKLHRVLRGHKDELYVL 473
mNDRP: 413  QNLQGIEDKITKMKVTMVAWDRHDNTVITAVNNMTLKVWNSYTGQLIHVLMGHEDEVFVL 472

dWR11: 474  ESNPRDEHVLLSAGHDGQVFLWDIEQGVCVANFLNDIDGQGHGSVFDAKWSPDGTMIAAT 533
mNDRP: 473  EPHPFDPRVLFSAGHDGNVIVWDLARGVKVRSYFNMIEGQGHGAVFDCKCSPDGQHFACT 532

dWR11: 534  DSHGHILIFGLGVCIEKYKMLPTELFFHTDFRPLLRDAQHHVVDEQTQIMPHLMPPPFLV 593
mNDRP: 533  DSHGHLLIFGFG-SSSKYDKIADQMFFHSDYRPLIRDANNFVLDEQTQQAPHLMPPPFLV 591

dWR11: 594  DADGNPHPSRFQRFVPGRESCSLDQLIPNLTVGVDGVVIDDGGAGGDAVVAAAPAEAPPA 653
mNDRP: 592  DVDGNPHPSRYQRLVPGRENCREEQLIPQM----------------------------GVTS 625

dWR11: 654  ALPPAAAGGPQGANYSHIDRMIAALANRQSVNVNANDANPTNGNQSFERLTNRQMPDSNG 713
mNDRP: 626  SGLNQVLSQQANQDISPLDSMIQRLQQEQDLR-RSGEAGVSNASR-----VNRGSVSSTS 679

dWR11: 714  RQSSRGNVLGSRLSTPRQGWGAA-AAAPVEDQAGPSQPFAEPAAEPGQAQVQQALPLKFI 772
mNDRP: 680  EVHSPPNI-GLRRSGQIEGVRQMHSNAPRSEIATERDL----------------VAWS 720

dWR11: 773  RRTYVRPMKYPQLQNLKQTIYSAGQFEKQEYKREMRRRPIMINTASAASSQQPGSVVGRP 832
mNDRP: 721  RRVVVPELSAGVASRQEEWRTAKGEEEIKSYRSEEKRKHLTV----------AKENKI 768

dWR11: 833  RNTRGNGGGARAGRRRGPQPAGGQPQPAYRTRAVRDQEPEHYDEVAPPPEEEEEDVSSNS 892
mNDRP: 769  LTVSKNHAHEHFLDLGDSKKQQANQHN-YRTRSALEETPRPLEEL--ENGTSSSDEGEVL 826

dWR11: 893  SGDTSYSNVEENLEDSSDESETDSSDYSDWVADTPGPNLEPPKRSKRKPLSRRPRSSDDS 948
mNDRP: 827  AVSGGTSEEEERAWHSDGSSSDYSSDYSDWTADA-GINLQPPKKVPKHKTKKPESSSDEE 885

dWR11: 949  SDDERAGRSRGGQVTAR----KVG----------RKTVLFPPTDANGEIPELYRPAE 995
mNDRP: 886  EESENQKQKHIKKERKKANEEKDGPTSPKKKKPKERKQKRLAVGELTENGLTLEEWLPSA 945

dWR11: 996  WLSEVIPRKAPYYPQMGDEVVYFRQGHAKYLDAVRLKKVYKLSHSSEPWNFHTLRDHELV 1055
mNDRP: 946  WITDTLPRRCPFVPQMGDEVYYFRQGHEAYVEMARKNKIYSINPKKQPWHKMELRVN--- 1001

dWR11: 1056 RVIGIKYEIR 1065
mNDRP: 1002 --IGIFFNVK 1010
```

binding region is located at the amino-terminus of the protein (residues 5-209). The only defined structural motifs within PHIP are two bromodomains, BD1 (residues 230 to 345) and BD2 (387 to 503), located in tandem in the centre of the molecule (Figure 3.2). Bromodomains are conserved sequences of approximately 100aa that have been proposed to mediate protein-protein interactions (Jeanmougin et al., 1997). A homology search revealed that PHIP BD sequences were most homologous (44% identity, 61% homology) to the bromodomain of mouse CBP (CREB binding protein) (Figure 3.7) a transcriptional coactivator (Chrivia et al., 1993).

PHIP proteins contain multiple putative tyrosine, serine and threonine residues in consensus sequences for many protein kinases, including cAMP and cGMP-dependent protein kinase, casein kinase II, protein kinase C and tyrosine kinases.

NDRP proteins contain six WD-repeats motifs (residues 181-211, 223-253, 265-299, 353-393, 417-452, and 464-495) and multiple potential nuclear localization signals (NLS) in the C-terminal region (Kato et al., 2000). WD-repeats motifs are defined by the presence of four to eight repeating units containing a conserved core of approximately 40 aa that often end with tryptophan-aspartic acid (WD). These motifs are found in many signaling proteins that regulate essential biological functions including gene transcription, cell division, apoptosis, vesicle fusion, and protein ubiquitination and degradation. Multiple NLSs have been shown to be involved in differential localization of NDRP proteins to the neuronal cell nucleus, depending on the stage of neuronal differentiation (Kato et al., 2000).

Figure 3.7. Alignment of human and mouse PHIP bromodomains. Structure-based sequence alignment between first and second hPHIP and mPHIP bromodomains (h/mPHIPBD1 and h/mPHIPBD2, respectively) with human CBP (CREB binding protein, GenBank Accession number 1345703). Structural subdomains are shown in dark gray boxes and highly conserved residues are highlighted in bold.

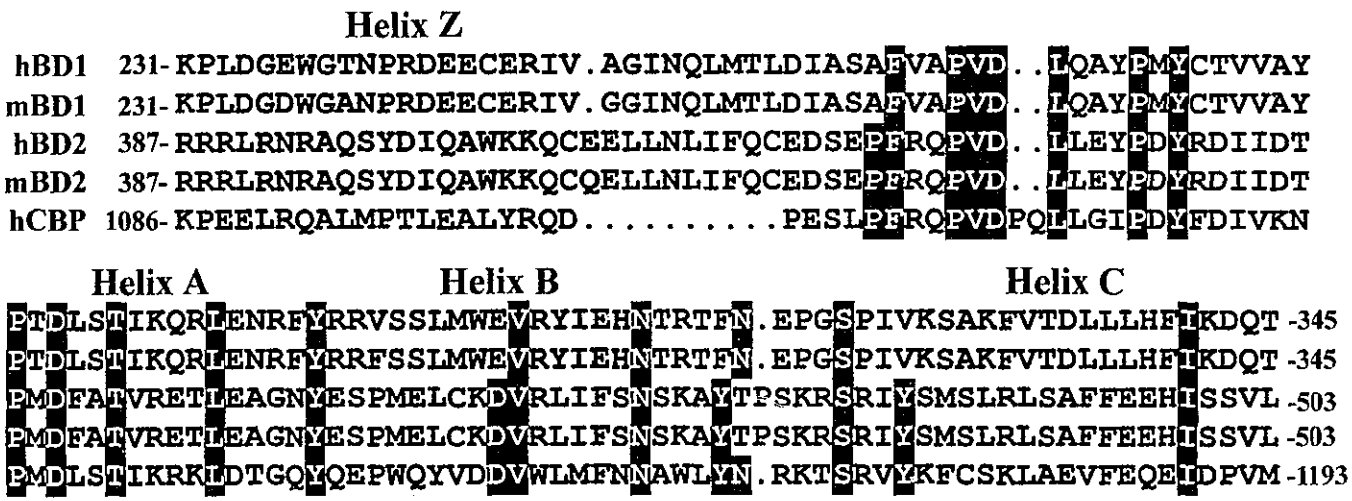
Helix Z
hBD1 231- KPLDGEWGTNPRDEECERIV.AGINQLMTLDIASAFVAPVD..LQAYPMYCTVVAY
mBD1 231- KPLDGDWGANPRDEECERIV.GGINQLMTLDIASAFVAPVD..LQAYPMYCTVVAY
hBD2 387- RRRLRNRAQSYDIQAWKKQCEELLNLIFQCEDSEPFRQPVD..LLEYPDYRDIIDT
mBD2 387- RRRLRNRAQSYDIQAWKKQCQELLNLIFQCEDSEPFRQPVD..LLEYPDYRDIIDT
hCBP 1086- KPEELRQALMPTLEALYRQD.....PESLPFRQPVDPQLLGIPDYFDIVKN
Helix A
Helix B
Helix C
PTDLSTIKQRLENRFYRRVSSLMWEVRYIEHNTRTFN.EPGSPIVKSAKFVTDLLLHFIKDQT -345
PTDLSTIKQRLENRFYRRFSSLMWEVRYIEHNTRTFN.EPGSPIVKSAKFVTDLLLHFIKDQT -345
PMDFATVRETLEAGNYESPMELCKDVRLIFSNSKAYTPSKRSRIYSMSLRLSAFFEEHISSVL -503
PMDFATVRETLEAGNYESPMELCKDVRLIFSNSKAYTPSKRSRIYSMSLRLSAFFEEHISSVL -503
PMDLSTIKRKLDTGQYQEPWQYVDDVWLMFNNAWLYN.RKTSRVYKFCSKLAEVFEQEIDPVM -1193

3.2.5 Anti-PHIP antibodies recognize ectopically expressed and endogenous PHIP.

In order to assay initial biochemical characterization of PHIP, an antibody specific to this protein was generated. A glutathione S-transferase (GST)-PHIP fusion protein containing amino acids 5-209 of mouse PHIP ($PHIP^{5-209}$) was expressed in bacterial cells and subsequently purified using glutathione sepharose beads. To ensure the purity and to estimate the protein amount, one microgram of the purified GST-PHIP fusion protein was electrophoresed on a SDS-PAGE gel and total protein was visualized by Coomassie Blue stain (Figure 3.8A). Polyclonal anti-PHIP antibodies were subsequently generated after several subcutaneous injections of the GST-PHIP fusion protein into two rabbits (A and B, See 2.7.1) and the serum containing the antibody fraction was later isolated. The anti-PHIP antibodies derived from rabbit A were exclusively used in the experiments presented in this study. To confirm that anti-PHIP antibodies recognize PHIP proteins, an *in vitro* transcription-translation assay with a linearized pCMV-PHIP construct encoding hemagglutinin (HA)-PHIP (residues 5-209) was performed. A single major product of about 24 KDa was immunoprecipitated from the cell-free rabbit reticulocyte extract using anti-PHIP antibodies and not pre-immune sera (Figure 3.8B). In addition, ectopically expressed HA-$PHIP^{5-209}$ in 293 cells, which was immunoprecipitated with anti-HA antibodies were detected with anti-PHIP antibodies by Western blot analysis (Figure 3.8C). These data demonstrate that antibodies specific to PHIP were successfully generated which could be employed in both immunoprecipitation and immunoblot analysis.

To test for anti-PHIP antibody immunoreactivity towards endogenous PHIP, lysates from mammalian cells were used in Western blot analysis. Anti-PHIP antibodies identified a

Figure 3.8. Anti-PHIP antibodies recognize ectopically expressed PHIP. **(A)** Anti-PHIP antibodies are generated against GST-PHIP fusion proteins containing PHIP PH binding region (PBR, residues 5-209). A small aliquot (1/200) of the purified protein was run on 10% SDS-PAGE and the purity and the concentration of the GST-PHIP fusion protein was assessed by comparison with the standard bovine serum albumin (BSA, 2μg, 6 μg, 12 μg) on Coomassie Blue stained gel. The expressed fusion protein was approximately 45 kilodaltons (KDa), corresponding to GST (approximately 23 KDa) and residues 5-209 of PHIP (approximately 22 KDa). **(B)** Anti-PHIP antibodies recognize a 22 KDa *in-vitro* transcribed and translated $PHIP^{5-209}$ protein. One tenth of the reaction lysate was diluted in 1 ml of PLC lysis buffer and subjected to immunoprecipiation (IP) assays using preimmune or anti-PHIP containing serum. The precipitated proteins were electrophoresed on a 10% SDS-PAGE and the dried gel was exposed to an X-ray film **(C)** Anti-PHIP antibodies recognize ectopically expressed truncated hemagglutinin antigen (HA)-PHIP proteins. Human embryonic kidney 293 cells were transiently transfected with either pCAN vector control or pCAN/DN-$PHIP^{5-209}$ construct with lipofectamine reagent (Gibco BRL) according to manufacturer's protocol. Transfected cell lysates were subjected to immunoprecipitation and subsequent Western blotting using anti-HA and anti-PHIP antibodies, respectively.

A.

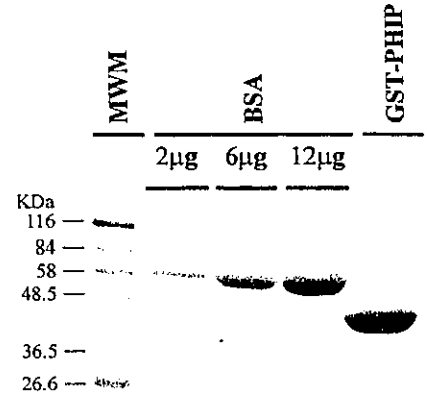
MWM
BSA
GST-PHIP
2μg
6μg
12μg
KDa
116
84
58
48.5
36.5
26.6

B.


IP:
α–PreImm.
α–PHIP
PHIP

C.

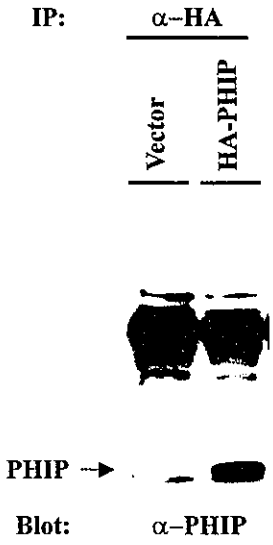
IP:
α–HA
Vector
HA-PHIP
PHIP
Blot:
α–PHIP

Figure 3.9. Immunoblot analysis of PHIP protein. (A) PHIP migrates with an apparent molecular mass of 104 kDa. PHIP was immunoprecipitated from multiple myeloma U266 cell lysates and immunoblotted with anti-PHIP antibodies. Rabbit preimmune serum was used as a control. (**B**) Two forms of PHIP (97 and 104 KDa) observed in anti-PHIP immunoprecipitates from cell lysates of U266, human A431 epidermoid carcinoma, Rat-2 and mouse NIH/3T3 fibroblasts.

A.

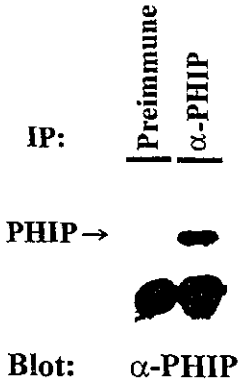
IP:
Preimmune
α-PHIP
PHIP→
Blot:
α-PHIP

B.

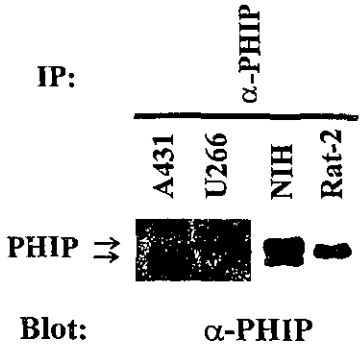
IP:
α-PHIP
A431
U266
NIH
Rat-2
PHIP ⇊
Blot:
α-PHIP

104 KDa protein from U266 cell lysates, which was not precipitated by pre-immune sera (Figure 3.9A). Further analysis of PHIP expression in mammalian cell extracts revealed two forms of PHIP protein, the long 104 KDa form and a shorter 97 KDa form (Figure 3.9B). The 97 KDa and 104 KDa polypeptides likely result from alternative usage of two putative translation initiation sites (Met1 and Met41, see Figure 3.1) as ectopic expression of full-length hPHIP containing both sites produced a doublet in PHIP immunoblots (data not shown).

3.2.6 An intact PH domain is required for PHIP/IRS-1 association. To recapitulate the interaction of PHIP with the IRS-1 PH domain in mammalian cells and to examine whether a functional PH domain or a smaller motif within the domain is responsible for PHIP binding, three independent mutants of the IRS-1 PH domain that disrupt the PH fold were generated. PH^{NT} encompasses the first half of the IRS-1 PH domain, spanning residues 3-67, PH^{CT} comprises the C-terminal residues 55-133, and PH^{W106A} defines a mutant where the Tryptophan at position 106, a residue conserved in all PH domains, was changed to Alanine. Cell extracts isolated from Cos-1 transiently expressing these PH domain mutants were mixed with bacterially expressed GST-$PHIP^{5-209}$ fusion protein. As expected, all three PH-domain mutants did not detectably associate with GST-PHIP, consistent with the notion that an intact PH domain is required for PHIP binding (Figure 3.10).

3.2.7 PHIP stably associates with IRS-1 *in vivo*. To investigate the interaction of PHIP and IRS-1 *in vivo*, lysates from NIH/IR cells (NIH3T3 cells overexpressing the insulin

Figure 3.10. PHIP interaction with IRS-1 requires an intact PH domain. Binding of IRS-1 PH domain mutants to PHIP. Left, anti-HA antibodies are used in immunodetection of HA-tagged IRS-1 PH domain mutants from whole cell lysates of transiently transfected COS-1 cells with PH^{WT}, PH^{NT}, PH^{CT}, PH^{W106A}; Right, cell lysates expressing the indicated IRS-1 PH domain mutant were mixed with either GST or GST-PHIP (PBR) proteins. Immunecomplexes immobilized on glutathione sepharose beads were then separated on 10% SDS-PAGE and subjected to western blot analysis with anti-HA antibodies.

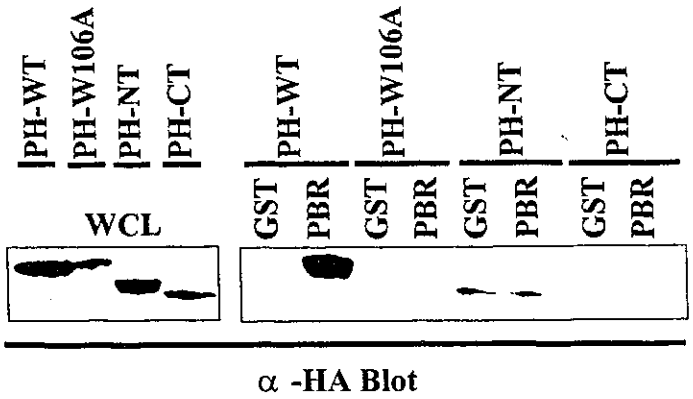
PH-WT
PH-W106A
PH-NT
PH-CT
WCL
GST
PBR
PH-WT
PH-W106A
PH-NT
PH-CT
GST
PBR
GST
PBR
GST
PBR
α -HA Blot

receptor) were immunoprecipitated with anti-IRS-1 antibodies directed against the C-terminus of IRS-1. Endogenous PHIP was found to associate with IRS-1 in both unstimulated and insulin-treated cells. (Figure 3.11, lanes 1 and 2). In contrast, when antibodies directed against the IRS-1 PH domain were used in similar co-immunoprecipitation assays, no interaction was detected, confirming that structural determinants within the PH domain of IRS-1 confer binding to PHIP. Based on the observation that IRS-1 and IRS-2 PH domains are highly conserved (60% amino acid identity) and have been shown to be functionally interchangeable in promoting substrate recognition by the insulin receptor (Burks et al., 1997), it was predicted that IRS-2 might also associate with PHIP *in vivo*. To test this hypothesis, anti-IRS-2 antibodies were used in analogous co-immunoprecipitation studies. Indeed, PHIP could be readily detected in anti-IRS-2 immunoprecipitates, consistent with the notion that PHIP may have a conserved function in recruiting members of the IRS protein family to activated insulin receptor complexes (Figure 3.11, lane 7).

3.2.8 Stoichiometric analysis of PHIP and IRS-1 association. In order to address the stoichiometry of PHIP/IRS-1 interaction in cells expressing endogenous levels of these proteins, [^{35}S]methionine labeled proteins from L6GLUT4myc (L6 myoblasts stably expressing myc-tagged GLUT4 glucose transporter) cell extracts were analyzed by immunoprecipitation with either anti-PHIP or anti-IRS-1 antibodies (Figure 3.12A). Immunoprecipitation with anti-IRS-1 antibodies resulted in coprecipitation of approximately 50% of PHIP proteins as compared to the amount of PHIP that was directly precipitated with anti-PHIP antibodies. No corresponding PHIP protein band was

Figure 3.11. PHIP stably associates with IRS-1 *in vivo*. Coimmunoprecipitation of PHIP and IRS-1 proteins. Serum deprived NIH/IR cells were either left unstimulated or stimulated with insulin (2 μM, 5 minutes). Cell lysates immunoprecipitated with anti-IRS-1^{PCT} , anti-IRS-1^{PH} or anti-PHIP antibodies and subjected to western blotting with anti-PHIP antibodies. Anti-IRS-2 antibodies were used to coimmunoprecipitate IRS-2/PHIP complexes from asynchronized cells.

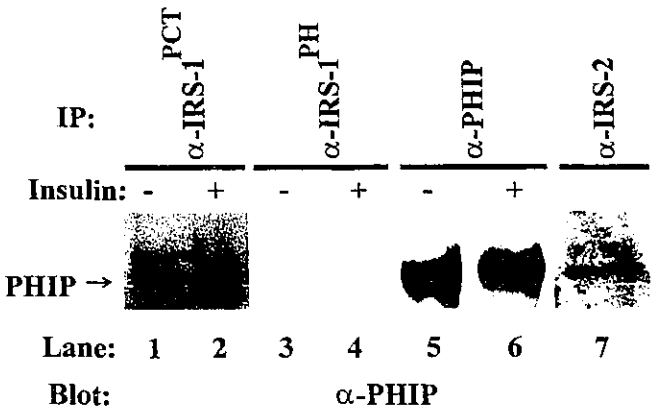
IP:
α-IRS-1PCT
α-IRS-1PH
α-PHIP
α-IRS-2
Insulin: - + - + - + -
PHIP →
Lane: 1 2 3 4 5 6 7
Blot: α-PHIP

Figure 3.12. Stoichiometric analysis of the PHIP-IRS-1 interactions. **(A)** Preimmune serum, anti-IRS-1^{PCT} and anti-PHIP antibodies were used in coimmunoprecipitation analysis of metabolically labeled cellular lysates from L6GLUT4myc cells. The precipitated proteins were electrophoresed on a 7.5% SDS-PAGE and the dried gel was exposed to an X-ray film. **(B)** PHIP is the major component of IRS-1 complexes in L6 cells. Fifty migrogram of whole cell lysate (WCL) from L6GLUT4myc cells was subjected to western blotting with anti-IRS-1 or anti-PHIP antibodies as indicated. One milligram of the same lysate was used in coimmunoprecipitation analysis using preimmune serum, anti-PHIP and anti-IRS-1 antibodies (lanes 2, 3, and 5). Anti-IRS-1 immunodepleted (ID) supernatant was subsequently used to immunprecipitate PHIP with anti-PHIP antibodies (lane 5).

A.

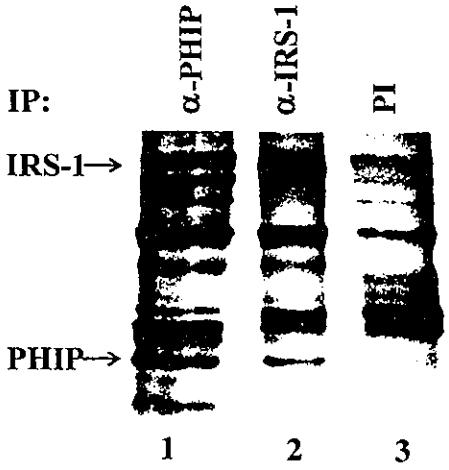
IP:
α-PHIP
α-IRS-1
PI
IRS-1→
PHIP→
1
2
3

B.

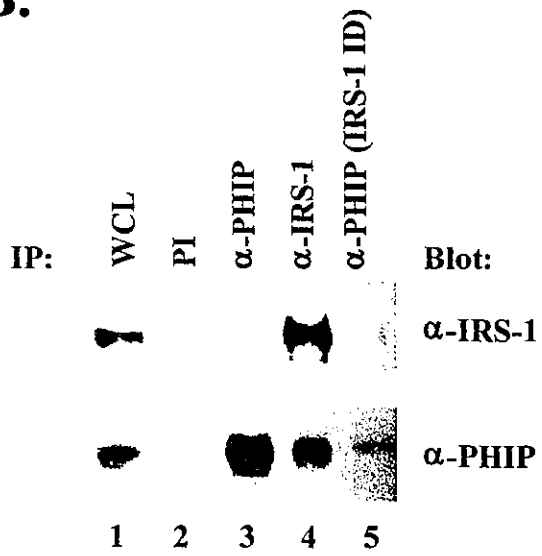
IP:
WCL
PI
α-PHIP
α-IRS-1
α-PHIP (IRS-1 ID)
Blot:
α-IRS-1
α-PHIP
1
2
3
4
5

observed when preimmune serum was used in the same immunoprecipitation assays. To ascertain the specificity of the proteins coprecipitated with anti-PHIP antibodies, the serum was pretreated with either immobilized GST or GST-PHIP fusion protein before immunoprecipitation. Immunodepleted anti-PHIP serum was then used to precipitate protein complexes from L6GLUT4myc cell lysate. GST-PHIP but not GST pre-treated serum effectively depleted the PHIP antibodies from rabbit polyclonal IgG pool as it alleviated precipitation of PHIP and its associated complexes, confirming the specificity of anti-PHIP antibodies in precipitating these proteins (data not shown).

In order to determine whether PHIP is a major component of IRS-1 interacting proteins, anti-IRS-1 antibodies were used in coprecipitation assays on lysates form L6GLUT4myc cells. Consistent with the results obtained by *in-vivo* labeling of L6GLUT4myc cells, approximately half of PHIP proteins coprecipitated with anti-IRS-1 antibodies (Figure 3.12B). IRS-1 immunodepletion from cell lysates using anti-IRS-1 antibodies prior to precipitation of PHIP proteins with anti-PHIP antibodies resulted in a major depletion of PHIP as well. Based on these observations, it was concluded that in L6 myoblasts a significant portion of native PHIP is within a physical complex with IRS-1.

3.2.9 PHIP is not a substrate of the activated insulin receptor. To establish whether PHIP directly interacts with the insulin receptor, coimmunoprecipitation assays were performed using anti-PHIP antibodies. Immunoblot analysis with anti-IR antibodies failed to reveal a direct interaction (data not shown). Similar results have previously been reported for the association of the IR with either IRS-1 or the Shc adaptor protein, suggesting that IR/effector interactions are weak or transient in nature and not detected in

receptor immune complexes (Backer et al., 1993; Pronk et al., 1993; Yenush et al., 1996a).

As there are several potential tyrosine phosphorylation sites in the PHIP sequence, it is conceivable that PHIP may serve as a substrate of the insulin receptor *in vivo*. To examine this idea, anti-PHIP antibodies were employed in immunoprecipitations experiments with unstimulated or insulin-stimulated 293 cell lysates. Anti-PHIP immunoprecipitates failed to show any discernable PHIP phosphorylation upon insulin stimulation on anti-phosphotyrosine immunoblots (Figure 3.13). PHIP however inducibly associated with a prominent 103 KDa phosphoprotein whose identity remains unknown.

Figure 3.13 PHIP is not a substrate of IR. PHIP was immunoprecipitated from untreated and insulin-treated (100 nM, 5 minutes) human kidney 293 cell extracts using anti-PHIP antibodies. Immune-complexes were resolved by 7.5% SDS-PAGE and immunoblotted with anti-phosphotyrosine antibodies (anti-pTyr). The blot was stripped and reprobed with anti-PHIP antibodies. A 103 KDa phosphoprotein of unknown identity is denoted by an asterisk.

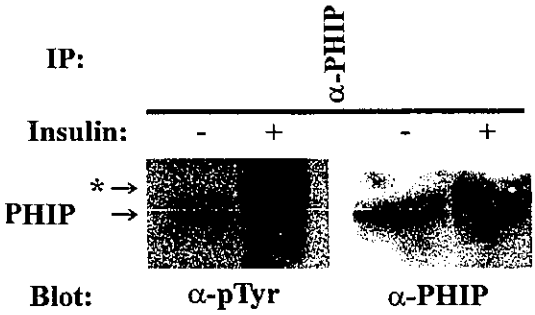
IP:
α-PHIP
Insulin:
-
+
-
+
*→
PHIP
→
Blot:
α-pTyr
α-PHIP

3.3 DISCUSSION

In this chapter, I have identified a novel protein, named PHIP for **PH** Interacting **P**rotein that selectively binds to the PH domain of IRS-1 *in vitro* and complexes with IRS-1 and IRS-2 *in vivo*. Full-length mouse and human PHIP cDNAs revealed an open reading frame of 2706 and 2694 nucleotides, encoding 902 and 898 amino acids, respectively. Sequence analysis of mouse PHIP cDNA identified 219 nucleotides of 5'-untranslated and 903 nucleotides of 3'-untranslated sequences. The latter contained a putative poly adenylation signal of ACTAAA, which fits the pattern of the consensus polyadenylation NNTANA sequence (Beaudoing et al., 2000) , 843 nucleotides downstream of the TAA termination codon and 49 nucleotides upstream of a polyadenine tract. Human PHIP cDNA revealed only a short 121 nucleotide 3'-UTR which contained a putative TATAAA polyadenylation signal 29 nucleotides downstream from the stop codon. It was followed by a 16 nucleotide polyadenine tract. Several cDNA screening and 5'RACE attempts failed to isolate complete human PHIP N-terminal region. This could be due to a complex secondary mRNA structure present at PHIP 5'-UTR, preventing complete denaturation of the transcript, hence progression of the reverse transcriptase enzyme during the cDNA creation.

Sequence comparison between mouse and human PHIP revealed a remarkable 88% identity at the nucleotide level, and 92.3% identity at the level of deduced amino acid sequence. While IRS-1 PH binding region of human PHIP was 98.5% identical to mouse PHIP, it was 53.6% identical to that of Drosophila. Amino acid sequence similarity between human/mouse and Drosophila PHIP is confined to the PBR region. This is

consistent with approximately 40% identity observed between CHICO, the Drosophila homologue of IRS proteins (Bohni et al., 1999), and IRS1-4 N-terminal region, encompassing the PH and PTB domains, suggesting an evolutionary conserved function of these regions in insulin signaling. Further analysis of Drosophila PHIP function will broaden our vision on the evolutionary importance of this molecule in regulating insulin responses.

The quest to identify PH domain binding motifs has lead to the discovery of two categories of ligands, proteins and lipids. The physiological relevance of the PH domain interactions with the latter remains controversial for the majority of the PH-domain containing proteins. The PH domain interactions with proteins however have identified both linear and conformational epitopes. For example, the PH domains from βARK and BTK bind to the βγ subunit of the heterotrimeric G proteins, which is composed of a coiled-coil region (Pitcher et al., 1995; Tsukada et al., 1994), a superhelical structure, suggesting that PH domains might recognize a conformational epitope. Interestingly, IRS-1 PH binding region of PHIP forms a highly helical three-dimensional structure, supporting the latter hypothesis. More recently however, one study indicated that the PH domain of IRS-1 binds to short stretches of acidic residues such as KVAEEEDDEE found in nucleolin I (Burks et al., 1998). Although, PHIP PBR contains several acidic residues that could potentially form a motif at the surface of its helices, these residues don't shape a linear motif. Noticeably, consistent with the earlier study, there is a stretch of acidic residues DDPIDEEEEFEE at PHIP C-terminus that could potentially associate with the PH domain. Future structural and mutational analysis would provide crucial insights into the nature of PHIP and IRS-1 interactions.

PHIP proteins also contain two bromodomains whose function remains to be defined. Bromodomains are structural modules involved in various protein-protein interactions through their association with acetylated lysine residues. Although, the majority of bromodomain-containing proteins also contain acetyltransferase activity involved in transcriptional regulation, the enzymatic activity is not always required for transcriptional activation. One example is CREB (cAMP response element-binding protein) binding protein (CBP), a transcriptional coactivator whose histone acetyltransferase (HAT) activity is not essential for nuclear receptor gene transcription (Korzus et al., 1998; Kurokawa et al., 1998). A homology search revealed that PHIP BD sequences were 61% homologous to the bromodomain of mouse CBP, suggesting that although PHIP proteins do not contain any enzymatic activity they may yet function as scaffolds to assemble multiprotein transcriptional complexes. Consistent with this idea, indirect immunofluorescence analysis by polyclonal anti-PHIP antibodies detected proteins localized in the nucleus of some cells (data not shown). Although, PHIP does not possess canonical nuclear localization sequences to promote its import into the nucleus, PHIP might be interacting with proteins that are nuclear bound. Moreover, as it will be discussed in the next chapter, while, ectopic expression of PHIP enhanced insulin-induced transcriptional responses via MAP kinase signaling pathway, PHIP overexpression promoted SRE-fos luciferase gene transactivation independent of MAP kinases in untreated cells, providing evidence for a potential direct transcriptional regulatory role of PHIP. In addition, CBPs have been shown to activate c-fos gene transcription, raising the intriguing speculation that PHIP might form complexes with CBPs thereby regulating transcription factor assembly. It would be interesting to

determine whether PHIP can bind to CBPs or other transcriptional coactivators. Future analysis of the role of PHIP in association with transcriptional coactivators and regulators would shed light to its function in regulating transcription.

The conceptual translation of PHIP cDNA predicts a protein of relative molecular mass of 100 KDa. Anti-PHIP antibodies however specifically immunoprecipitated proteins of 104 KDa in size, suggesting post-translational modifications might be affecting PHIP migration during SDS gel electrophoresis. In addition, PHIP contains several putative tyrosine, serine and threonine that if phosphorylated could give rise to a significant retardation in the mobility of the protein. PHIP proteins are tyrosine phosphorylated at low levels under basal conditions that remains constant upon insulin stimulation and could at least partially account for the differences between the predicted and observed molecular masses. It is worth noting that while PHIP might also be phosphorylated at serine and threonine residues in quiescent cells, this event does not seem to be inducible as insulin stimulation does not detectibly affect migration of PHIP proteins during SDS-PAGE, over time. Phosphoamino acid analysis and tryptic peptide mapping are required to corroborate basal and insulin-induced phosphorylation state of PHIP.

CHAPTER FOUR

CHARACTERIZATION OF THE ROLE OF PHIP IN INSULIN SIGNALING

4.1 INTRODUCTION

As major substrates of the insulin receptor, IRS-1 proteins play a central role in transducing many of the diverse biological effects of insulin including mitogenesis, gene expression and glucose transport. The C-terminal portion of IRS-1 contains multiple tyrosine phosphorylation motifs, which serve as docking sites for various SH2 (Src-Homology 2) domain containing signaling molecules. Two such molecules are PI 3-kinase and Grb-2 adaptor proteins that through their association with IRS-1 elicit the activation of biochemical network that promote the metabolic and growth responses, respectively, during insulin stimulation (White and Yenush, 1998). While, PI-3 kinase activity is required for insulin-stimulated glucose transport, Grb-2 provides the link between the insulin receptor and the guanine nucleotide exchange factor Sos which activates the small GTP binding protein Ras, subsequently leading to the activation of MAP Kinases cascade involved in gene expression and DNA synthesis (De Fea and Roth, 1997; Ito et al., 1996; Rose et al., 1994).

Recent studies have documented that lack of IRS-1/Grb-2 association due to expression of an IRS-1 mutant protein carrying $Tyr^{895}Phe$ substitution impairs MAPK activation and DNA synthesis in brown adipocytes (Valverde et al., 2001). This phenomenon is

observed despite intact phosphorylation of Shc, another substrate of activated insulin receptor also known to bind to Grb-2 and activate MAP Kinases. This provides a strong support for the essential role of IRS-1 and its direct association with Grb-2 in the insulin signaling pathway leading to MAP kinase activation and mitogenesis. In addition, previous studies have demonstrated that deletion of the IRS-1 PH domain attenuates its phosphorylation and mitigates insulin-mediated mitogenesis (Myers et al., 1995; Voliovitch et al., 1995; Yenush et al., 1996b), suggesting the critical function of the PH domain in efficient substrate phosphorylation by the activated insulin receptor and subsequent biological responses.

One of the main metabolic effects of insulin action on fat and muscle cells is the regulation of glucose uptake by inducing the redistribution of the glucose transporter, GLUT4, from intracellular compartments to the plasma membrane (Czech and Corvera, 1999). Although activation of the p85/p110 isoform of PI 3-kinase through its recruitment to phosphotyrosine sites on IRS-1 is a necessary component of insulin-stimulated GLUT4 translocation (Quon et al., 1995; Sharma et al., 1998), the role of IRS-1 proteins in insulin action on glucose transport remains controversial. Several lines of evidence support the involvement of IRS-1 for GLUT4 externalization. For example, expression of anti-sense ribozyme directed against rat IRS-1 significantly reduces GLUT4 translocation to the plasma membrane of rat adipose cells in response to insulin (Quon et al., 1994). Moreover, mutations of IR Tyr960, which do not alter receptor kinase activity, but are critical for IRS-1 binding and phosphorylation, abolish glucose transport (Backer et al., 1990; Kanai et al., 1993a; White et al., 1988). However, in contrast to these findings, other reports indicate that microinjection of anti-IRS-1

antibodies or expression of dominant inhibitory PTB domains of IRS-1 are able to block the mitogenic effects of insulin in fibroblasts but not GLUT4 trafficking in cultured adipocytes (Morris et al., 1996; Sharma et al., 1997). Interpretation of the results in adipocytes, is confounded by the observation that glucose uptake proceeds unabated in IRS-1 PTB-expressing cells, despite a near complete inhibition of not only IRS-1 tyrosine phosphorylation but of IR kinase activity (Sharma et al., 1997).

One of the early cellular events in insulin signaling is the reorganization of actin filaments. Recent evidence points to the potential participation of the actin microfilament network in promoting not only insulin-dependent redistribution of PI 3-kinase to GLUT4-containing vesicles but also in mobilizing GLUT4 to the cell surface (Khayat et al., 2000; Tsakiridis et al., 1994; Wang et al., 1998). Treatment of insulin responsive L6 myotubes and 3T3-L1 adipocytes with cytochalasin D, a potent inhibitor of actin assembly, completely abolishes glucose uptake upon insulin stimulation (Tsakiridis et al., 1997). Moreover, actin reorganization has been implicated in TC10 GTP-binding protein recruitment to the caveolae and its activation, which is also critical for GLUT4 plasma membrane translocation (Chiang et al., 2001; Watson et al., 2001). Thus, a proposed model for the mechanism of actin rearrangements in regulating glucose transport has been depicted by the insulin-induced translocation of the TC10 and IRS-1/PI 3-kinase to the intracellular glucose transporter, mainly GLUT4 containing vesicles, that cooperatively guide the latter en route to the cell surface (Heller-Harrison et al., 1996).

While it is clear that IRS-1 proteins are key mediators in transducing insulin-dependent biological effects, the relative contribution of PHIP in these cellular processes remains to be defined. In this chapter, I describe experiments performed to assess the role of PHIP

in both metabolic and mitogenic responses of insulin. Data obtained for this part of the study have been accomplished in collaborations with Anjaruwee Nimnual and Varinder Randhawa. Anjaruwee Nimnual performed the microinjection studies and Varinder Randhawa carried out the GLUT4 localization and actin remodeling experiments.

4.2 RESULTS

4.2.1 PHIP potentiates insulin-stimulated 5X SRE-LUC transactivation. To evaluate the involvement of PHIP in insulin-mediated transcriptional responses, its ability to induce transcription from a synthetic reporter, 5X SRE-LUC, which contains five copies of the serum responsive element (SRE) from the human c-fos promoter (Graham and Gilman, 1991), was examined. COS-1 cells transiently transfected with the 5X SRE-LUC reporter gene and increasing amounts of pCGN-PHIP, an expression plasmid encoding full-length PHIP, led to a dose-dependent increase in basal levels of transcription in untreated cells which was further enhanced in response to insulin (Figure 4.1). In order to investigate the relative importance of the MAP kinase pathway as a downstream effectors of PHIP-mediated gene expression, the MEK1 inhibitor, PD98059 (Alessi et al., 1995), was used to block MAP kinase activation during insulin stimulation of COS-1 cells which had been transiently transfected with the highest levels of pCGN-PHIP. The complete sensitivity of ligand-dependent PHIP SRE-LUC activity to

Figure 4.1. Effect of PHIP on insulin-induced transcriptional activation of the SRE-Fos promoter. COS-1 cells were transiently transfected with increasing amounts of pCGN/hPHIP (6 μg, 9 μg, 12 μg) or empty vector as control (12 μg) together with 3 μg of 5X SRE-fos luciferase reporter construct (5X SRE-LUC). Serum-starved cells were either left untreated or treated with Mek-1 inhibitor (PD98059, 2 hours). Cells were then incubated for with (100 nM, 10 hours) or without insulin and relative luciferase activity was measured in cell lysates. Results are expressed as the mean ± SD of triplicates from a representative experiment.

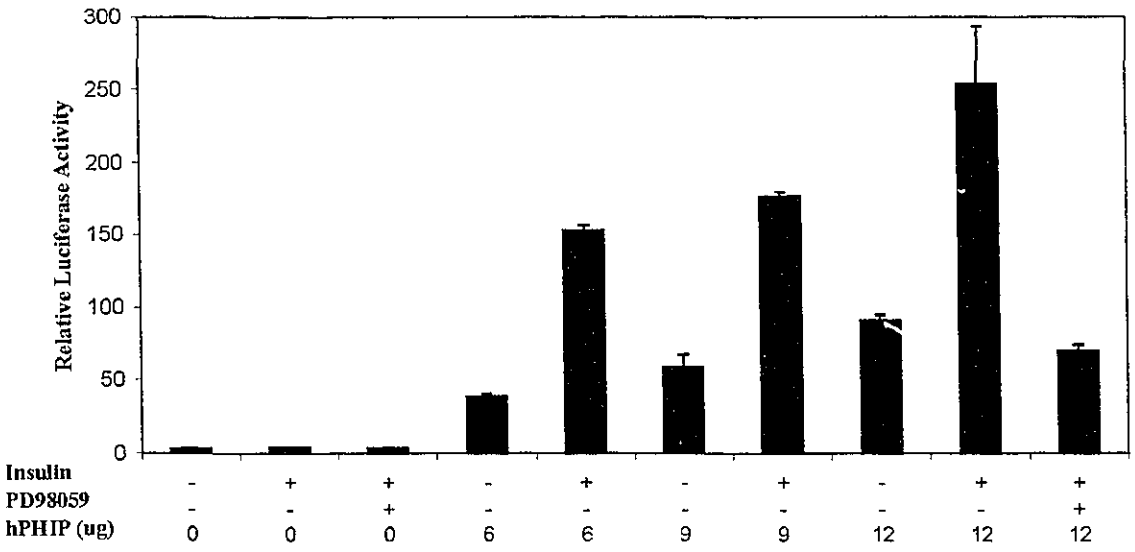
Relative Luciferase Activity
300
250
200
150
100
50
0
Insulin - + + - + - + - + +
PD98059 - - + - - - - - - +
hPHIP (ug) 0 0 0 6 6 9 9 12 12 12

PD98059, suggests that the MAP kinase cascade is an important component of insulin-stimulated PHIP transcriptional responses.

4.2.2 PH-binding region of PHIP disrupts insulin-stimulated MAP kinase activity. In order to determine the relative contribution of PHIP in insulin-induced MAP kinase activation, a hemagglutinin antigen (HA)-tagged PHIP construct that encode the IRS-1 PH binding region (PBR, residues 5-209) alone was used. Expression of PHIP PBR was predicted to function in a dominant inhibitory fashion by competing with the endogenous PHIP for the IRS-1 PH domain. Indeed, ectopically expressed dominant-negative PHIP (DN-PHIP) binds to endogenous IRS-1 in both untreated and insulin-stimulated cell lysates (Figure 4.2A). To evaluate the effect of DN-PHIP on IRS-1-mediated MAP kinase activation, COS cells were cotransfected with DN-PHIP and HA-tagged $p44^{MAPK}$, and anti-HA immune complexes from serum-starved and insulin-stimulated cell lysates were subjected to an *in vitro* kinase assay using myelin basic protein (MBP) as the substrate. As shown in Figure 4.2B, insulin-stimulated MAP kinase activation was reduced to basal levels by DN-PHIP expression. As expected, Shc phosphorylation remained refractile to the effects of DN-PHIP, suggesting that in these cells the PHIP/IRS-1 signaling pathway is essential for promoting MAP kinase activation during insulin stimulation.

To further dissect the effect of DN-PHIP on MAP kinase activation, various doses of insulin was used in similar *in vitro* kinase assays. Remarkably, maximum inhibitory effects of DN-PHIP was only observed at the highest dose of insulin (100 nM) (Figure 4.2C), suggesting that at unsaturated insulin receptor activation levels other signaling

Figure 4.2. Effect of dominant-negative (DN) PHIP mutants on MAP kinase activation. **(A)** DN/PHIP mutant protein interacts with endogenous IRS-1. COS cells were transiently transfected with either control pCGN vector or plasmid pCGN/DN-PHIP encoding HA-tagged $PHIP^{5-209}$ truncated protein. Serum starved cells were either left untreated or treated with insulin (100 nM, 5 minutes). Cleared cell lysates were then subjected to immunoprecipitaion with anti-IRS-1 antibodies and subsequently western blotted with anti-HA antibodies. **(B)** DN/PHIP inhibits MAPK activity through IRS-1 and not SHC adaptor protein. COS cells were transiently transfected with pCDNA1/HA-$p44^{MAPK}$ and either pCGN/HA-DN-PHIP or empty vector. Cell cultures were treated with (100 nM, 5 minutes) or without insulin. Cell lysates were precipitated with anti-HA antibodies and subjected to an in-vitro kinase assay with MBP (myelin basic protein) as substrate. The HA-depleted lysates were then precipitated with anti-Shc antibodies and subjected to analysis with anti-pTyr antibodies. **(C)** DN/PHIP exhibits maximal inhibition at high insulin doses. The same *in-vitro* MAP kinase assays were performed at different insulin doses (0, 1, 10, and 100 nM, 5 minutes) as described in (B).

A.

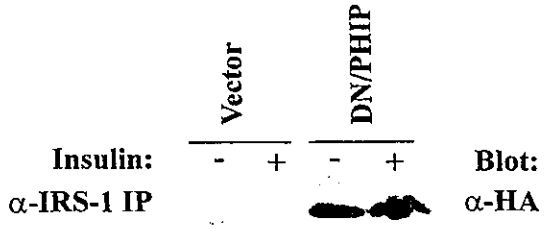
Vector
DN/PHIP
Insulin:
- + - +
Blot:
α-IRS-1 IP
α-HA

B.

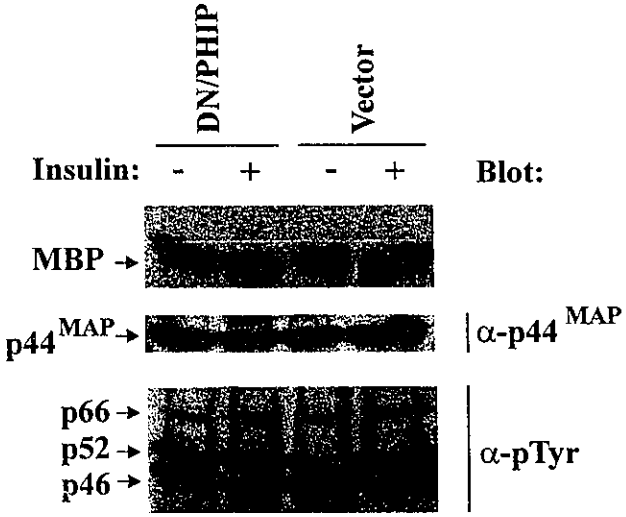
DN/PHIP
Vector
Insulin:
- + - +
Blot:
MBP
p44 MAP
α-p44 MAP
p66
p52
p46
α-pTyr

C.

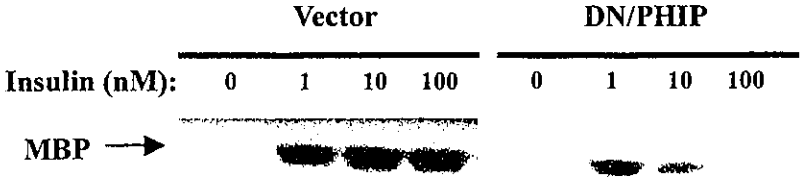
Vector
DN/PHIP
Insulin (nM):
0 1 10 100 0 1 10 100
MBP

molecules lead to MAP kinase activation. Indeed, tyrosine phosphorylated Shc has been shown to associate with Grb2/Sos (Goalstone et al., 2001; Yamauchi and Pessin, 1994b), providing a potential alternate mechanism for MAP kinase activation at low insulin levels.

4.2.3 Expression of the IRS-1 PH domain blocks PHIP-mediated transcriptional responses. To determine whether IRS-1 PH binding is required for the ability of PHIP to potentiate insulin responses, the effect of overexpressing the N-terminal IRS-1 PH domain (IRS-1-PH) on PHIP-stimulated SRE-LUC activity was evaluated in COS-1 cells. It was reasoned that overexpression of the isolated PH domain of IRS-1 would transdominantly interfere with PHIP binding to endogenous IRS-1. As shown in Figure 4.3A, increasing expression of the IRS-1-PH domain progressively blocked the PHIP signal, supporting the notion that PH-domain–directed interaction between PHIP and IRS-1 is required for PHIP-mediated transcriptional responses. In order to confirm that the IRS-1-PH exerted its effects by disrupting PHIP/IRS-1 complexes, high levels of IRS-1 expression was constituted by transiently transfecting an IRS-1 encoding vector into cells expressing ectopic PHIP and IRS-1-PH. Indeed, co-expression of excess IRS-1 overcame the inhibition imposed by IRS-1-PH in a dose-dependent manner, suggesting that wild-type IRS-1 outcompetes the IRS-1 PH domain for PHIP complex formation (Figure 4.3B).

4.2.4 Expression of DN-PHIP blocks insulin but not serum-stimulated transcriptional responses. To further establish the physiological significance of

Figure 4.3. Effect of IRS-1 PH domain on PHIP- mediated transcriptional activation of the SRE-Fos promoter. **(A)** IRS-1 PH domain inhibits PHIP-induced SRE-LUC activity. COS cells were cotransfected with pCGN/hPHIP (4 μg) and the indicated amount of pCGN/IRS-1 PH together with 2 μg of 5X SRE-LUC. Cells were treated with (100 nM, 10 hours) or without insulin and relative luciferase activity was measured in cell lysates. **(B)** IRS-1 PH mediated inhibition of PHIP-stimulated luciferase activity is restored by wild-type IRS-1 in a dose-dependent manner. COS cells were cotransfected with 1μg of pCGN/hPHIP, 2 μg of 5XSRE-LUC, either 1μg of pCGN/IRS-1 PH or vector DNA and increasing amounts of pCGN/IRS-1 cDNA as indicated. Cells were then treated and processed as in (A).

A.

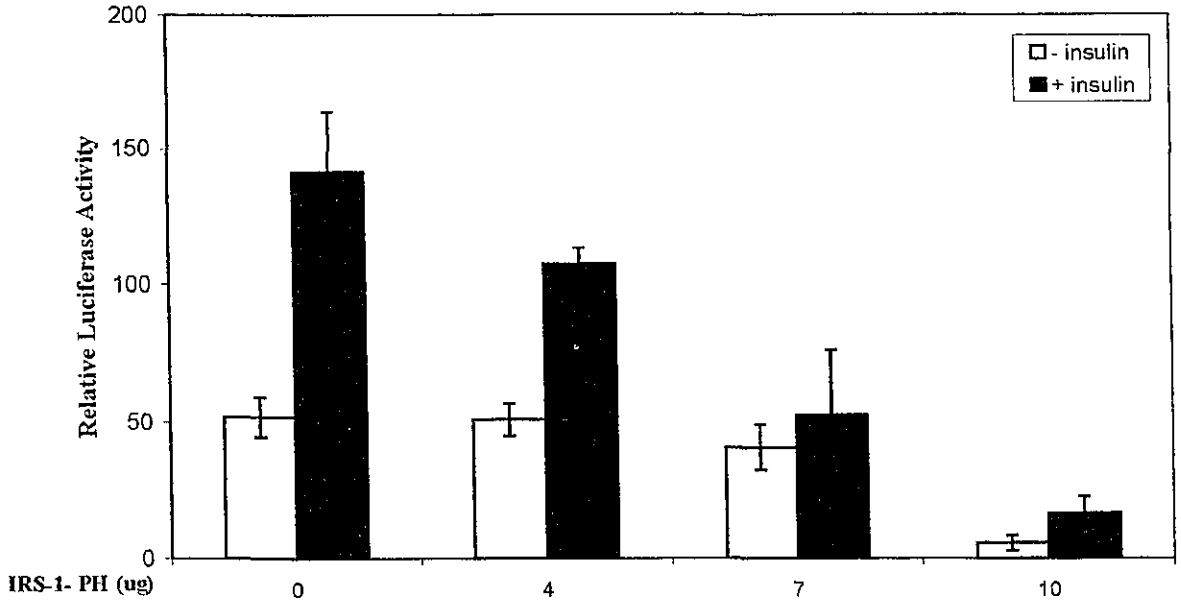
200
150
100
50
0
Relative Luciferase Activity
- insulin
+ insulin
IRS-1- PH (ug)
0
4
7
10

B.

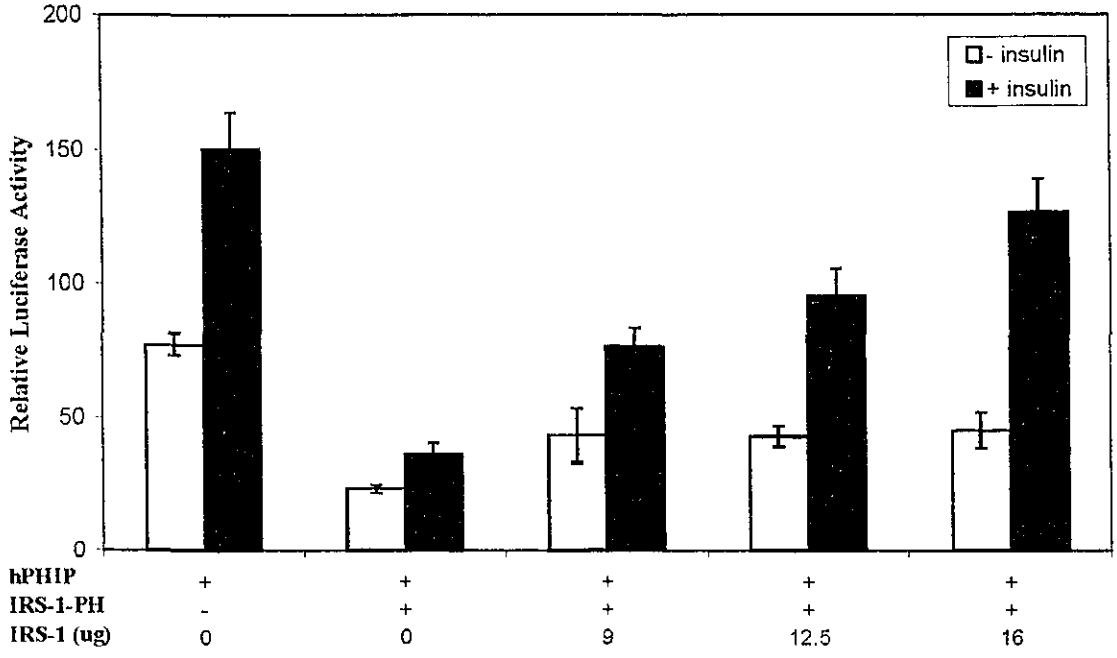
200
150
100
50
0
Relative Luciferase Activity
- insulin
+ insulin
hPHIP + + + + +
IRS-1-PH - + + + +
IRS-1 (ug) 0 0 9 12.5 16

IRS-1/PHIP interactions for gene expression, Dr. Nimnual from Dr. BarSagi's group used DN-PHIP in microinjection experiments. To this end, serum-starved Rat-1 fibroblast cells were coinjected with constructs encoding HA-epitope tagged DN-PHIP and 5X SRE-CAT (serum response element - chroramphenicol acetyltransferase) reporter plasmids. The expression of CAT and DN-PHIP were detected by indirect immunostaining using anti-CAT and anti-HA antibodies, respectively. In order to ensure that the effects observed are specific to insulin, serum, which contains a variety of growth factors, was included as control in this set of experiments. Insulin and serum treatment of parental Rat-1 fibroblasts microinjected with the reporter plasmid 5XSRE-CAT resulted in expression of the CAT protein readily detectable by immunofluorescence staining with anti-CAT antibodies (Figure 4.4A). However, cells coinjected with the construct expressing HA-tagged DN-PHIP completely blocked insulin- but not serum-stimulated CAT expression, which implicates PHIP as an integral component of the signaling pathway used by IR to regulate gene expression (Figure 4.4A, B). In order to address whether the effects of DN-PHIP on SRE-CAT in response to insulin occur at the level of IRS-1 or at some distal point in the IR signaling pathway, Rat-1 cells expressing DN-PHIP were co-injected with excess IRS-1. Consistent with the idea that PHIP functions upstream of IRS-1, it was found that overexpression of IRS-1 fully restored SRE-CAT expression in DN-PHIP expressing cells (Figure 4.4C). This data suggests that increased expression of IRS-1 in these cells effectively displaced DN-PHIP from endogenous IRS-1 complexes and interacted with wild type PHIP molecules, hence rescued the inhibitory effects of DN-PHIP.

Figure 4.4. Effect of DN-PHIP on insulin-mediated transcriptional activation of the SRE-CAT promoter. **(A)** DN-PHIP inhibits insulin-induced 5X SRE-CAT. Serum deprived Rat-1 fibroblasts were co-injected with constructs expressing HA-tagged DN-PHIP and the 5X SRE-CAT reporter construct. Cells were either left untreated or treated with insulin (0.5 μM, 5 hours) or serum (20%, 5 hours). The expression of CAT or DN/PHIP was monitored by immunostaining with anti-CAT or anti-HA antibodies , respectively. **(B)** The results shown in (A) are expressed as % of maximum which represents the average number of cells expressing SRE-CAT, upon serum stimulation. The values represent averages of 5 independent experiments in which at least 50 cells were injected for each condition. **(C)** IRS-1 rescues SRE-CAT expression. Serum deprived Rat-1 cells were coinjected with plasmids encoding 5X SRE-CAT and either pCGN vector or HA-tagged DN/PHIP in the presence or absence of HA-tagged IRS-1 as indicated. The results are expressed as % maximum, which represents the average number of cells expressing SRE-CAT upon insulin stimulation. The values represent the average of 5 independent experiments in which at least 50 cells were injected for each condition.

A.

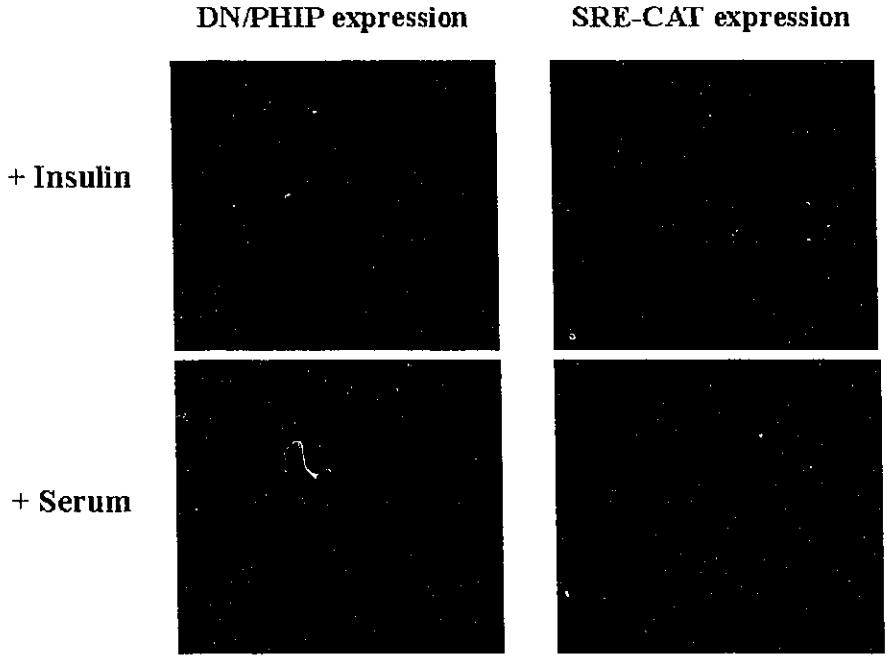
DN/PHIP expression
SRE-CAT expression
+ Insulin
+ Serum

B.

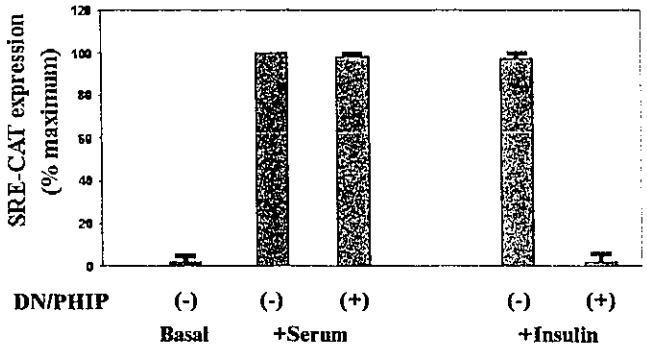
SRE-CAT expression
(% maximum)
120
100
80
60
40
20
0
DN/PHIP
(-)
(-)
(+)
(-)
(+)
Basal
+Serum
+Insulin

C.

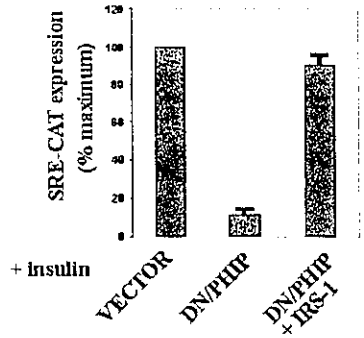
SRE-CAT expression
(% maximum)
120
100
80
60
40
20
0
+ insulin
VECTOR
DN/PHIP
DN/PHIP
+IRS-1

4.2.5 Expression of DN-PHIP blocks insulin but not serum-stimulated mitogenesis. As previously mentioned, studies have demonstrated that the growth stimulatory effects of insulin are dependent on IRS-1 (Rose et al., 1994; Wang et al., 1993). To examine the role of PHIP in insulin mediated mitogenic signaling, Dr. Nimnual microinjected HA-tagged DN-PHIP into NIH fibroblasts overexpressing human insulin receptor (NIH/IR) to study its effect on 5-bromodeoxyuridine (BrdU) incorporation into newly synthesized DNA. Rabbit anti-rat IgG was coinjected into the same cells as DN-PHIP to monitor the microinjected cells. Here, anti-BrdU was employed to observe the levels of DNA synthesis under various conditions. Again, serum was used as control to study the effect of PHIP mutants in response to different growth factors present in serum. Compared to quiescent cells, stimulation with insulin or serum led to a marked increase in the proportion of cells staining positive for BrdU incorporation (Figure 4.5A). However, whereas the growth stimulatory effects of serum were not affected by microinjection of DN-PHIP, insulin-induced stimulation of DNA synthesis was markedly attenuated in NIH/IR cells injected with DN-PHIP, consistent with the notion that PHIP/IRS-1 PH interactions are essential in promoting the proliferative actions of insulin (Figure 4.5A,B).

4.2.6 Expression of DN-PHIP impedes insulin-induced GLUT4 membrane translocation. In order to examine whether PHIP/IRS-1 complexes participate in the signal transduction pathway linking the insulin receptor to GLUT4 traffic in muscle cells, Varinder Randhawa transiently transfected L6 myoblasts stably expressing a myc-tagged GLUT4 construct (L6GLUT4myc) with either wild-type or dominant-interfering forms of PHIP. In general, L6 myoblasts do not express detectable levels of endogenous GLUT4,

Figure 4.5. Effect of DN-PHIP on insulin-mediated mitogenesis. **(A)** DN-PHIP inhibits insulin-induced DNA synthesis. Serum-deprived NIH/IR cells were coinjected with HA-tagged DN/PHIP and rabbit anti-rat IgG. The injected cells are indicated by arrows. Cells were treated with BrdU followed by insulin (0.5 μM) or serum (20%). DNA synthesis was observed by immunostaining with antibody to BrdU. **(B)** The results shown in (A) are expressed as % of maximum, which represents the average number of cells incorporating BrdU upon serum stimulation. The values represent averages of 5 independent experiments in which at least 50 cells were injected for each condition.

A.

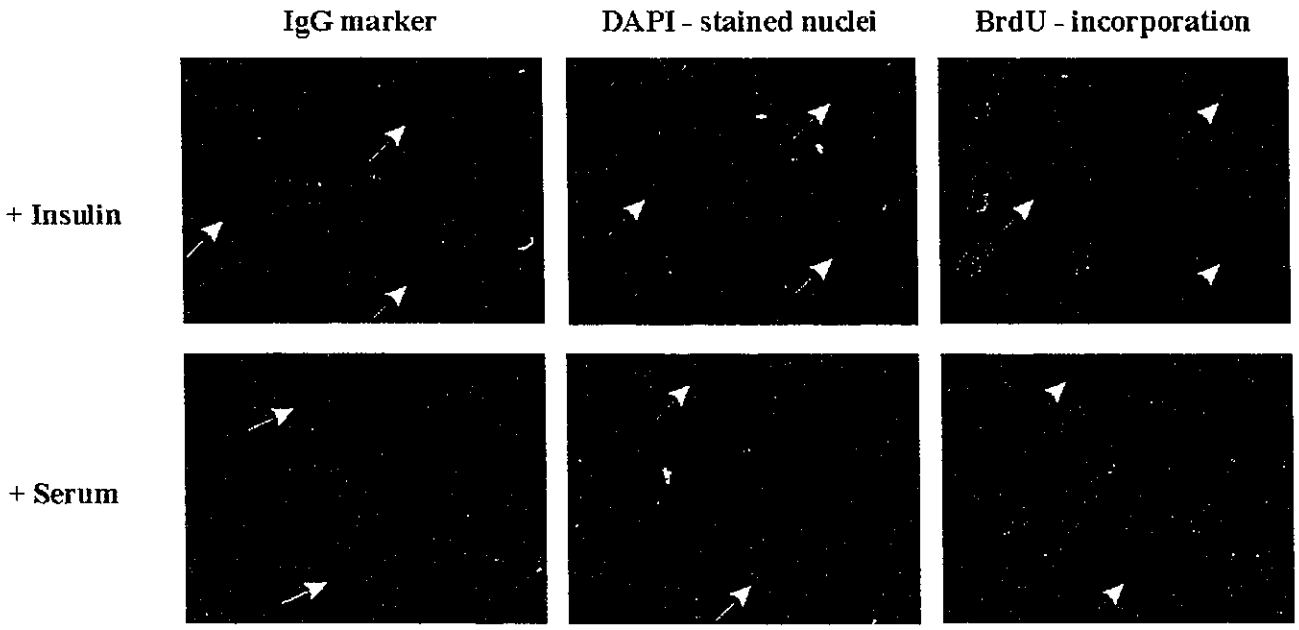
IgG marker
DAPI - stained nuclei
BrdU - incorporation
+ Insulin
+ Serum

B.

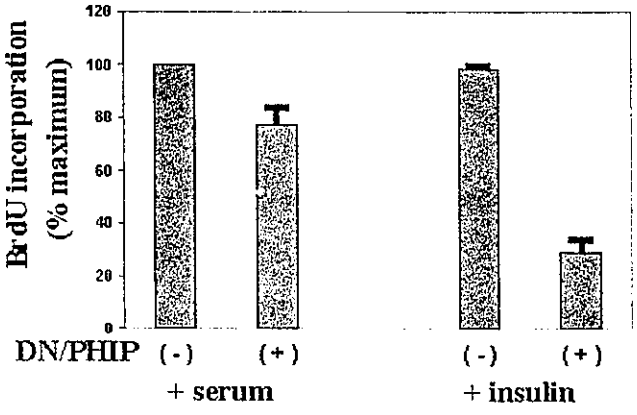
BrdU incorporation (% maximum)
120
100
80
60
40
20
0
DN/PHIP
(-)
(+)
(-)
(+)
+ serum
+ insulin

yet stable expression of GLUT4myc in these cells has been previously shown to mimic the effects of insulin on GLUT4 membrane translocation similar to that observed in physiological myotubes (Kanai et al., 1993b; Kishi et al., 1998; Mitsumoto et al., 1991). Co-expression of green fluorescent protein (GFP) cDNA was used to facilitate recognition of transfected cells. As previously shown, insulin treatment of L6GLUT4myc myoblasts generates a two-fold gain in cell-surface GLUT4myc detected by immunofluorescence labeling of the exofacial myc epitope (Randhawa et al., 2000; Ueyama et al., 1999) (Figure 4.6A,D). Ectopic expression of DN-PHIP caused a near complete inhibition of insulin-dependent GLUT4myc membrane translocation (>90%), in a manner identical to that observed with a dominant-negative mutant of the p85 subunit of PI 3-kinase (Δp85) (Quon et al., 1995; Wang et al., 1999)(Figure 4.6B,D). The effect of DN-PHIP was specific for the insulin-stimulated state, as the PHIP mutant did not alter the content of cell surface GLUT4myc in unstimulated cells.

4.2.7 Expression of IRS-1 PH domain mutant significantly reduces insulin-stimulated GLUT4 membrane translocation. To investigate whether ectopic expression of the IRS-1 PH domain, which would uncouple IRS-1 from PHIP could also mitigate insulin's effects on GLUT4 translocation, Randhawa V. transiently transfected L6GLUT4myc cells with a plasmid encoding the PH domain of IRS-1 alone. Data from these studies demonstrate that the IRS-1 PH domain caused a significant reduction in insulin-dependent GLUT4myc incorporation into the plasma membrane, albeit somewhat less robust (60%) than that induced by DN-PHIP (Figure 4.6C,D). The incomplete inhibition may be accounted for in part by the presence of other IRS proteins that may

Figure 4.6. Effect of PHIP and IRS-1 mutants on insulin-induced GLUT4 translocation. **(A)** Insulin promotes GLUT4 translocation to the plasma membrane. Serum-starved L6 myoblast cells ectopically expressing myc-GLUT4 (L6GLUT4myc) were either left untreated or treated with insulin (100 nM, 5 minutes) and then immunostained with anti-myc antibodies to monitor cell surface incorporated myc-GLUT4. **(B)** DN/PHIP inhibits insulin-mediated GLUT4 translocation to the cell surface. L6GLUT4myc cells were transiently cotransfected with 0.3 μg of plasmid encoding green fluorescent protein (pEGFP) and 0.9 μg of either pCGN/hPHIP, pCGN/DN-PHIP, or Δp85 plasmid containing the SH2 domain of the p85 subunit of PI 3-kinase. Forty-eight hours after transfection cells were starved for three hours and treated with insulin (100 nM, 5 minutes). Arrows point toward the transfected cells as monitored by GFP expression. Shown are representative images from at least 3 independent experiments. **(C)** IRS-1 PH domain inhibits insulin-stimulated GLUT4 membrane translocation. L6GLUT4myc cells were transiently co-transfected with 0.3 μg of pEGFP and 0.9 μg of either pCGN vector control, pCGN/IRS-1, or pCGN/IRS-1 PH. Insulin-stimulated cell surface incorporated GLUT4 was then monitored as described in (B). **(D)** Graphic representation of GLUT4myc translocation to the plasma membrane. The results shown in (A), (B) and (C) are expressed as fold stimulation relative to basal levels of surface GLUT4myc in untransfected cells. The values presented are representative images of at least 3 independent experiments.

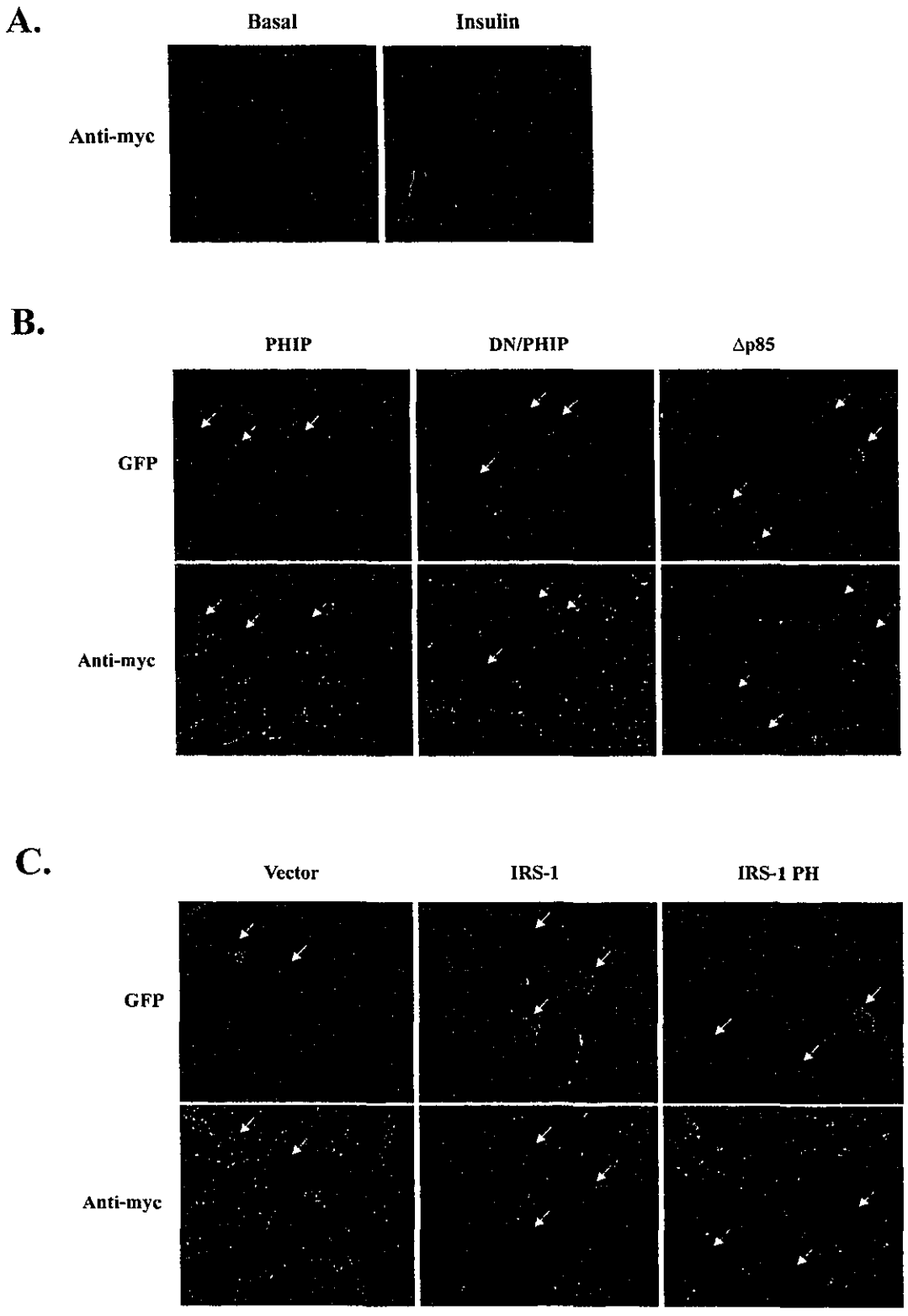
A.
Basal
Insulin
Anti-myc
B.
PHIP
DN/PHIP
Δp85
GFP
Anti-myc
C.
Vector
IRS-1
IRS-1 PH
GFP
Anti-myc

D.

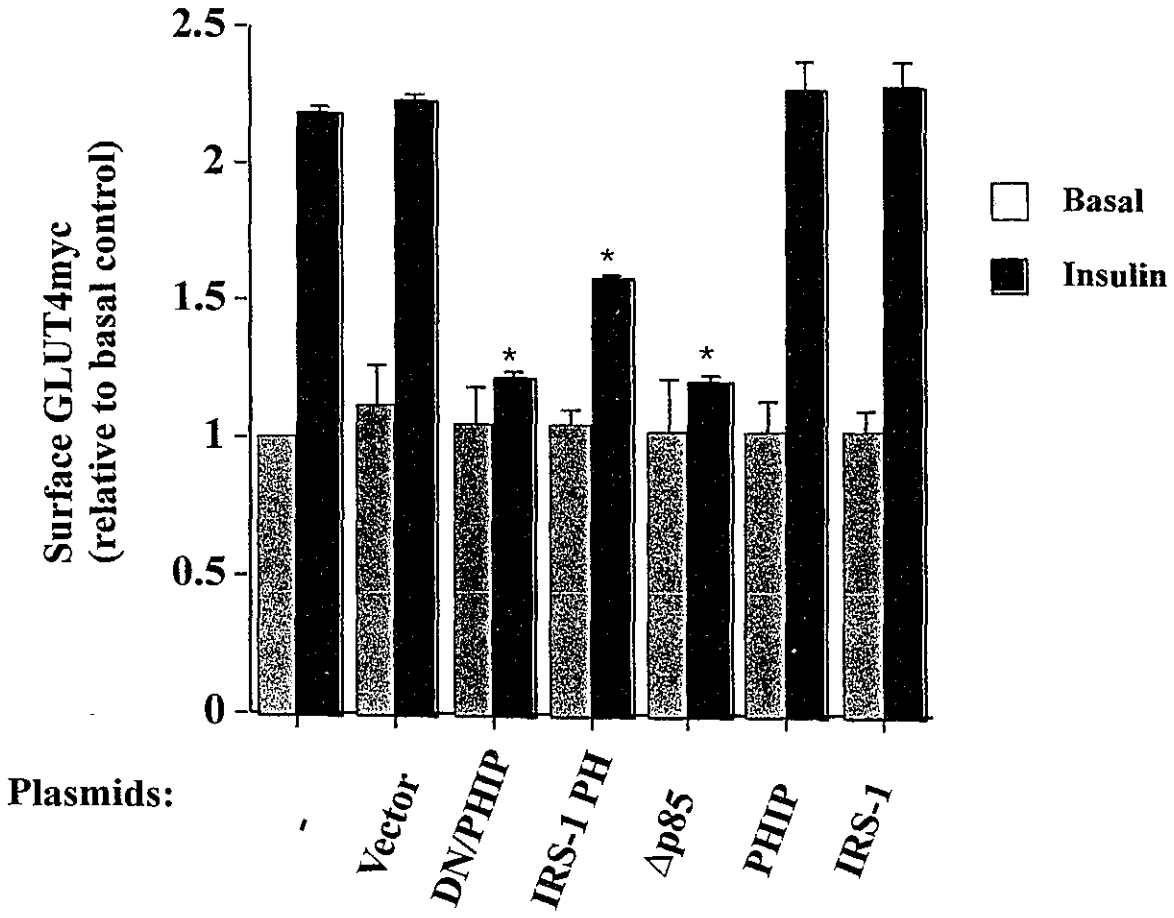
Surface GLUT4myc
(relative to basal control)
2.5
2
1.5
1
0.5
0
Basal
Insulin
Plasmids:
-
Vector
DN/PHIP
IRS-1 PH
Δp85
PHIP
IRS-1

partially substitute for IRS-1 function. These findings are in accordance with previous reports that overexpression of the IRS-1 PH domain in 3T3-L1 adipocytes can inhibit insulin's ability to stimulate IRS-1 tyrosine phosphorylation and activate the PI 3-kinase/AKT pathway (Goalstone et al., 2001). By contrast, neither full-length PHIP nor full-length IRS-1 caused any measurable change in GLUT4myc redistribution under basal or insulin-stimulated conditions (Figure 4.6B,C,D). Taken together, these results support the idea that PHIP/IRS-1 complex formation is necessary but not sufficient in promoting the metabolic effects of insulin in L6 muscle cells.

4.2.8 Expression of DN-PHIP disrupts insulin-induced actin rearrangement in L6 myoblasts. In light of previous evidence supporting the requirement of functional IRS-1 for insulin-stimulated actin cytoskeletal rearrangement (Morris et al., 1996), the role of PHIP in this process was explored. To this end, Randhawa V. utilized rhodamine-conjugated phalloidin to detect changes in the pattern of filamentous actin in L6GLUT4myc cells ectopically expressing either wild-type PHIP or DN-PHIP. Whereas actin staining in the basal state exhibits a filamentous pattern that runs along the longitudinal axis of the cell, a marked reorganization of actin into dense structures throughout the myoplasm was observed upon insulin stimulation (Figure 4.7). This effect was dramatically decreased by the expression of DN-PHIP but not by the empty vector or wild-type PHIP. Intriguingly, overexpression of wild-type PHIP appeared to induce remodeling of the actin cytoskeleton even under basal conditions in a fraction of transfected cells (Figure 4.7). Taken together, these observations implicate PHIP in the

Figure 4.7. Effect of DN-PHIP on insulin-induced actin remodeling. L6GLUT4myc cells were transiently cotransfected with 0.3 μg of pEGFP and 0.9 μg of either pCGN vector control, pCGN/hPHIP or pCGN/DN-PHIP. Serum starved cells were either left unstimulated or stimulated with insulin (100 nM, 10 minutes). GFP expression was used to monitor transfected cells. Filamentous actin was detected by rhodamine-conjugated phalloidin.

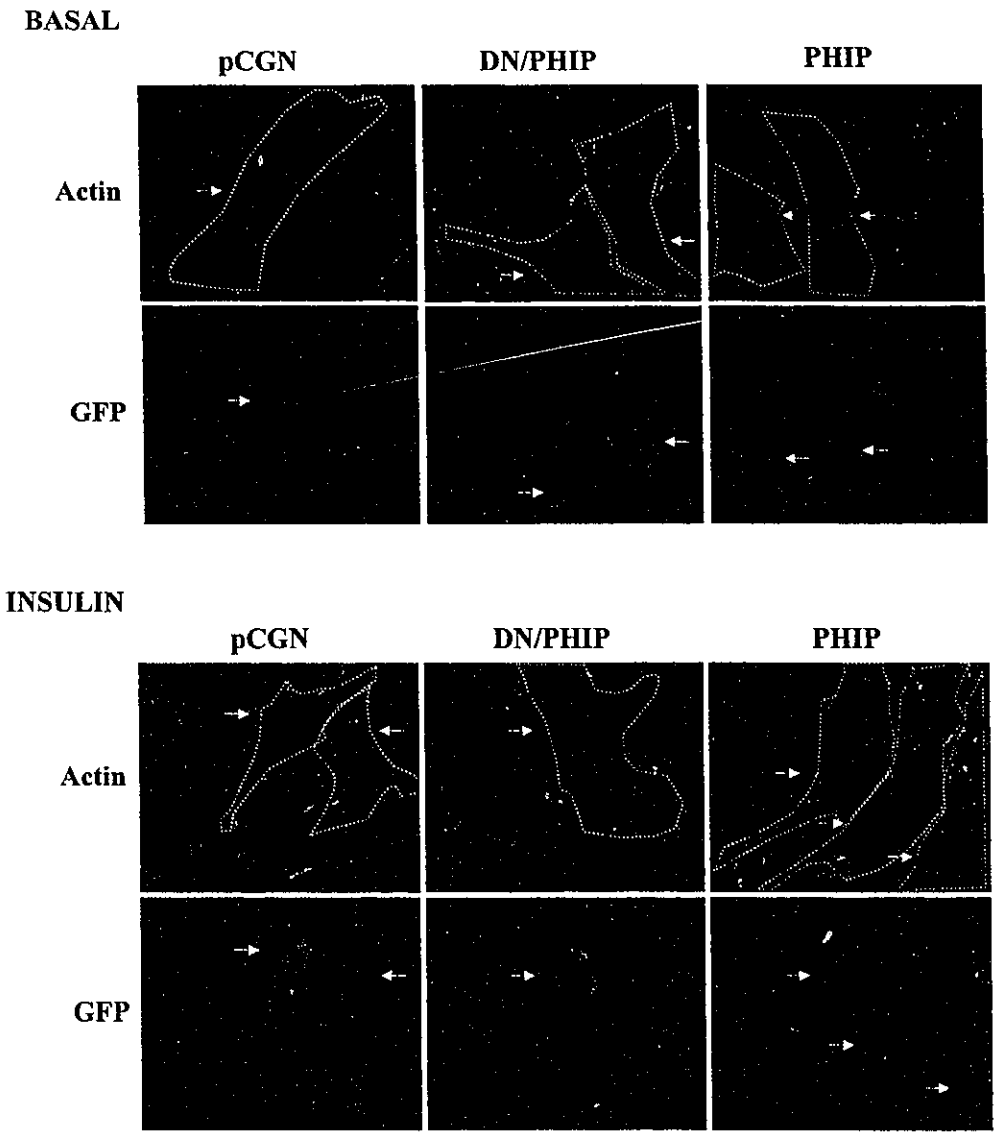
BASAL
pCGN
DN/PHIP
PHIP
Actin
GFP
INSULIN
pCGN
DN/PHIP
PHIP
Actin
GFP

regulation of cellular processes that promote cytoskeletal remodeling and accompany incorporation of GLUT4 vesicles at the plasma membrane surface of muscle cells.

4.2.9 Effects of DN-PHIP on insulin-induced PI 3-kinase activity. To investigate whether the effects of DN-PHIP on insulin-stimulated GLUT4 membrane translocation and actin reorganization was exerted through inhibition of PI 3-kianse activation, L6GLUT4myc cells were transiently transfected with DN-PHIP. Anti-IRS-1 immune complexes from serum-starved and insulin-stimulated cell lysates were subjected to an *in vitro* kinase assay using phosphotidylinositol (PI) as substrate. Surprisingly, DN-PHIP displayed no detectable inhibitory effects on PI 3-kinase activity upon insulin stimulation (Figure 4.8). This is in contrast to the inhibitory effects of DN-PHIP on two other PI 3-kinase-dependent biochemical processes, namely insulin-mediated GLUT4 translocation and actin rearrangements. Therefore, it is likely that the lack of any detectable effects of DN-PHIP on PI 3-kinase activation is due to experimental problems associated with the transient transfection in which only a small minority of cells express sufficient levels of the ectopic protein to exert any detectable effects. Other methods of ectopic protein expression such as adenoviral-mediated DN-PHIP expression may overcome this problem by infecting the majority of cells.

Figure 4.8. Effects of DN-PHIP on insulin-stimulated IRS-1-associated PI 3-kinase activity. DN/PHIP overexpression does not exhibit any detectable effect on PI 3-kinase activation. L6GLUT4myc cells were transiently transfected with either pCGN contol pCGN/hPHIP, pCGN/HA-DN-PHIP or empty vector. Untransfected NIH/IR cells were used as control for the kinase assay. Cell cultures were treated with (100 nM, 5 minutes) or without insulin. Cell lysates were precipitated with anti-IRS-1 antibodies and subjected to an *in-vitro* kinase assay with phosphotidylinositol (PI) as substrate. The phospholipid products were separated on thin layer chromatography (TLC) plates, dried and exposed in PhosphoImager cassette.

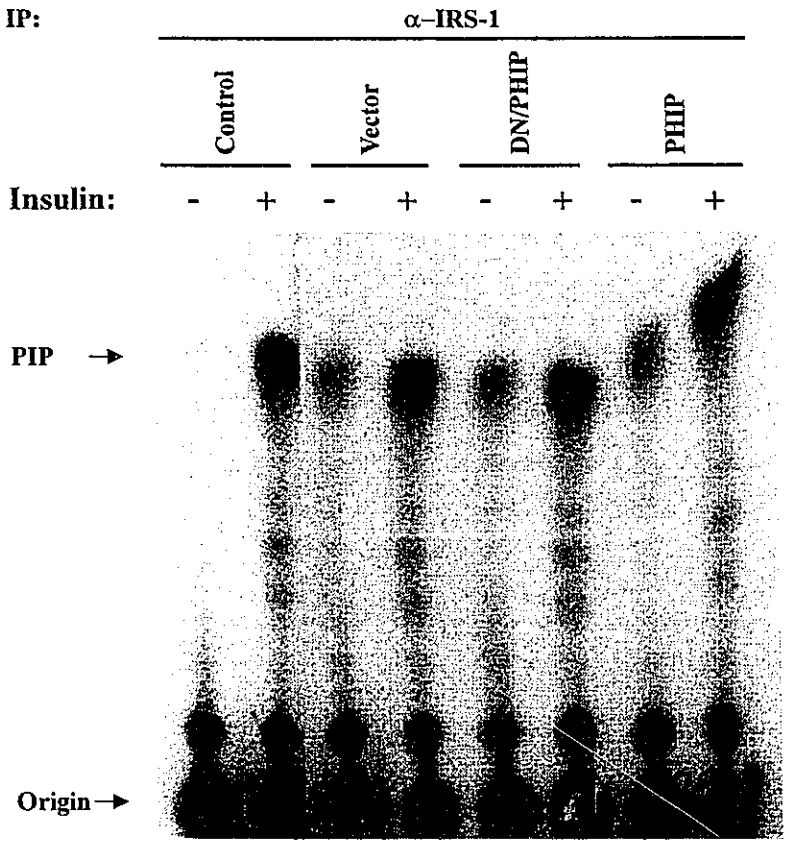
IP:
α–IRS-1
Control
Vector
DN/PHIP
PHIP
Insulin:
- + - + - + - +
PIP
Origin

4.3 DISCUSSION

Here, I have described a dominant negative N-terminal truncation mutant of PHIP, DN-PHIP, which potently inhibits MAP kinase activation in an insulin-dose dependent manner. The maximum inhibition is virtually observed only at higher doses of insulin, suggesting the operation of alternate signaling molecules than IRS-1 and PHIP downstream of the insulin receptor important for MAP kinase activation at lower insulin doses. One strong candidate is the Shc adaptor protein, which is known to be phosphorylated by the activated insulin receptor and promote MAP kinase activation (Pronk et al., 1993). Consistent with this observation, previous studies have documented that in fact Shc/Grb2 is the predominant signaling pathway leading to MAP kinase activation upon insulin stimulation in CHO cells overexpressing IR (Yamauchi and Pessin, 1994b), supporting the premise that at unsaturated IR activation levels, either due to IR overexpression or lower insulin concentrations, other molecules than IRS-1 and PHIP are involved in MAP kinase activation. Therefore, I propose a model in which at low concentrations, insulin only activates dispersed receptors in isolation and this is sufficient for Shc-mediated signaling. Whereas, higher insulin concentrations lead to maximal receptors activation, aggregation and internalization, providing the appropriate kinetics for proper IRS-1/PHIP-mediated signaling. Indeed, previous reports describe that increasing concentrations of insulin enhance receptor endocytosis by fluid-phase mechanism, a phenomenon that is absent under low insulin concentrations (Carpentier, 1994; Kotani et al., 1995; Smith et al., 1997). One note of caution is that high or low insulin levels should be discussed in correlation with the levels of the insulin receptor in

the context of a particular cell type or tissue. In other words, the level of occupied receptors saturation is the determining factor in differential signaling pathways activated in response to insulin. Of course, the ramifications of the proposed hypothesis remain to be investigated. As anticipated, DN-PHIP impeded insulin-induced transcriptional and proliferative responses. This inhibition is remarkably specific for insulin, as serum induced transactivation and DNA synthesis is unaffected by DN-PHIP. Moreover this inhibition is overcome by co-expression of IRS-1. Taken together, these data suggest that regions of PHIP implicated in interactions with the IRS-1 PH domain can disengage IR from IRS-1 proteins and subsequently decrease sensitivity to growth-promoting responses of insulin.

Unlike the effect of PHIP observed under insulin-triggered conditions, PHIP-mediated gene transcription was orchestrated independent of MAP kinase signaling pathway under basal conditions. Given that PHIP contains two bromodomain modules, known to be involved in transcriptional regulation, one could speculate that PHIP may regulate transcriptional responses through dual mechanisms. One that is indirect and depends on MAP kinases and the other may occur directly via interactions with the multiprotein complex transcriptional machinery. These may represent two distinct but not mutually exclusive functions of PHIP in regulating gene transcription. Arguably, these data leave open the possibility of an indirect yet MAP kinase-independent PHIP-mediated transcriptional regulation. The latter hypothesis is consistent with an earlier report that demonstrated, while c-fos gene transcription was markedly reduced in embryonic fibroblasts and 3T3 cells derived from mice with targeted disruption of IRS-1, MAP

kinase activity was unabated, supporting the involvement of IRS-1-dependent but MAP kinase-independent mechanisms of gene transcription (Bruning et al., 1997).

In this current study, we provide strong support for the involvement of PHIP/IRS-1 complexes in glucose transport in muscle cells. The use of PHIP or IRS-1 constructs known to interfere with efficient IR/IRS-1 protein interaction and hence productive signal transduction from IRS-1 to PI 3-kinase, are capable of interfering with insulin-stimulated GLUT4 translocation in L6 myoblasts. One might argue that the inhibitory effects of IRS-1 PH domain mutant might be due to titration of phospholipid ligands at the plasma membrane, and thus inhibition of binding of endogenous IRS-1 to the membrane. If this were indeed the case, one would expect that IRS-1 PH domain mutant overexpression should non-specifically inhibit other growth factor signaling pathways that require phospholipid ligands as second messengers. Several recent studies however provide evidence against this hypothesis. First, IRS-1 PH domain binds only weakly and non-specifically to phospholipid molecules, supporting the idea that IRS-1 PH/phospholipid interaction might not be physiologically relevant (Razzini et al., 2000). Second, expression of IRS-1 PH domain in Xenopus oocytes inhibited oocyte maturation in response to insulin and not progesterone, two growth factors known to regulate oocyte maturation, suggesting that IRS-1 PH domain expression alone functioned in a dominant inhibitory fashion in an insulin-specific manner (Ohan et al., 1998). Lastly, overexpression of the IRS-1 PH domain impairs IRS-1 tyrosine phosphorylation and PI 3-kinase activation upon insulin stimulation with no effects on prenyltransferase activity known to require phospholipid ligands (Goalstone et al., 2001). Together, these data

support the role of IRS-1 PH domain in retaining biological specificity through interaction with specific protein ligands such as PHIP.

Data presented also indicated that overexpression of either PHIP or IRS-1 alone in muscle cells was not sufficient in promoting transport of GLUT4 to plasma membrane surfaces. This is consistent with other observations indicating that activation of IRS-1-associated signaling effectors such as PI 3-kinase, although necessary, is not sufficient for GLUT4 activation. Notably, growth factors such as PDGF and IL4 can activate PI 3-kinase as efficiently as insulin yet fail to stimulate glucose transport in insulin-sensitive cells (Guilherme and Czech, 1998; Isakoff et al., 1995). One possible explanation is that additional PHIP/IRS-1/PI3 kinase-independent pathways are required to coordinate GLUT4 intracellular routing. Indeed, recent evidence points to a novel insulin-responsive pathway that recruits flotillin/CAP/CBL complexes to IR-associated lipid rafts in the plasma membrane, an event which is thought to potentiate GLUT4 docking to the cell surface following insulin receptor activation (Baumann et al., 2000).

In view of the recent advances in understanding the cellular mechanisms of GLUT4 transit to the cell surface upon insulin stimulation, cytoskeletal rearrangements have proven to be crucial. In this regard, fractionation studies have found both IRS-1 and PI 3-kinase in a cytoskeletal fraction, an insoluble protein matrix mainly composed of actin filaments, of the intracellular membrane compartments (Clark et al., 1998; Khayat et al., 2000), proposing a potential mechanism for their role in GLUT4 exocytosis. Although, PI 3-kinase is presumed to be localized to this site by coupling with tyrosine phosphorylated IRS-1, the molecular basis for IRS-1 targeting has not yet been clearly established. One obvious candidate is the IRS-1 PH domain. Previous studies have

demonstrated the importance of PH domains in targeting proteins to cellular membranes by binding to phospholipids (Lemmon and Ferguson, 2000). More importantly, the PH domain of several proteins such as Pleckstrin and Bruton's tyrosine kinase (Btk) have been shown to bind to filamentous actin and regulate actin remodelling in response to various stimuli (Ma and Abrams, 1999; Yao et al., 1999). Consistent with this data, ectopic expression of PHIP can induce filamentous actin reorganization at discrete sites in the myoplasm, suggesting that PHIP engages in the spatial control of actin assembly. It has yet to be determined whether PHIP itself can bind directly or indirectly to LDM-associated actin. Furthermore, it should be noted that the effects of PHIP overexpression on actin remodelling was not observed in all unstimulated cells. This again could be due to the nature of the transient transfection in which the amount DNA taken up by the cells may vary. Single cell microinjection assays in which controlled amounts of DNA are introduced into the cells will verify these results. Furthermore, it is of particular interest to determine the mechanism of PHIP action on the cytoskeleton using dominant-negative variants of proteins known to be involved in insulin-induced cytoskeletal dynamics.

CHAPTER FIVE

BIOCHEMICAL CHARACTERIZATION OF THE MECHANISMS OF PHIP FUNCTION IN INSULIN SIGNALING

5.1 INTRODUCTION

Hitherto, I have presented data supporting PHIP as a physiological protein ligand of the IRS-1 PH domain, which plays an important role in transducing insulin-instigated IRS-1-mediated signals. However, the precise mechanism of PHIP function remains to be established. As demonstrated in the previous chapter, dominant inhibitory mutants of PHIP inhibited insulin-stimulated MAP kinase activation leading to gene transcription, an event that could be reversed by overexpression of IRS-1, providing evidence for the PHIP function upstream of IRS-1 that may serve to link IRS-1 to the activated IR. However, coimmunoprecipitation studies failed to detect a direct PHIP/IR interaction, arguing for alternative mechanisms by which PHIP might reinforce effective IRS-1/IR coupling. Biochemical studies in 3T3-L1 adipocytes indicate that IRS-1 is preferentially tyrosine phosphorylated in the LDM compartment (Clark et al., 2000; Heller-Harrison et al., 1995). Given that PHIP is stably associated and cosegregates with IRS-1 in the LDM, suggests that PHIP may regulate tethering of IRS-1 molecules to the LDM. Moreover, overexpression of PHIP induces filamentous actin reorganization under basal conditions, indicating that PHIP may facilitate the preassembly of IRS-1 proteins onto a cytoskeletal

scaffold that is in close apposition to IR-enriched lipid rafts, providing a kinetic advantage in IRS-1 substrate recognition following receptor ligation.

To better understand the biochemical mechanisms of PHIP function in insulin signaling, I started by investigating the role of PHIP in insulin-induced IRS-1 tyrosine and serine/threonine phosphorylation. Insulin treatment induces rapid tyrosine phosphorylation followed by a pronounced retardation in the electrophoretic mobility of IRS-1 in a timely fashion, due to hyperphosphorylation on serine/threonine (Ser/Thr) residues (Heller-Harrison et al., 1995; Kublaoui et al., 1995). Recent studies have demonstrated that in general IRS-1 Ser/Thr phosphorylation acts as a negative regulator of insulin signaling through inhibition of IRS-1 tyrosine phosphorylation by the activated insulin receptor (Hotamisligil et al., 1996; Kanety et al., 1995; Tanti et al., 1994). Furthermore, these studies also suggested the Ser/Thr phosphorylation of IRS-1, subsequently leading to IRS-1 degradation plays an important role in the development of insulin resistance. Several groups have attempted to identify kinases responsible for phosphorylation of IRS-1 that leads to insulin signaling attenuation. Activation of PI 3-kinase by PDGF has been shown to enhance the electrophoretic mobility of IRS-1, leading to the inhibition of subsequent insulin-dependent signaling. This supports the role of PI 3-kinase in mediating IRS-1 Ser/Thr phosphorylation (Elbashir et al., 2001; Ricort et al., 1996). Consistent with this idea, Harute T. and colleagues have shown that pharmacological inhibitors of PI 3-kinase such as Wortmanin and LY294002 blocked insulin-induced electrophoretic mobility shift of IRS-1 (Haruta et al., 2000). The same group has also demonstrated that inhibition of mammalian target of rapamycin (mTOR), by treating the cells with Rapamycin prior to insulin stimulation, also exhibited

pronounced inhibitory effects on IRS-1 Ser/Thr phosphorylation and degradation, suggesting that mTOR is an important component of the mechanisms involved in IRS-1 Ser/Thr phosphorylation. Furthermore, activation of Ser/Thr kinases such as $I_K\beta$ kinase (IKK) by inflammatory agents including tumour necrosis factor - α (TNF-α), the prolonged activation of which is known to promote insulin resistance, have also been implicated in promoting IRS-1 Ser/Thr phosphorylation (Hotamisligil et al., 1996; Yin et al., 1998). Together, these data provide strong evidence for the involvement of mechanisms inducing Ser/Thr phosphorylation of IRS-1 in the development of insulin resistance, potentially leading to diabetes.

Serine/Threonine phosphorylation of IRS-1 has also been proposed to trigger the release of IRS-1 from the LDM to the cytosol, providing a potential mechanism through which Ser/Thr phosphorylation negatively regulates IRS-1 signaling (Clark et al., 2000; Inoue et al., 1998; Ricort et al., 1996). This has lead to the hypothesis that Ser/Thr phosphorylation of IRS-1 modulates IRS-1/LDM interactions. To explore the role of PHIP on IRS-1 tyrosine phosphorylation, I have studied the effects of DN-PHIP expression on IRS-1 phosphorylation in response to insulin. Moreover, to address the potential role of PHIP in IRS-1 subcellular compartmentalization and intracellular trafficking, I have employed an adenoviral construct to ectopically express PHIP in insulin-responsive cells such as L6 myotubes and 3T3-L1 adipocytes.

5.2 RESULTS

5.2.1 PH-Binding region of PHIP disrupts IRS-1 tyrosine phosphorylation. To analyze whether DN-PHIP interaction with endogenous IRS-1 leads to disruption of IRS-1 tyrosine phosphorylation in response to insulin, DN-PHIP was ectopically expressed in COS-7 and Rat-1 cells. Transient expression of DN-PHIP, but not full-length PHIP significantly impaired IRS-1 tyrosine phosphorylation (> 5 -fold) in insulin-treated cells (Figure 5.1A, B). To ascertain whether the reduction in IRS-1 phosphorylation occurred through interference with receptor function, changes in phosphotyrosine levels of immunoprecipitated insulin receptor and Shc, a direct substrate of the activated insulin receptor, were monitored. To this end, anti-Shc antibodies were used in immunoprecipitation followed by western blot with anti-phosphotyrosine antibodies. These results demonstrated that diminution of IRS-1 tyrosine phosphorylation levels was not attributable to inhibition of IR kinase activity in at least two cell backgrounds (Figure 5.1 A, C).

5.2.2 Effect of PHIP overexpression on insulin-stimulated IRS-1 serine/threonine phosphorylation. To gain some insight into the role of PHIP in IRS-1 Ser/Thr phosphorylation, the effect of PHIP overexpression on IRS-1 Ser/Thr phosphorylation levels was tested by monitoring the electrophoretic properties of IRS-1 by sodium dodecyl sulfate-polyacrylamide gel electrophoresis (SDS-PAGE) in COS-7 cells. Under basal conditions, increasing amounts of ectopically expressed PHIP induced a dose-dependent increase in the electrophoretic mobility of IRS-1 (Figure 5.2). Given

Figure 5.1. Dominant negative PHIP inhibits insulin-induced tyrosine phosphorylation of IRS-1. **(A,B)** COS-7 cells were transiently transfected with either pCGN/HA-DN-PHIP, pCGN/HA-PHIP or empty vector. Cell cultures were treated with or without insulin (0.2 μM, 5 minutes). Whole cell lysates or anti-IRS-1^{PCT} immunoprecipitates were subjected to immunoblot analysis with either anti-IRS-1^{PCT}, anti-pTyr or anti-HA antibodies as indicated. Anti-insulin receptor (IR) immunoprecipitates were blotted with anti-pTyr antibodies. The membrane was stripped and reprobed with anti-IR antibodies. **(C)** Rat-1 fibroblasts were transiently transfected with either pCGN/HA-DN-PHIP or empty vector. Cell cultures were treated with insulin (100 nM, 5 minutes). Cell lysates were precipitated with anti-IRS-1^{PCT} or anti-Shc antibodies and were subjected to immunoblot analysis with anti-pTyr antibodies. The membrane containing Shc immune complexes was stripped and reprobed with anti-Shc antibodies.

A.

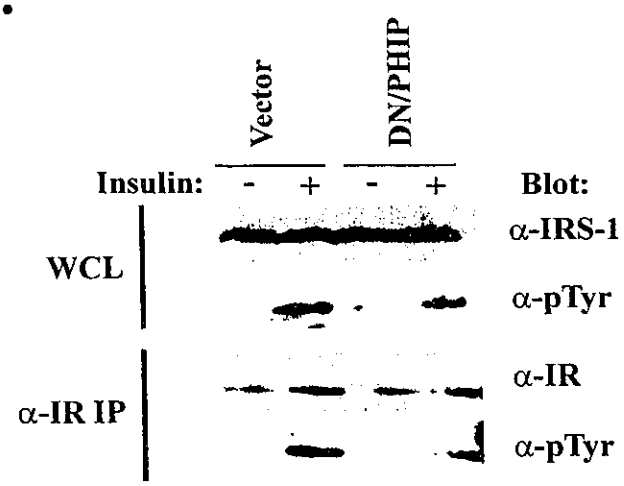
Vector
DN/PHIP
Insulin: - + - +
Blot:
WCL
α-IRS-1
α-pTyr
α-IR IP
α-IR
α-pTyr

B.

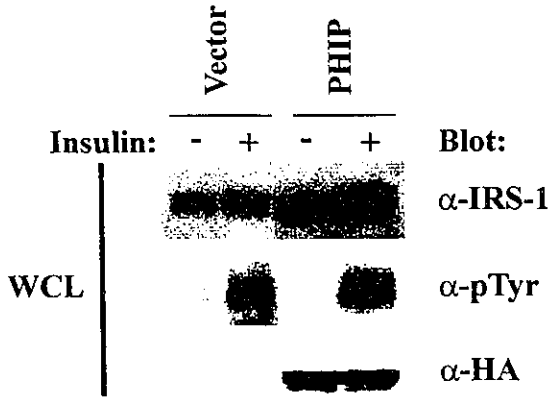
Vector
PHIP
Insulin: - + - +
Blot:
WCL
α-IRS-1
α-pTyr
α-HA

C.

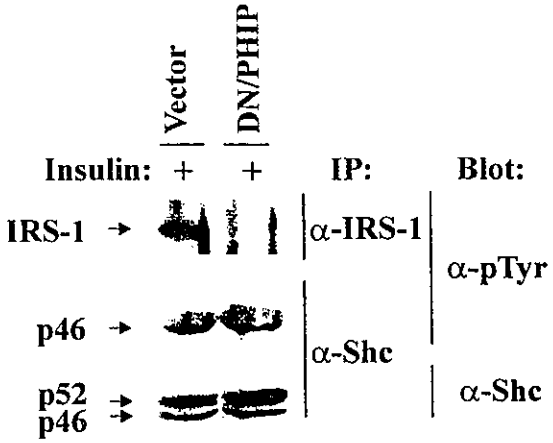
Vector
DN/PHIP
Insulin: + +
IP:
Blot:
IRS-1
α-IRS-1
α-pTyr
p46
α-Shc
p52
p46
α-Shc

Figure 5.2. Ectopically expressed PHIP induces an enhanced insulin-induced Ser/Thr phosphorylation of IRS-1 in COS cells. COS-7 cells were transiently transfected with 20 μg of pCGN control plasmid or increasing amounts (5 μg, 10 μg, 20 μg) of pCGN/HA-PHIP. One hundred micrograms of unstimulated or insulin-stimulated (100 nM, 5 minutes) cell lysate were resolved by 7.5% SDS-PAGE and subjected to western blotting with anti-IRS-1^{PCT} and anti-HA to detect endogenous IRS-1 and ectopic PHIP, respectively. Anti-IRS-1^{PCT} blot was then stripped and re-probed with anti-phosphotyrosine antibodies (anti-pTyr).

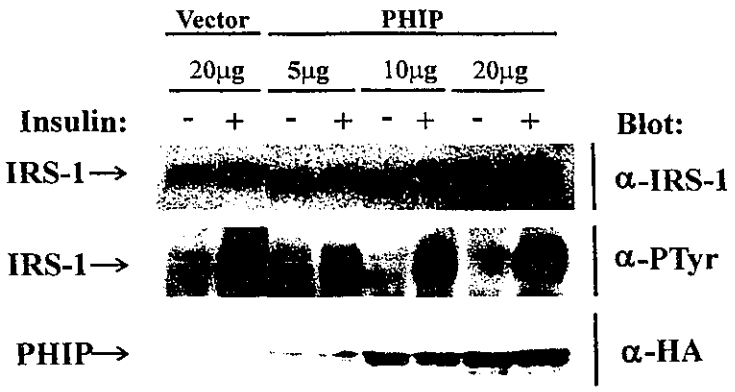
Vector
PHIP
20μg
5μg
10μg
20μg
Insulin:
- + - + - + - +
Blot:
IRS-1→
α-IRS-1
IRS-1→
α-PTyr
PHIP→
α-HA

that hypophosphorylated forms of IRS-1 display increased association with LDM fractions (Clark et al., 2000; Inoue et al., 1998), this data suggests that PHIP overexpression may modulate a Ser/Thr phosphorylation event that enhances sequestration of IRS-1 to the LDM compartment. By contrast, acute insulin stimulation (5 minutes) of PHIP transfectants, produced a significant retardation in the mobility of IRS-1, consistent with an increase in the phospho-Ser/Thr content of IRS-1. This shift is typically observed with prolonged insulin treatment (15-60 minutes) (Clark et al., 2000; Haruta et al., 2000; Heller-Harrison et al., 1995). Importantly, the amount of tyrosine phosphorylated IRS-1 remained fairly constant if not slightly increased in the highest PHIP expressors, when normalized for protein levels (Figure 5.2). These findings raise the possibility that PHIP-dependent phosphorylation of IRS-1 Ser/Thr residues may elicit a positive regulatory effect on downstream signaling events. Indeed, a recent study revealed that phosphorylation of serine residues within the PTB domain of IRS-1 by insulin-stimulated PKB, protects IRS-1 proteins from the rapid action of protein tyrosine phosphatases, and enables serine-phosphorylated IRS-1 proteins to maintain their tyrosine-phosphorylated active conformation (Paz et al., 1999).

In order to determine whether the same effect is observed in physiological insulin-responsive systems, an adenovirus construct encoding HA-tagged PHIP was used to transduce both undifferentiated L6GLUT4myc myoblasts and differentiated myotubes. The effect of PHIP overexpression on IRS-1 electrophoretic mobility was monitored over a time course of insulin stimulation by western blotting using anti-IRS-1 antibodies. Anti-HA and anti-PHIP antibodies were used to detect ectopic and endogenous levels of PHIP, respectively. In contrast to the results obtained from COS-7 cells, PHIP

overexpression did not exhibit any significant effect on the mobility of IRS-1 (Figure 5.3). To verify the latter results, similar assays were performed in another insulin-responsive cell type, 3T3-L1 adipocytes in which Ser/Thr phosphorylation of IRS-1 has been extensively studied. Analogously, ectopic expression of PHIP brought about no change in IRS-1 electrophoretic mobility in response to different doses of insulin, suggesting that increased PHIP expression does not enhance insulin-induced IRS-1 Ser/Thr phosphorylation in these cells under these experimental conditions (Figure 5.4). Although, these data do not rule out a functional role of PHIP in IRS-1 Ser/Thr phosphorylation, they suggest that PHIP overexpression alone might not be sufficient to promote IRS-1 Ser/Thr phosphorylation in these cells.

5.2.3 PHIP colocalizes with IRS-1 both in intact cells and subcellular fractions. Given that PHIP stably associates with IRS-1, it was important to examine whether PHIP colocalizes with IRS-1 in intact cells. To address this issue, indirect immunfluorescence analysis was carried on L6GLUT4myc myoblast cells using anti-PHIP or anti-IRS-1 antibodies. Merged images obtained by immunofluorescence microscopy demonstrated that PHIP and IRS-1 co-immunolocalize to punctate structures in the cytoplasm (Figure 5.5). Interestingly, PHIP proteins were also detected in the nucleus of some cells; whether this phenomenon is regulated by insulin remains to be elucidated.

Previous studies in cultured 3T3-L1 adipocytes have shown that IRS-1 molecules preferentially associate with the intracellular low density microsomes (LDM) (Anai et al., 1998; Clark et al., 2000; Heller-Harrison et al., 1995; Inoue et al., 1998; Kriauciunas et al., 2000). To further determine the subcellular distribution pattern of endogenous PHIP

Figure 5.3. Ectopically expressed PHIP has no effects on IRS-1 Ser/Thr phosphorylation in L6 myotubes. L6GLUT4myc myotubes were infected with either empty adenovirus vector or adenovirus encoding HA-PHIP at an MOI of 5000. Fifty micrograms of unstimulated or insulin-stimulated (100 nM; 5, 15, 30, 60 minutes (min)) cell lysate were separated on 7.5% SDS-PAGE and subjected to western blotting with anti-IRS-1^{PCT}, anti-HA or anti-PHIP antibodies to detect endogenous IRS-1, ectopic PHIP, or endogenous PHIP, respectively.

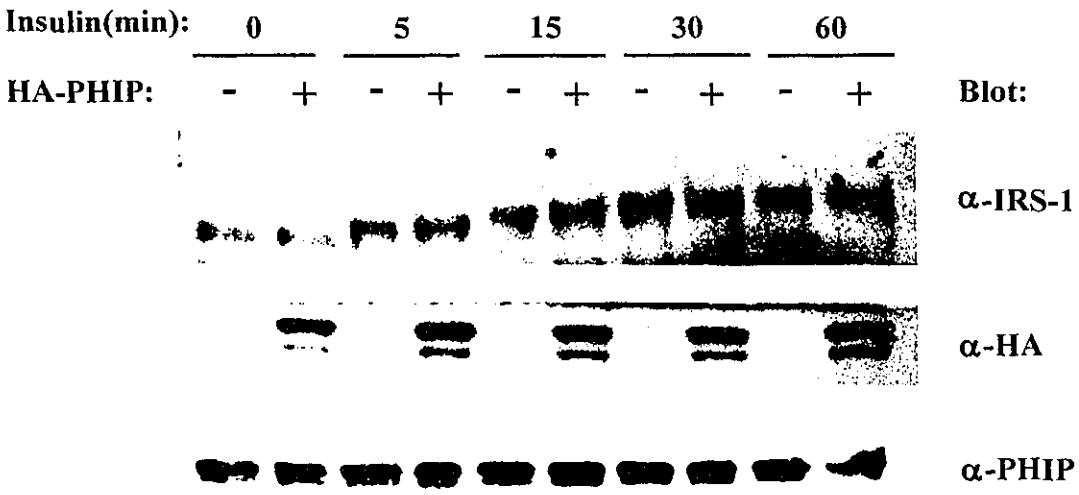
Insulin(min):
0
5
15
30
60
HA-PHIP:
- + - + - + - + - +
Blot:
α-IRS-1
α-HA
α-PHIP

Figure 5.4. Ectopically expressed PHIP does not affect IRS-1 Ser/Thr phosphorylation in 3T3-L1 adipocytes. Differentiated 3T3-L1 cells were infected and processed as described in Figure 5.4. Fifty micrograms of unstimulated or insulin-stimulated (1, 10, 100 nM; 5, 20, 60 minutes) cell lysates were separated on 7.5% SDS-PAGE and subjected to western blotting with anti-IRS-1^{PCT}, anti-HA antibodies to detect endogenous IRS-1, and ectopic PHIP, respectively.

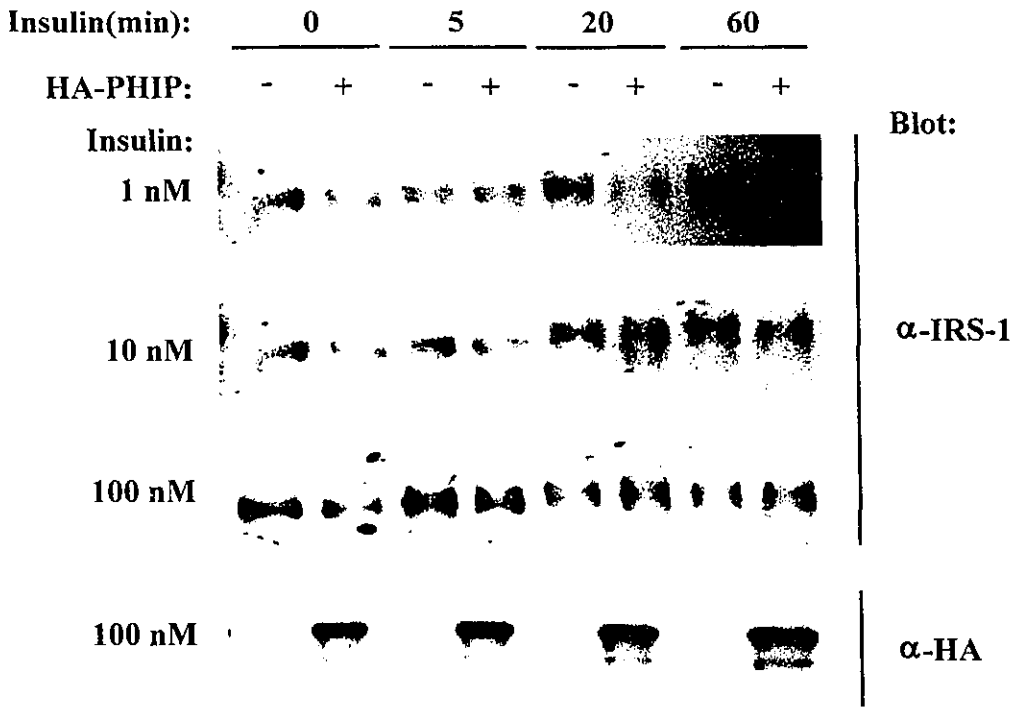
Insulin(min):
0
5
20
60
HA-PHIP:
- + - + - + - +
Insulin:
1 nM
10 nM
100 nM
100 nM
Blot:
α-IRS-1
α-HA

Figure 5.5. PHIP and IRS-1 colocalize within intact cells. Polyclonal anti-PHIP and monoclonal anti-IRS-1 were used in immunostaining analysis of L6GLUTmyc myoblasts. Representative images of four independent experiments are shown at two different magnifications, 40X and 100X.

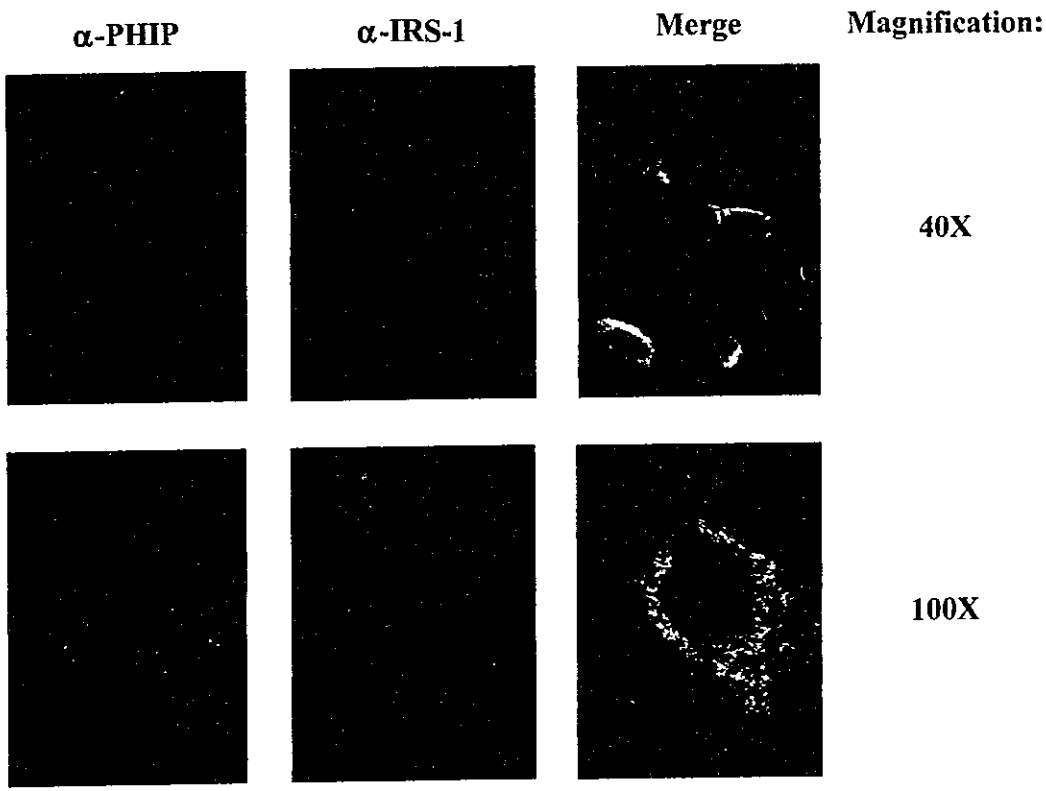
α-PHIP
α-IRS-1
Merge
Magnification:
40X
100X

and IRS-1 proteins, LDM, cytosol and plasma membrane (PM) fractions were isolated from both undifferentiated and differentiated L6GLUT4myc cell lysates by differential centrifugation. In order to monitor the fidelity of the fractionation procedure anti-transferrin receptor antibodies (anti-TfR) were originally used as control for detection of LDM and PM fractions by immunoblotting analysis (Farhang-Fallah et al., 2002). Data from these studies revealed that under basal conditions, about two third of IRS-1 proteins were localized to the LDM compartment and insulin stimulation resulted in a progressive decrease in both the levels and electrophoretic mobility of IRS-1 proteins in this fraction. Concomitantly, the levels of IRS-1 increased in the cytosolic fraction upon insulin stimulation over time. Following 30-60 minutes of insulin stimulation the IRS-1 proteins levels start to decrease in the cytosolic fraction as well, presumably due to IRS-1 degredation (Figure 5.6). Significantly, PHIP segregated with IRS-1 in both LDM and cytosolic fractions, although insulin did not appear to alter the subcellular distribution of PHIP between these compartments. Plasma membrane fractions revealed strong PHIP and weak IRS-1 signals. Thus it is conceivable that PHIP through its association with the IRS-1 PH domain may direct targeting of IRS-1 to specific subcellular compartments and serve as a key determinant for the signaling specificity of IRS-1 with respect to the insulin receptor pathway.

5.2.4 Ectopic expression of PHIP has no effect on IRS-1 subcellular distribution. Cellular compartmentalization and intracellular trafficking of IRS-1 are essential in its ability to elicit insulin responses (Kriauciunas et al., 2000). Given that PHIP cosegregates with IRS-1 in LDM compartments, it was important to establish whether

Figure 5.6. PHIP and IRS-1 colocalize in the same subcellular compartments. Fifty micrograms of low-density microsomes (LDM), cytosol (CYT) and plasma membrane (PM) fractions isolated from unstimulated or insulin-stimulated (100 nM; 5, 15, 30, and 60 minutes) L6GLUT4myc myotube extracts were separated on 7.5% SDS-PAGE and subjected to western blotting with anti-PHIP and anti-IRS-1^{PCT} antibodies.

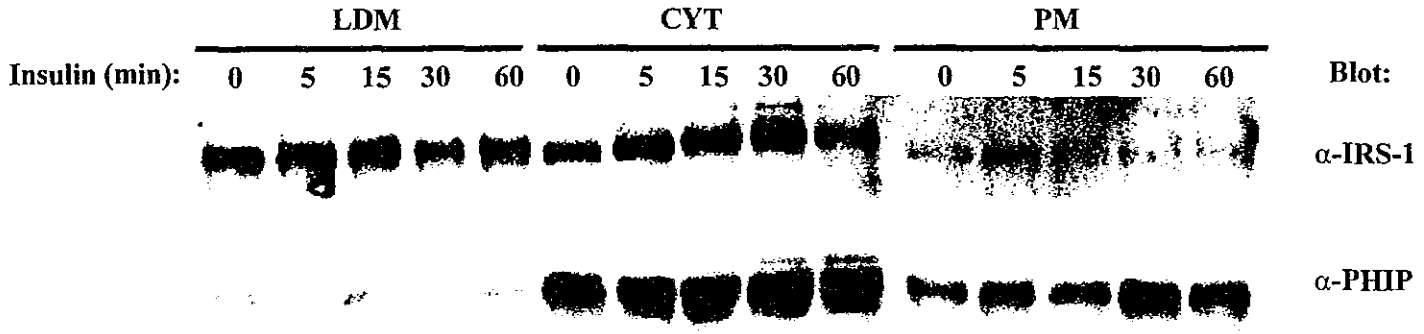
LDM
CYT
PM
Insulin (min):
0 5 15 30 60 0 5 15 30 60 0 5 15 30 60
Blot:
α-IRS-1
α-PHIP

ectopic PHIP expression would alter IRS-1 subcellular compartmentalization. To this end, L6GLUT4myc myotubes were infected with adenovirus construct encoding HA-tagged wild-type PHIP. Homogenized serum-starved or insulin-stimulated cells were subjected to repeated ultracentrifugation to separate LDM and cytosol as described in section 2.19. While ectopic HA-PHIP distribution was similar to that of endogenous PHIP, there was no significant effect on IRS-1 intracellular localization upon PHIP overexpression under basal or insulin stimulation (Figure 5.7). These data suggest that PHIP overexpression alone is insufficient to induce IRS-1 redistribution in these cells.

5.2.5 The PH domain is required for Ser/Thr phosphorylation but not subcellular distribution of IRS-1. In order to recapitulate the role of the IRS-1 PH domain in IRS-1 Ser/Thr phosphorylation, COS-7 cells were transiently transfected with pCGN constructs encoding either wild type IRS-1 or IRS-1 lacking the PH domain (pCGN/IRS-1$^{\Delta PH}$). Cellular extracts were separated on SDS-PAGE and subjected to immunoblotting with anti-IRS-1 antibodies. Consistent with the effects observed with ectopic PHIP expression in COS-7 cells, there was no discernable difference in electrophoretic mobility migration of IRS-1$^{\Delta PH}$ upon insulin stimulation, suggesting that PHIP/IRS-1 PH domain interactions are necessary for IRS-1 Ser/Thr phosphorylation in these cells (Figure 5.8A). Surprisingly, unlike endogenous IRS-1 where a time-dependent progressive mobility shift is seen upon insulin stimulation, ectopically expressed IRS-1 displayed no retarded migration (Figure 5.8A). One possibility is that massive overexpression of IRS-1 proteins in a small population of cells, due to limitations of transient transfection, disturbs

Figure 5.7. Ectopically expressed PHIP has no significant effects on IRS-1 intracellular distribution. **(A)** L6GLUT4myc myotubes were transiently transduced with HA-PHIP encoding adenoviral plasmids as described in Figure 5.3. Fifty micrograms of unstimulated and insulin-stimulated (100 nM; 5, 15, 30, and 60 minutes) LDM and CYT fractions were analyzed by immunoblotting with anti-IRS-1^{PCT} and anti-HA antibodies to detect endogenous IRS-1 and ectopic PHIP, respectively. **(B)** The same fractions as in (A) were re-run on a 7.5% SDS-PAGE next to control uninfected fractions for comparison of IRS-1 migration.

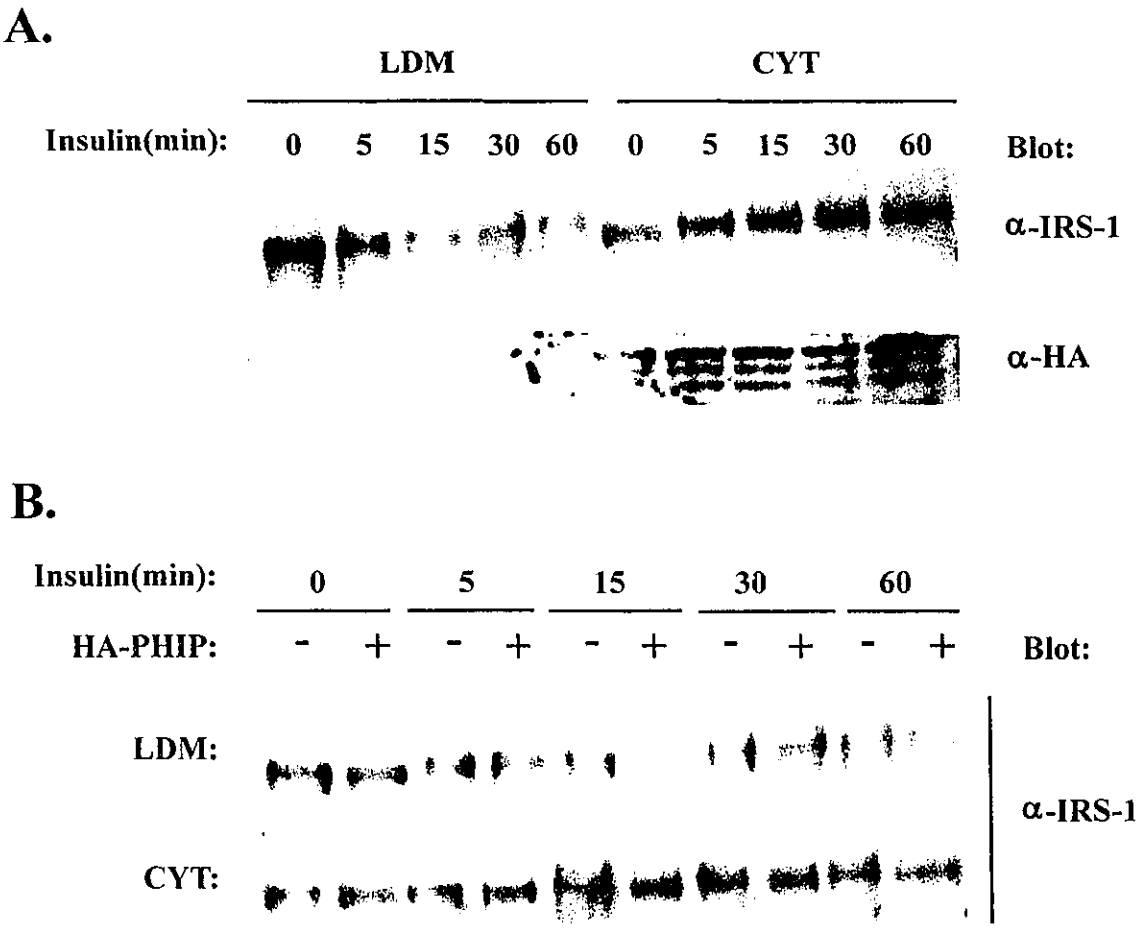
A.
LDM
CYT
Insulin(min):
0 5 15 30 60 0 5 15 30 60
Blot:
α-IRS-1
α-HA
B.
Insulin(min):
0 5 15 30 60
HA-PHIP:
- + - + - + - + - +
Blot:
LDM:
CYT:
α-IRS-1

Figure 5.8. Effects of deletion of the IRS-1 PH domain on IRS-1 Ser/Thr phosphorylation and subcellular localization. **(A)** Deletion of the PH domain of IRS-1 desensitizes it to insulin-induced Ser/Thr phosphorylation. COS-7 cells were transiently transfected with pCGN plasmids encoding either full-length IRS-1 or IRS-$1^{\Delta PH}$ (IRS-1 mutant lacking the PH domain). Fifty micrograms of total cell lysate from unstimulated or insulin-stimulated (100 nM; 5, 20 and 60 minutes) were subjected to western blotting using anti-HA antibodies to detect ectopically expressed HA-tagged full-length or mutant IRS-1. **(B)** IRS-$1^{\Delta PH}$ localizes to LDM. COS-7 cells were transfected as previously described in (A). Fifty micrograms of LDM or CYT fractions were resolved by 7.5% SDS-PAGE and subjected to immunoblot analysis with anti-HA antibodies.

A.

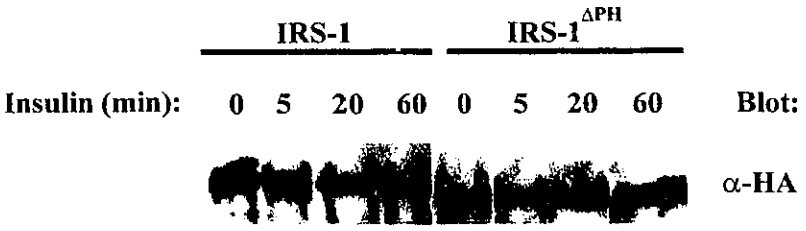
IRS-1
IRS-1ΔPH
Insulin (min):
0 5 20 60 0 5 20 60
Blot:
α-HA

B.

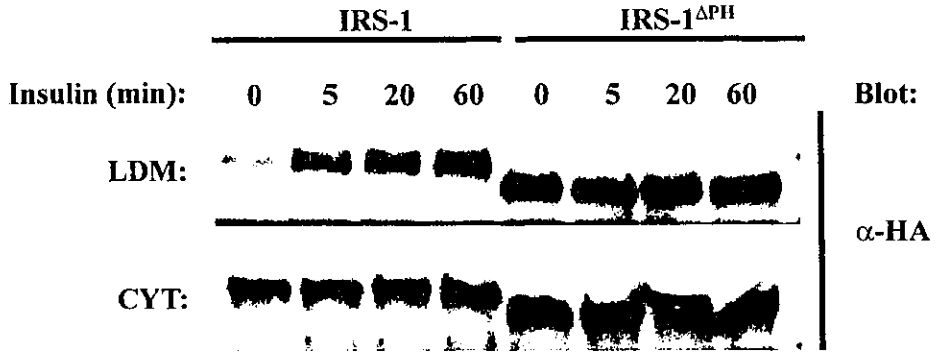
IRS-1
IRS-1ΔPH
Insulin (min):
0 5 20 60 0 5 20 60
Blot:
LDM:
CYT:
α-HA

the stoichiometric balance between the IRS-1 proteins and the upstream insulin receptor or downstream signaling molecules such as PI 3-kinase. Indeed, previous studies have shown that while IRS-$1^{\Delta PH}$ fails to undergo insulin-induced tyrosine phosphorylation in 32D cells, overexpression of IR in these cells, restores its tyrosine phosphorylation (Myers et al., 1995). Alternatively, ectopically expressed wild type IRS-1 might have mislocalized to wrong intracellular compartments, thereby failing to respond to insulin. To address this issue, subcellular fractions of LDM and cytosol were isolated from COS-7 cell extracts ectopically expressing HA-tagged wild-type IRS-1. The results of these experiments demonstrated that HA-IRS-1 distributed between both LDM and cytosol ruling out the possibility of inappropriate intracellular distribution of ectopically expressed IRS-1 (Figure 5.8B).

To determine the role of the PH domain in IRS-1 subcellular localization, COS-7 cells were transiently transfected with pCGN/IRS-$1^{\Delta PH}$ and intracellular fractions were isolated. IRS-$1^{\Delta PH}$ proteins localized to the LDM as well as cytosol, suggesting that the PH domain is not essential for IRS-1/LDM association (Figure 5.8B). This is consistent with previous observations where transient overexpression of PH/PTB had no effect on IRS-1 localization to the LDM (Inoue et al., 1998). Collectively, these data suggest that other regions than the PH domain are involved in IRS-1 localization to the LDM compartments.

5.3 DISCUSSION

The data presented herein suggests that PHIP is essential for productive coupling of IRS-1 to the insulin receptor. However, I have not clearly established, from the present study, the molecular basis by which PHIP facilitates IRS-1/IR interactions. Overexpression of PHIP exerted differential effects on IRS-1 Ser/Thr phosphorylation monitored by IRS-1 electrophoretic mobility on SDS-PAGE. The results demonstrated that the extent of PHIP-induced IRS-1 Ser/Thr phosphorylation is cell type specific; such that overexpression of PHIP increased IRS-1 Ser/Thr phosphorylation initiated by insulin in COS-7 cells, a phenomenon undetected in L6 or 3T3-L1 cells. One possible explanation may come from the levels of individual molecules that affect the stoichiometry of multiprotein complex formation in the insulin signaling pathways. Indeed, the levels of endogenous IRS-1 and PHIP are much higher in insulin-sensitive L6GLUT4myc myotubes as compared to an insulin-insensitive cell line such as COS-7. Consistent with these observations, other studies have also shown that different levels of IRS-1 proteins in CHO cells lead to either enhancement or inhibition of insulin signaling in a cell context dependent manner, further confirming the requirement of a specific stoichiometry of interaction between signaling proteins to achieve certain biological responses (Yamauchi and Pessin, 1994a). Another reason could be due to the fact that because of high levels of PHIP and IRS-1 in myoblasts and myotubes, simply expressing a bit more PHIP in these cells in not likely to give an enhanced response on the Ser/Thr phosphorylation status of IRS-1. In addition, in contrast to L6GLUT4myc myoblasts in which the level of PHIP proteins increases upon differentiation into myotubes, the level

of PHIP proteins decreases in 3T3-L1 cells upon differentiation into adipocytes for unknown reasons (Data not shown). One possibility is that due to different nature of insulin responses in these two systems distinct stoichiometry of PHIP/IRS-1 interactions might be required to mediate various insulin biological outputs. Alternatively, other PHIP family of proteins, undetectable with the current polyclonal antibodies, might be mediating insulin signaling in 3T3-L1 cells.

It should be noted that anti-Ser/Thr antibodies were not used to confirm that the IRS-1 electrophoretic mobility shift observed was indeed due to enhanced Ser/Thr phosphorylation of IRS-1. However, extensive work to date has established that insulin-induced mobility shift of IRS-1 is mainly due to IRS-1 Ser/Thr phosphorylation as determined by phosphoaminoacid and phosphopeptide mapping analysis (Sun et al., 1992).

In contrast to the results obtained by another group where IRS-1 protein mutants lacking the PH domain undergo Ser/Thr phosphorylation in response to insulin (Sun et al., 1992), transient expression of IRS-$1^{\Delta PH}$ in COS-7 cells displayed no detectable insulin-triggered mobility retardation. This apparent discrepancy might be due to the fact that in the former study CHO cells overexpressing insulin receptor has been used, creating a circumstance in which the PH domain was dispensable for IRS-1 Ser/Thr phosphorylation and signaling emanated by insulin. Consequently, these results suggest that under low levels of the insulin receptor as in COS-7 cells, PHIP, through its interaction with the PH domain of IRS-1 provides a significant advantage for the endogenous IRS-1 during competition for a limited number of insulin receptors thereby displacing ectopic IRS-$1^{\Delta PH}$ away from the receptor.

CHAPTER SIX

CONCLUDING REMARKS AND FUTURE DIRECTIONS

Despite our growing advancements in dissecting molecular pathways leading to biological responses of cell growth and metabolism, understanding the mechanisms of signaling specificity associated with the insulin signaling remains a major challenge. An emerging concept raises the importance of subcellular compartmentalization, as one of the major mechanisms through which temporal and spatial assembly of signaling molecules directs activation of specific molecular events in accordance with cell physiology. Using this hypothesis several investigators have attempted to rationalize association of IRS-1, a low-density membrane resident protein, and its phosphorylation by the activated insulin receptor, a plasma membrane-embedded tyrosine kinase. Traditionally, it was thought that insulin-mediated internalized endosomal-bound insulin receptors are responsible for tyrosine phosphorylation of the LDM-tethered IRS-1 (Backer et al., 1989; Khan et al., 1989). By contrast, recent evidences has indicated that under conditions where insulin receptor internalization is inhibited, IRS-1 is phosphorylated and activates downstream signaling, consistent with the idea that the activated insulin receptor intercepts IRS-1 at plasma-proximal sites (Ceresa et al., 1998; Heller-Harrison et al., 1995). Here, I summarize observations that support this latter hypothesis and argue for the potential role of PHIP in IRS-1 tyrosine phosphorylation and signaling originated at the plasma membrane microdomains. Furthermore, I elaborate on

the implications of PHIP subcellular compartmentalization in eliciting insulin-mediated signal transduction.

Using subcellular fractionation assays, I have demonstrated that PHIP proteins localize to the LDM, cytosol and plasma membrane. PHIP protein localization to the plasma membrane provides it with a unique opportunity to regulate IRS-1 compartmentalization in proximity to the insulin receptor and allow its phosphorylation by the activated receptor. Recent studies argue for the distribution of the insulin receptor to cholesterol- and caveolin-enriched lipid raft microdomains of the plasma membrane called caveolae (Gustavsson et al., 1999; Watson et al., 2001; Wu et al., 1997). The integrity of caveolae has been proven vital for insulin and IRS-1 actions as the treatment of adipocytes with plasma membrane cholesterol extracting drugs, which disrupt lipid rafts, inhibits insulin-stimulated IRS-1 tyrosine phosphorylation and subsequent Akt activation without impairing receptor autophosphorylation(Gustavsson et al., 1996; Parpal et al., 2001). A recent study by Zacharias and colleagues has elegantly demonstrated distinct spatial submicrodomain localization of fluorescent test protein attached to different lipid anchors using fluorescence resonance energy transfer (FRET)(Zacharias et al., 2002). Test proteins carrying the myristoylation and palmitoylation lipid chains localized in caveolae whereas those containing prenylation tail clustered in non-caveolae structures. It is noteworthy that targeting of IRS-1 proteins to non-caveolae compartments of the plasma membrane through addition of a prenylation chain containing CAAX motif, disrupts insulin-stimulated IRS-1 signaling, lending support to the concept that IRS-1 localization to caveolae is important in transducing insulin signaling (Kriauciunas et al., 2000). Intriguingly, the PHIP protein sequence also contain three putative myristoylation sites

that might be responsible for localization of PHIP proteins with lipid raft microdomains of the plasma membrane, and which may promote recruitment of IRS-1 molecules to these compartments via association of PHIP with the IRS-1 PH domain. Indeed, weak IRS-1 immunoreactive signals have also been detected in the plasma membrane fraction in the same subcellular fractionation studies of L6GLUT4myc cells. Alternatively, PHIP might be interacting with caveolin, the major protein component of the rafts, as a mechanism that may contribute to the segregation of PHIP at the plasma membrane. Even though PHIP localization to the caveolae and its interaction with caveolin has yet to be investigated, it is noteworthy that PHIP contains a putative caveolin-interacting motif (ΨXΨXXXXΨ or ΨXXXXΨXXΨ, where Ψ represents any aromatic and X any amino acid, (Couet et al., 1997), EPLQPEYPDSLFQCYNVCW$^{170\text{-}188}$ (See Figure 3.1A) that could potentially mediate PHIP/Caveolin association. Moreover, the insulin receptor also contains this motif, TTSSDMWSFGVVIWEITS$^{1175\text{-}2292}$ and has been shown to bind to caveolin-1 and -3 *in vitro* and cofractionates with caveolin-1 in CHO cells overexpressing the insulin receptor (Yamamoto et al., 1998). Taken together, these observations raise the intriguing possibility that PHIP might recruit IRS-1 to caveolin-enriched lipid rafts by interacting with caveolin, and thereby promote IRS-1 phosphorylation in these microdomain compartments of the plasma membrane where the insulin receptor is localized (Figure 6.1). Several observations support this hypothetical model in which caveolin/PHIP/IRS-1 PH domain interactions might be required for IRS-1 localization to plasma membrane microdomains. First, although, PH domains are commonly known to bind to phospholipids and result in the recruitment of the host protein to the plasma membrane, IRS-1 PH domain binds to phospholipids with very low affinity and weak

Figure 6. A hypothetical model describing insulin-induced PHIP-mediated IRS-1 plasma membrane localization. Potential interaction of PHIP with caveolin (black coiled-shaped proteins) in caveolae is proposed to mediate recruitment of IRS-1 to these lipid raft microdomains upon insulin stimulation.

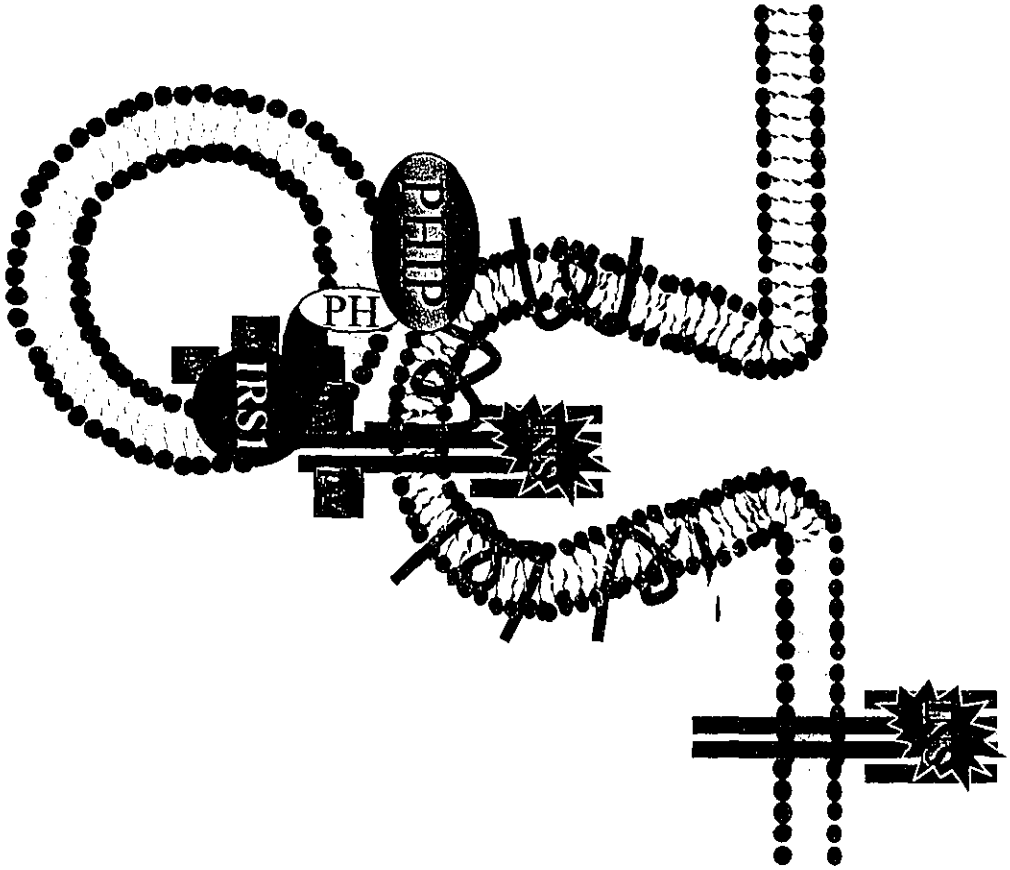
PH
IRS1

specificity, questioning the *in vivo* physiological relevance of IRS-1 PH/phospholipid interactions observed *in vitro* (Razzini et al., 2000). Moreover, mutations of the IRS-1 PH domain designed to disrupt its interactions with the phospholipids have no bearing on IRS-1 tyrosine phosphorylation or PI 3-kinase activation, suggesting that phospholipid/IRS-1 PH interactions are dispensable in IRS-1-mediated signaling *in vivo* (Jacobs et al., 2001; Vainshtein et al., 2001). Second, phospholipids are also relatively depleted in the caveolin containing lipid rafts (Brown and London, 1998), supporting the view that IRS-1 is potentially recruited to the caveolae through protein-protein interactions. Third, both IRS-1 and PHIP proteins are localized to plasma membrane fractions under basal conditions as shown in Figure 5.6, suggesting that PHIP/IRS-1 complexes are preassembeled in the membrane. Together, these data support the role of PHIP as an anchor that positions LDM-associated IRS-1 proteins in juxtaposition to the insulin receptor in lipid rafts possibly trough association with caveolin, which in turn might provide a kinetic advantage for rapid phosphorylation of IRS-1. Indeed, tyrosine phosphorylation of IRS-1 is observed as early as 30 seconds after insulin stimulation (Sun et al., 1992). Given that both putative caveolin binding motif and two of the myristoylation sites are located at the amino-terminus of PHIP, one might expect that a truncated PHIP mutant encompassing this region would be sufficient to link IRS-1 to the insulin receptor and for insulin-mediated IRS-1 phosphorylation. In contrast, overexpression of mutants of PHIP containing the IRS-1 PH binding region function in a dominant inhibitory manner and block IRS-1 tyrosine phosphorylation by the activated insulin receptor. One possibility is that if indeed DN-PHIP has caveolin-binding properties, it may disrupt caveolae structures when overexpressed which might contribute

to its inhibitory properties. Alternatively, it may be that DN-PHIP is not sufficient to stably associate with caveolar domains and as such it may uncouple IRS-1 from endogenous plasma membrane-associated PHIP thus acting in a transdominant fashion. In addition, other regions of PHIP might be required for the potential caveolin/PHIP/IRS-1/insulin receptor complex formation. Indeed, PHIP also contains a short stretch of acidic amino acid residues at its carboxy-terminus, DDPIDEEEEFEE$^{828\text{-}839}$ (See Figure 3.1A) similar to KVAEEEDDEE found in nucleolin I (Burks et al., 1998), that might be involved in intermolecular interactions that regulate PHIP and IRS-1 association. Future biochemical and structure-function analysis with specific mutations or deletion of the myristoylation and caveolin-binding motif within PHIP would determine the physiological significance of PHIP distribution in the plasma membrane.

Given the localization of PHIP in other cellular compartments such as LDM, cytosol and nucleus supports the functional plasticity of PHIP proteins in the regulation of insulin-mediated signaling at multiple stages, the exact molecular mechanism of which remain obscure. Based on preliminary data, PHIP expression was shown to be increased during L6GLUT4myc myoblast differentiation into myotubes, suggesting a potential role of PHIP in myoblast differentiation. By contrast, an opposite effect was observed upon differentiation of fibroblast or preadipocyte 3T3-L1 into adipocyte where a decrease in PHIP protein levels was observed. Data presented here support a differential role of PHIP in various insulin-responsive cells. On the one hand, enhanced PHIP expression in myotubes might support a role of PHIP in glucose transport and metabolic function of insulin mediated through IRS-1. Indeed PHIP was proven to be essential for mobilization of GLUT4 to the cell surface, as dominant inhibitory mutants of PHIP markedly

diminished GLUT4 membrane translocation. Moreover, the role of PHIP in insulin-induced actin remodeling, known to be essential for GLUT4 translocation, further supports the role of PHIP in maintaining the appropriate microfilament network necessary for the metabolic actions of insulin in muscle cells. Together, these data support the notion that enhanced PHIP expression is linked to a possible role in muscle differentiation. This is analogous to the observation in which caveolin 3 expression is very low in myoblasts and is tremendously overexpressed upon myoblast differentiation, implicating caveolin 3 in muscle differentiation (Galbiati et al., 2001). On the other hand, PHIP might not be as important for lipogenic aspects of insulin in adipocytes. Given the indispensable role of PHIP in DNA synthesis or mitogenesis, it is tantalizing to speculate that in these cells PHIP function might be required for DNA synthesis and proliferation. This is consistent with the elevated levels of PHIP expression observed in actively growing 3T3-L1 fibroblasts as compared to differentiated adipocytes. In support of the role of PHIP in mitogenesis, expression of dominant-inhibitory mutant of PHIP in NIH3T3 fibroblasts overexpressing the insulin receptor resulted in a near complete attenuation of DNA synthesis induced by insulin. Analogously, such differential function has also been observed for IRS-1 in 32D hematopoietic cells. While, overexpression of IRS-1 resulted in increased IGF-1-instigated mitogenesis and proliferation, ectopically expressed IRS-1 inhibited IGF-1-mediated differentiation of 32D cells into granulocytes and caused malignant transformation (Valentinis et al., 1999). Therefore these developmentally regulated patterns of PHIP expression suggest that it may regulate unique signaling pathways involved in L6 cell proliferation, survival and differentiation. Given that PHIP contains two bromodomains commonly known to facilitate

transcription, it is tempting to speculate that PHIP might be involved in differentiation of L6 myoblasts by facilitating specific gene transcription in response to insulin in these cells. It would be interesting to see whether PHIP can activate genes required for L6 differentiation and find out whether PHIP has the ability to bind to their promoter independently or in conjunction with other coactivators such as CBPs.

In conclusion, given the physiological significance of PHIP function in mediating both mitogenic and metabolic responses of insulin, suggests that interruption of PHIP function might lead to insulin resistance and diabetes. Future *in vivo* studies in which PHIP gene has been disrupted would elucidate on the role of PHIP in these diseases and its potential therapeutic value in their treatment.

REFERENCES

Abe, H., Yamada, N., Kamata, K., Kuwaki, T., Shimada, M., Osuga, J., Shionoiri, F., Yahagi, N., Kadowaki, T., Tamemoto, H., Ishibashi, S., Yazaki, Y., and Makuuchi, M. (1998). Hypertension, hypertriglyceridemia, and impaired endothelium-dependent vascular relaxation in mice lacking insulin receptor substrate-1. *J.Clin.Invest.* ***101***, 1784-1788.

Alessi, D.R., Cuenda, A., Cohen, P., Dudley, D.T., and Saltiel, A.R. (1995). PD 098059 is a specific inhibitor of the activation of mitogen- activated protein kinase kinase in vitro and in vivo. *J Biol.Chem* ***270***, 27489-27494.

Anai, M., Ono, H., Funaki, M., Fukushima, Y., Inukai, K., Ogihara, T., Sakoda, H., Onishi, Y., Yazaki, Y., Kikuchi, M., Oka, Y., and Asano, T. (1998). Different subcellular distribution and regulation of expression of insulin receptor substrate (IRS)-3 from those of IRS-1 and IRS-2. *J Biol Chem* ***273***, 29686-29692.

Araki, E., Lipes, M.A., Patti, M.E., Bruning, J.C., Haag, B., Johnson, R.S., and Kahn, C.R. (1994). Alternative pathway of insulin signaling in mice with targeted disruption of the IRS-1 gene. *Nature* ***372***, 186-190.

Backer, J.M., Kahn, C.R., Cahill, D.A., Ullrich, A., and White, M.F. (1990). Receptor-mediated internalization of insulin requires a 12-amino acid sequence in the juxtamembrane region of the insulin receptor beta-subunit. *J. Biol. Chem.* ***265***, 16450-16454.

Backer, J.M., Kahn, C.R., and White, M.F. (1989). Tyrosine phosphorylation of the insulin receptor during insulin-stimulated internalization in rat hepatoma cells. *J. Biol. Chem.* ***264***, 1694-1701.

Backer, J.M., Myers, M.G.J., Sun, X.J., Chin, D.J., Shoelson, S.E., Miralpeix, M., and White, M.F. (1993). Association of IRS-1 with the insulin receptor and the phosphatidylinositol 3'-kinase. Formation of binary and ternary signaling complexes in intact cells. *J. Biol. Chem.* ***268***, 8204-8212.

Backer, J.M., Shoelson, S.E., Weiss, M.A., Hua, Q.X., Cheatham, R.B., Haring, E., Cahill, D.C., and White, M.F. (1992). The insulin receptor juxtamembrane region contains two independent tyrosine/beta-turn internalization signals. *J. Cell Biol.* ***118***, 831-839.

Baumann, C.A., Ribon, V., Kanzaki, M., Thurmond, D.C., Mora, S., Shigematsu, S., Bickel, P.E., Pessin, J.E., and Saltiel, A.R. (2000). CAP defines a second signaling pathway required for insulin-stimulated glucose transport. *Nature* ***407***, 202-207.

Beaudoing, E., Freier, S., Wyatt, J.R., Claverie, J.M., and Gautheret, D. (2000). Patterns of variant polyadenylation signal usage in human genes. *Genome Res.* ***10***, 1001-1010.

Beitner-Johnson, D., Blakesley, V.A., Shen-Orr, Z., Jimenez, M., Stannard, B., Wang, L.M., Pierce, J., and LeRoith, D. (1996). The proto-oncogene product c-Crk associates with insulin receptor substrate-1 and 4PS. Modulation by insulin growth factor-I (IGF) and enhanced IGF-I signaling. *J. Biol. Chem.* ***271***, 9287-9290.

Bickel, P.E. (2002). Lipid rafts and insulin signaling. *Am.J.Physiol.Endocrinol.Metab.* ***282***, E1-E10

Blomberg, N., Baraldi, E., Nilges, M., and Saraste, M. (1999). The PH superfold: a structural scaffold for multiple functions. *Trends.Biochem.Sci.* ***24***, 441-445.

Bohni, R., Riesgo-Escovar, J., Oldham, S., Brogiolo, W., Stocker, H., Andruss, B.F., Beckingham, K., and Hafen, E. (1999). Autonomous control of cell and organ size by CHICO, a Drosophila homolog of vertebrate IRS1-4. *Cell **97***, 865-875.

Bottomley, M.J., Salim, K., and Panayotou, G. (1998). Phospholipid-binding protein domains. *Biochim.Biophys.Acta **1436***, 165-183.

Bowtell, D., Fu, P., Simon, M., and Senior, P. (1992). Identification of murine homologues of the Drosophila son of sevenless gene: potential activators of ras. *Proc.Natl.Acad.Sci.U.S A. **89***, 6511-6515.

Brown, D.A. and London, E. (1998). Functions of lipid rafts in biological membranes. *Annu.Rev.Cell Dev.Biol. **14***, 111-136.

Bruning, J.C., Gautam, D., Burks, D.J., Gillette, J., Schubert, M., Orban, P.C., Klein, R., Krone, W., Muller-Wieland, D., and Kahn, C.R. (2000). Role of brain insulin receptor in control of body weight and reproduction. *Science **289***, 2122-2125.

Bruning, J.C., Michael, M.D., Winnay, J.N., Hayashi, T., Horsch, D., Accili, D., Goodyear, L.J., and Kahn, C.R. (1998). A muscle-specific insulin receptor knockout exhibits features of the metabolic syndrome of NIDDM without altering glucose tolerance. *Mol.Cell 2*, 559-569.

Bruning, J.C., Winnay, J., Cheatham, B., and Kahn, C.R. (1997). Differential signaling by insulin receptor substrate 1 (IRS-1) and IRS- 2 in IRS-1-deficient cells. *Mol Cell Biol **17***, 1513-1521.

Burgering, B.M., Medema, R.H., Maassen, J.A., van de Wetering ML, van der Eb AJ, McCormick, F., and Bos, J.L. (1991). Insulin stimulation of gene expression mediated by p21ras activation. *EMBO J 10*, 1103-1109.

Burkhard, P., Stetefeld, J., and Strelkov, S.V. (2001). Coiled coils: a highly versatile protein folding motif. *Trends.Cell Biol 11*, 82-88.

Burks, D.J., Pons, S., Towery, H., Smith-Hall, J., Myers, M.G.J., Yenush, L., and White, M.F. (1997). Heterologous pleckstrin homology domains Do not couple IRS-1 to the insulin receptor [In Process Citation]. *J. Biol. Chem. 272*, 27716-27721.

Burks, D.J., Wang, J., Towery, H., Ishibashi, O., Lowe, D., Riedel, H., and White, M.F. (1998). IRS pleckstrin homology domains bind to acidic motifs in proteins. *J. Biol.Chem. 273*, 31061-31067.

Carpentier, J.L. (1994). Insulin receptor internalization: molecular mechanisms and physiopathological implications. *Diabetologia 37 Suppl 2*, S117-S124

Carpentier, J.L., Hamer, I., Gilbert, A., and Paccaud, J.P. (1996). Molecular and cellular mechanisms governing the ligand-specific and non-specific steps of insulin receptor internalization. *Z.Gastroenterol. 34 Suppl 3*, 73-75.

Carpentier, J.L., Paccaud, J.P., Backer, J., Gilbert, A., Orci, L., Kahn, C.R., and Baecker, J. (1993). Two steps of insulin receptor internalization depend on different domains of the beta-subunit. *J.Cell Biol. 122*, 1243-1252.

Carvalho, E., Jansson, P.A., Nagaev, I., Wenthzel, A.M., and Smith, U. (2001). Insulin resistance with low cellular IRS-1 expression is also associated with low

GLUT4 expression and impaired insulin-stimulated glucose transport. *FASEB J.* ***15***, 1101-1103.

Ceresa, B.P., Kao, A.W., Santeler, S.R., and Pessin, J.E. (1998). Inhibition of clathrin-mediated endocytosis selectively attenuates specific insulin receptor signal transduction pathways. *Mol.Cell Biol* ***18***, 3862-3870.

Chen, D., Van, H.D., White, M.F., and Backer, J.M. (1995). Insulin receptor substrate 1 rescues insulin action in CHO cells expressing mutant insulin receptors that lack a juxtamembrane NPXY motif. *Mol Cell Biol* ***15***, 4711-4717.

Chiang, S.H., Baumann, C.A., Kanzaki, M., Thurmond, D.C., Watson, R.T., Neudauer, C.L., Macara, I.G., Pessin, J.E., and Saltiel, A.R. (2001). Insulin-stimulated GLUT4 translocation requires the CAP-dependent activation of TC10. *Nature* ***410***, 944-948.

Chou, M.M., Fajardo, J.E., and Hanafusa, H. (1992). The SH2- and SH3-containing Nck protein transforms mammalian fibroblasts in the absence of elevated phosphotyrosine levels. *Mol.Cell Biol.* ***12***, 5834-5842.

Chrivia, J.C., Kwok, R.P., Lamb, N., Hagiwara, M., Montminy, M.R., and Goodman, R.H. (1993). Phosphorylated CREB binds specifically to the nuclear protein CBP. *Nature* ***365***, 855-859.

Clark, S.F., Martin, S., Carozzi, A.J., Hill, M.M., and James, D.E. (1998). Intracellular localization of phosphatidylinositide 3-kinase and insulin receptor substrate-1 in adipocytes: potential involvement of a membrane skeleton. *J Cell Biol* ***140***, 1211-1225.

Clark, S.F., Molero, J.C., and James, D.E. (2000). Release of insulin receptor substrate proteins from an intracellular complex coincides with the development of insulin resistance. *J. Biol. Chem. 275*, 3819-3826.

Conejo, R. and Lorenzo, M. (2001). Insulin signaling leading to proliferation, survival, and membrane ruffling in C2C12 myoblasts. *J.Cell Physiol. 187*, 96-108.

Couet, J., Li, S., Okamoto, T., Ikezu, T., and Lisanti, M.P. (1997). Identification of peptide and protein ligands for the caveolin-scaffolding domain. Implications for the interaction of caveolin with caveolae-associated proteins. *J.Biol.Chem. 272*, 6525-6533.

Czech, M.P. and Corvera, S. (1999). Signaling mechanisms that regulate glucose transport. *J. Biol.Chem. 274*, 1865-1868.

Das, B., Shu, X., Day, G.J., Han, J., Krishna, U.M., Falck, J.R., and Broek, D. (2000). Control of intramolecular interactions between the pleckstrin homology and dbl homology domains of vav and sos1 regulates rac binding. *J. Biol.Chem. 275*, 15074-15081.

De Fea, K. and Roth, R.A. (1997). Modulation of insulin receptor substrate-1 tyrosine phosphorylation and function by mitogen-activated protein kinase. *J. Biol.Chem. 272*, 31400-31406.

del Peso, L., Gonzalez-Garcia, M., Page, C., Herrera, R., and Nunez, G. (1997). Interleukin-3-induced phosphorylation of BAD through the protein kinase Akt. *Science 278*, 687-689.

Di Guglielmo, G.M., Drake, P.G., Baass, P.C., Authier, F., Posner, B.I., and Bergeron, J.J. (1998). Insulin receptor internalization and signaling. *Mol.Cell Biochem. 182*, 59-63.

Downward, J. (1998). Lipid-regulated kinases: some common themes at last. *Science 279*, 673-674.

Eck, M.J., Dhe-Paganon, S., Trub, T., Nolte, R.T., and Shoelson, S.E. (1996). Structure of the IRS-1 PTB domain bound to the juxtamembrane region of the insulin receptor. *Cell 85*, 695-705.

Egawa, K., Maegawa, H., Shimizu, S., Morino, K., Nishio, Y., Bryer-Ash, M., Cheung, A.T., Kolls, J.K., Kikkawa, R., and Kashiwagi, A. (2001). Protein-tyrosine phosphatase-1B negatively regulates insulin signaling in l6 myocytes and Fao hepatoma cells. *J.Biol.Chem. 276*, 10207-10211.

Elbashir, S.M., Harborth, J., Lendeckel, W., Yalcin, A., Weber, K., and Tuschl, T. (2001). Duplexes of 21-nucleotide RNAs mediate RNA interference in cultured mammalian cells. *Nature 411*, 494-498.

Fantin, V.R., Wang, Q., Lienhard, G.E., and Keller, S.R. (2000). Mice lacking insulin receptor substrate 4 exhibit mild defects in growth, reproduction, and glucose homeostasis. *Am.J.Physiol.Endocrinol.Metab. 278*, E127-E133

Farhang-Fallah, J., Yin, X., Trentin, G., Cheng, A.M., and Rozakis-Adcock, M. (2000). Cloning and characterization of PHIP, a novel insulin receptor substrate-1 pleckstrin homology domain interacting protein. *J. Biol. Chem. 275*, 40492-40497.

Farhang-Fallah, J., Randhawa, V.K., Nimnual, A., Klip, A., Bar-Sagi, D., and Rozakis-Adcock, M. (2002) PHIP couples the IRS-1 PH domain to insulin signaling pathways leading to mitogenesis and GLUT4 translocation. *Mol. Cell. Biol.* **in press**.

Franke, T.F., Kaplan, D.R., Cantley, L.C., and Toker, A. (1997). Direct regulation of the Akt proto-oncogene product by phosphatidylinositol-3,4-bisphosphate. *Science 275*, 665-668.

Frech, M., Andjelkovic, M., Ingley, E., Reddy, K.K., Falck, J.R., and Hemmings, B.A. (1997). High affinity binding of inositol phosphates and phosphoinositides to the pleckstrin homology domain of RAC/protein kinase B and their influence on kinase activity. *J. Biol. Chem. 272*, 8474-8481.

Galbiati, F., Razani, B., and Lisanti, M.P. (2001). Caveolae and caveolin-3 in muscular dystrophy. *Trends.Mol.Med. 7*, 435-441.

Giovannone, B., Scaldaferri, M.L., Federici, M., Porzio, O., Lauro, D., Fusco, A., Sbraccia, P., Borboni, P., Lauro, R., and Sesti, G. (2000). Insulin receptor substrate (IRS) transduction system: distinct and overlapping signaling potential. *Diabetes Metab.Res.Rev. 16*, 434-441.

Goalstone, M.L., Leitner, J.W., Berhanu, P., Sharma, P.M., Olefsky, J.M., and Draznin, B. (2001). Insulin signals to prenyltransferases via the Shc branch of intracellular signaling. *J. Biol. Chem. 276*, 12805-12812.

Goldstein, B.J., Bittner-Kowalczyk, A., White, M.F., and Harbeck, M. (2000). Tyrosine dephosphorylation and deactivation of insulin receptor substrate-1 by protein-tyrosine phosphatase 1B. Possible facilitation by the formation of a ternary complex with the Grb2 adaptor protein. *J. Biol.Chem.75*, 4283-4289.

Graham, R. and Gilman, M. (1991). Distinct protein targets for signals acting at the c-fos serum response element. *Science **251***, 189-192.

Guilherme, A. and Czech, M.P. (1998). Stimulation of IRS-1-associated phosphatidylinositol 3-kinase and Akt/protein kinase B but not glucose transport by beta1-integrin signaling in rat adipocytes. *J.Biol.Chem. **273***, 33119-33122.

Gustafson, T.A., He, W., Craparo, A., Schaub, C.D., and O'Neill, T.J. (1995). Phosphotyrosine-dependent interaction of SHC and insulin receptor substrate 1 with the NPEY motif of the insulin receptor via a novel non-SH2 domain. *Mol.Cell Biol **15***, 2500-2508.

Gustavsson, J., Parpal, S., Karlsson, M., Ramsing, C., Thorn, H., Borg, M., Lindroth, M., Peterson, K.H., Magnusson, K.E., and Stralfors, P. (1999). Localization of the insulin receptor in caveolae of adipocyte plasma membrane. *FASEB J. **13***, 1961-1971.

Gustavsson, J., Parpal, S., and Stralfors, P. (1996). Insulin-stimulated glucose uptake involves the transition of glucose transporters to a caveolae-rich fraction within the plasma membrane: implications for type II diabetes. *Mol.Med. **2***, 367-372.

Han, J., Luby-Phelps, K., Das, B., Shu, X., Xia, Y., Mosteller, R.D., Krishna, U.M., Falck, J.R., White, M.A., and Broek, D. (1998). Role of substrates and products of PI 3-kinase in regulating activation of Rac-related guanosine triphosphatases by Vav. *Science **279***, 558-560.

Harlan, J.E., Hajduk, P.J., Yoon, H.S., and Fesik, S.W. (1994). Pleckstrin homology domains bind to phosphatidylinositol-4,5- bisphosphate. *Nature **371***, 168-170.

Harlan, J.E., Yoon, H.S., Hajduk, P.J., and Fesik, S.W. (1995). Structural characterization of the interaction between a pleckstrin homology domain and phosphatidylinositol 4,5-bisphosphate. *Biochemistry **34***, 9859-9864.

Haruta, T., Uno, T., Kawahara, J., Takano, A., Egawa, K., Sharma, P.M., Olefsky, J.M., and Kobayashi, M. (2000). A rapamycin-sensitive pathway down-regulates insulin signaling via phosphorylation and proteasomal degradation of insulin receptor substrate-1. *Mol.Endocrinol. **14***, 783-794.

Haslam, R.J., Koide, H.B., and Hemmings, B.A. (1993). Pleckstrin domain homology. *Nature **363***, 309-310.

He, W., Craparo, A., Zhu, Y., O'Neill, T.J., Wang, L.M., Pierce, J.H., and Gustafson, T.A. (1996). Interaction of insulin receptor substrate-2 (IRS-2) with the insulin and insulin-like growth factor I receptors. Evidence for two distinct phosphotyrosine-dependent interaction domains within IRS-2. *J. Biol. Chem. **271***, 11641-11645.

Heller-Harrison, R.A., Morin, M., and Czech, M.P. (1995). Insulin regulation of membrane-associated insulin receptor substrate 1. *J. Biol. Chem. **270***, 24442-24450.

Heller-Harrison, R.A., Morin, M., Guilherme, A., and Czech, M.P. (1996). Insulin-mediated targeting of phosphatidylinositol 3-kinase to GLUT4-containing vesicles. *J. Biol. Chem. **271***, 10200-10204.

Hotamisligil, G.S., Peraldi, P., Budavari, A., Ellis, R., White, M.F., and Spiegelman, B.M. (1996). IRS-1-mediated inhibition of insulin receptor tyrosine kinase activity in TNF-alpha- and obesity-induced insulin resistance. *Science **271***, 665-668.

Hribal, M.L., Federici, M., Porzio, O., Lauro, D., Borboni, P., Accili, D., Lauro, R., and Sesti, G. (2000). The Gly-->Arg972 amino acid polymorphism in insulin receptor substrate-1 affects glucose metabolism in skeletal muscle cells. *J.Clin.Endocrinol.Metab.* ***85***, 2004-2013.

Hunter, S.J. and Garvey, W.T. (1998). Insulin action and insulin resistance: diseases involving defects in insulin receptors, signal transduction, and the glucose transport effector system. *Am.J Med.* ***105*** , 331-345.

Inoue, G., Cheatham, B., Emkey, R., and Kahn, C.R. (1998). Dynamics of insulin signaling in 3T3-L1 adipocytes. Differential compartmentalization and trafficking of insulin receptor substrate (IRS)-1 and IRS-2. *J. Biol. Chem.* ***273***, 11548-11555.

Isakoff, S.J., Cardozo, T., Andreev, J., Li, Z., Ferguson, K.M., Abagyan, R., Lemmon, M.A., Aronheim, A., and Skolnik, E.Y. (1998). Identification and analysis of PH domain-containing targets of phosphatidylinositol 3-kinase using a novel in vivo assay in yeast. *EMBO J* ***17***, 5374-5387.

Isakoff, S.J., Taha, C., Rose, E., Marcusohn, J., Klip, A., and Skolnik, E.Y. (1995). The inability of phosphatidylinositol 3-kinase activation to stimulate GLUT4 translocation indicates additional signaling pathways are required for insulin-stimulated glucose uptake. *Proc.Natl.Acad.Sci.U.S A* ***92***, 10247-10251.

Ito, T., Sasaki, Y., and Wands, J.R. (1996). Overexpression of human insulin receptor substrate 1 induces cellular transformation with activation of mitogen-activated protein kinases. *Mol Cell Biol* ***16***, 943-951.

Jacobs, A.R., LeRoith, D., and Taylor, S.I. (2001). Insulin receptor substrate-1 pleckstrin homology and phosphotyrosine-binding domains are both involved in plasma membrane targeting. *J.Biol.Chem. 276*, 40795-40802.

Jeanmougin, F., Wurtz, J.M., Le Douarin, B., Chambon, P., and Losson, R. (1997). The bromodomain revisited. *Trends Biochem.Sci. 22*, 151-153.

Kaburagi, Y., Satoh, S., Tamemoto, H., Yamamoto-Honda, R., Tobe, K., Veki, K., Yamauchi, T., Kono-Sugita, E., Sekihara, H., Aizawa, S., Cushman, S.W., Akanuma, Y., Yazaki, Y., and Kadowaki, T. (1997). Role of insulin receptor substrate-1 and pp60 in the regulation of insulin-induced glucose transport and GLUT4 translocation in primary adipocytes. *J. Biol. Chem. 272*, 25839-25844.

Kabuta, T., Hakuno, F., Asano, T., and Takahashi, S. (2002). Insulin receptor substrate-3 functions as transcriptional activator in the nucleus. *J.Biol.Chem. 277*, 6846-6851.

Kanai, F., Ito, K., Todaka, M., Hayashi, H., Kamohara, S., Ishii, K., Okada, T., Hazeki, O., Ui, M., and Ebina, Y. (1993a). Insulin-stimulated GLUT4 translocation is relevant to the phosphorylation of IRS-1 and the activity of PI3-kinase. *Biochem.Biophys.Res.Commun. 195*, 762-768.

Kanai, F., Nishioka, Y., Hayashi, H., Kamohara, S., Todaka, M., and Ebina, Y. (1993b). Direct demonstration of insulin-induced GLUT4 translocation to the surface of intact cells by insertion of a c-myc epitope into an exofacial GLUT4 domain. *J. Biol. Chem. 268*, 14523-14526.

Kanety, H., Feinstein, R., Papa, M.Z., Hemi, R., and Karasik, A. (1995). Tumor necrosis factor alpha-induced phosphorylation of insulin receptor substrate-1

(IRS-1). Possible mechanism for suppression of insulin- stimulated tyrosine phosphorylation of IRS-1. *J. Biol. Chem.* ***270***, 23780-23784.

Kato, H., Chen, S., Kiyama, H., Ikeda, K., Kimura, N., Nakashima, K., and Taga, T. (2000). Identification of a Novel WD Repeat-Containing Gene Predominantly Expressed in Developing and Regenerating Neurons. *J Biochem.(Tokyo.)* ***128***, 923-932.

Kelly, K.L. and Ruderman, N.B. (1993). Insulin-stimulated phosphatidylinositol 3-kinase. Association with a 185-kDa tyrosine-phosphorylated protein (IRS-1) and localization in a low density membrane vesicle. *J. Biol. Chem.* ***268***, 4391-4398.

Kelly, K.L., Ruderman, N.B., and Chen, K.S. (1992). Phosphatidylinositol-3-kinase in isolated rat adipocytes. Activation by insulin and subcellular distribution. *J. Biol. Chem.* ***267***, 3423-3428.

Khan, M.N., Baquiran, G., Brule, C., Burgess, J., Foster, B., Bergeron, J.J., and Posner, B.I. (1989). Internalization and activation of the rat liver insulin receptor kinase in vivo. *J.Biol.Chem.* ***264***, 12931-12940.

Kharitonenkov, A., Schnekenburger, J., Chen, Z., Knyazev, P., Ali, S., Zwick, E., White, M., and Ullrich, A. (1995). Adapter function of protein-tyrosine phosphatase 1D in insulin receptor/insulin receptor substrate-1 interaction. *J. Biol. Chem.* ***270***, 29189-29193.

Khayat, Z.A., Tong, P., Yaworsky, K., Bloch, R.J., and Klip, A. (2000). Insulin-induced actin filament remodeling colocalizes actin with phosphatidylinositol 3-kinase and GLUT4 in L6 myotubes. *J Cell Sci.* ***113 Pt 2***, 279-290.

Kishi, K., Muromoto, N., Nakaya, Y., Miyata, I., Hagi, A., Hayashi, H., and Ebina, Y. (1998). Bradykinin directly triggers GLUT4 translocation via an insulin-independent pathway. *Diabetes* ***47***, 550-558.

Klippel, A., Kavanaugh, W.M., Pot, D., and Williams, L.T. (1997). A specific product of phosphatidylinositol 3-kinase directly activates the protein kinase Akt through its pleckstrin homology domain. *Mol.Cell Biol.* ***17***, 338-344.

Konishi, H., Kuroda, S., and Kikkawa, U. (1994). The pleckstrin homology domain of RAC protein kinase associates with the regulatory domain of protein kinase C zeta. *Biochem.Biophys.Res.Commun.* ***205***, 1770-1775.

Korzus, E., Torchia, J., Rose, D.W., Xu, L., Kurokawa, R., McInerney, E.M., Mullen, T.M., Glass, C.K., and Rosenfeld, M.G. (1998). Transcription factor-specific requirements for coactivators and their acetyltransferase functions. *Science* ***279***, 703-707.

Kotani, K., Hara, K., Yonezawa, K., and Kasuga, M. (1995). Phosphoinositide 3-kinase as an upstream regulator of the small GTP-binding protein Rac in the insulin signaling of membrane ruffling. *Biochem.Biophys.Res.Commun.* ***208***, 985-990.

Kozak, M. (1986). Point mutations define a sequence flanking the AUG initiator codon that modulates translation by eukaryotic ribosomes. *Cell* ***44***, 283-292.

Kriauciunas, K.M., Myers, M.G.J., and Kahn, C.R. (2000). Cellular compartmentalization in insulin action: altered signaling by a lipid-modified IRS-1. *Mol.Cell Biol* ***20***, 6849-6859.

Kublaoui, B., Lee, J., and Pilch, P.F. (1995). Dynamics of signaling during insulin-stimulated endocytosis of its receptor in adipocytes. *J. Biol. Chem. 270*, 59-65.

Kulkarni, R.N., Bruning, J.C., Winnay, J.N., Postic, C., Magnuson, M.A., and Kahn, C.R. (1999). Tissue-specific knockout of the insulin receptor in pancreatic beta cells creates an insulin secretory defect similar to that in type 2 diabetes. *Cell 96*, 329-339.

Kurokawa, R., Kalafus, D., Ogliastro, M.H., Kioussi, C., Xu, L., Torchia, J., Rosenfeld, M.G., and Glass, C.K. (1998). Differential use of CREB binding protein-coactivator complexes. *Science 279*, 700-703.

Lavan, B.E., Fantin, V.R., Chang, E.T., Lane, W.S., Keller, S.R., and Lienhard, G.E. (1997a). A novel 160-kDa phosphotyrosine protein in insulin-treated embryonic kidney cells is a new member of the insulin receptor substrate family. *J. Biol. Chem. 272*, 21403-21407.

Lavan, B.E., Lane, W.S., and Lienhard, G.E. (1997b). The 60-kDa phosphotyrosine protein in insulin-treated adipocytes is a new member of the insulin receptor substrate family. *J. Biol. Chem. 272*, 11439-11443.

Lemmon, M.A., Falasca, M., Ferguson, K.M., and Schlessinger, J. (1997). Regulatory recruitment of signaling molecules to the cell membrane by plekstrin homology domains. *Trends Cell Biol. 7*, 237-242.

Lemmon, M.A. and Ferguson, K.M. (1998). Pleckstrin homology domains. *Curr.Top.Microbiol.Immunol. 228*, 39-74.

Lemmon, M.A. and Ferguson, K.M. (2000). Signal-dependent membrane targeting by pleckstrin homology (PH) domains. *Biochem.J 350 Pt 1*, 1-18.

Lemmon, M.A., Ferguson, K.M., and Abrams, C.S. (2002). Pleckstrin homology domains and the cytoskeleton. *FEBS Lett. 513*, 71-76.

Li, S.C., Zwahlen, C., Vincent, S.J., McGlade, C.J., Kay, L.E., Pawson, T., and Forman-Kay, J.D. (1998). Structure of a Numb PTB domain-peptide complex suggests a basis for diverse binding specificity. *Nat.Struct.Biol. 5*, 1075-1083.

Liu, S.C., Wang, Q., Lienhard, G.E., and Keller, S.R. (1999). Insulin receptor substrate 3 is not essential for growth or glucose homeostasis. *J.Biol.Chem. 274*, 18093-18099.

Liu, X., Wang, H., Eberstadt, M., Schnuchel, A., Olejniczak, E.T., Meadows, R.P., Schkeryantz, J.M., Janowick, D.A., Harlan, J.E., Harris, E.A., Staunton, D.E., and Fesik, S.W. (1998). NMR structure and mutagenesis of the N-terminal Dbl homology domain of the nucleotide exchange factor Trio. *Cell 95*, 269-277.

Ma, A.D. and Abrams, C.S. (1999). Pleckstrin homology domains and phospholipid-induced cytoskeletal reorganization. *Thromb.Haemost. 82*, 399-406.

Mahadevan, D., Thanki, N., Singh, J., McPhie, P., Zangrilli, D., Wang, L.M., Guerrero, C., LeVine, H., Humblet, C., and Saldanha, J. (1995). Structural studies on the PH domains of Dbl, Sos1, IRS-1, and beta ARK1 and their differential binding to G beta gamma subunits. *Biochemistry 34*, 9111-9117.

Mauvais-Jarvis, F. and Kahn, C.R. (2000). Understanding the pathogenesis and treatment of insulin resistance and type 2 diabetes mellitus: what can we learn from transgenic and knockout mice? *Diabetes Metab. 26*, 433-448.

Miki, H., Miura, K., and Takenawa, T. (1996). N-WASP, a novel actin-depolymerizing protein, regulates the cortical cytoskeletal rearrangement in a

PIP2-dependent manner downstream of tyrosine kinases. *EMBO J 15*, 5326-5335.

Miki, H., Yamaguchi, H., Suetsugu, S., and Takenawa, T. (2000). IRSp53 is an essential intermediate between Rac and WAVE in the regulation of membrane ruffling. *Nature 408*, 732-735.

Miki, T., Smith, C.L., Long, J.E., Eva, A., and Fleming, T.P. (1993). Oncogene ect2 is related to regulators of small GTP-binding proteins. *Nature 362*, 462-465.

Mitsumoto, Y., Burdett, E., Grant, A., and Klip, A. (1991). Differential expression of the GLUT1 and GLUT4 glucose transporters during differentiation of L6 muscle cells. *Biochem.Biophys.Res.Commun. 175*, 652-659.

Moreau, V., Frischknecht, F., Reckmann, I., Vincentelli, R., Rabut, G., Stewart, D., and Way, M. (2001). A complex of N-WASP and WIP integrates signaling cascades that lead to actin polymerization. *Nat.Cell Biol . 2*, 441-448.

Morris, A.J., Martin, S.S., Haruta, T., Nelson, J.G., Vollenweider, P., Gustafson, T.A., Mueckler, M., Rose, D.W., and Olefsky, J.M. (1996). Evidence for an insulin receptor substrate 1 independent insulin signaling pathway that mediates insulin-responsive glucose transporter (GLUT4) translocation. *Proc.Natl.Acad.Sci.U.S A 93*, 8401-8406.

Mur, C., Valverde, A.M., Kahn, C.R., and Benito, M. (2002). Increased insulin sensitivity in IGF-I receptor--deficient brown adipocytes. *Diabetes 51*, 743-754.

Musacchio, A., Gibson, T., Rice, P., Thompson, J., and Saraste, M. (1993). The PH domain: a common piece in the structural patchwork of signaling proteins. *Trends.Biochem.Sci 18*, 343-348.

Myers, M.G.J., Grammer, T.C., Brooks, J., Glasheen, E.M., Wang, L.M., Sun, X.J., Blenis, J., Pierce, J.H., and White, M.F. (1995). The pleckstrin homology domain in insulin receptor substrate-1 sensitizes insulin signaling. *J. Biol. Chem.* ***270***, 11715-11718.

Myers, M.G.J., Grammer, T.C., Wang, L.M., Sun, X.J., Pierce, J.H., Blenis, J., and White, M.F. (1994a). Insulin receptor substrate-1 mediates phosphatidylinositol 3'-kinase and p70S6k signaling during insulin, insulin-like growth factor-1, and interleukin-4 stimulation. *J. Biol. Chem.* ***269***, 28783-28789.

Myers, M.G.J., Wang, L.M., Sun, X.J., Zhang, Y., Yenush, L., Schlessinger, J., Pierce, J.H., and White, M.F. (1994b). Role of IRS-1-GRB-2 complexes in insulin signaling. *Mol Cell Biol* ***14***, 3577-3587.

Myers, M.G.J. and White, M.F. (1996). Insulin signal transduction and the IRS proteins. *Annu.Rev.Pharmacol.Toxicol.* ***36***, 615-658.

Nakashima, N., Rose, D.W., Xiao, S., Egawa, K., Martin, S.S., Haruta, T., Saltiel, A.R., and Olefsky, J.M. (1999). The functional role of CrkII in actin cytoskeleton organization and mitogenesis. *J. Biol. Chem.* ***274***, 3001-3008.

Nave, B.T., Haigh, R.J., Hayward, A.C., Siddle, K., and Shepherd, P.R. (1996). Compartment-specific regulation of phosphoinositide 3-kinase by platelet-derived growth factor and insulin in 3T3-L1 adipocytes. *Biochem.J* ***318***, 55-60.

Nimnual, A.S., Yatsula, B.A., and Bar-Sagi, D. (1998). Coupling of Ras and Rac guanosine triphosphatases through the Ras exchanger Sos. *Science* ***279***, 560-563.

O'Neill, T.J., Craparo, A., and Gustafson, T.A. (1994). Characterization of an interaction between insulin receptor substrate 1 and the insulin receptor by using the two-hybrid system. *Mol.Cell Biol* ***14***, 6433-6442.

Ogawa, W., Matozaki, T., and Kasuga, M. (1998). Role of binding proteins to IRS-1 in insulin signaling. *Mol.Cell Biochem.* ***182***, 13-22.

Ohan, N., Bayaa, M., Kumar, P., Zhu, L., and Liu, X.J. (1998). A novel insulin receptor substrate protein, xIRS-u, potentiates insulin signaling: functional importance of its pleckstrin homology domain. *Mol.Endocrinol.* ***12***, 1086-1098.

Okada, T., Kawano, Y., Sakakibara, T., Hazeki, O., and Ui, M. (1994). Essential role of phosphatidylinositol 3-kinase in insulin-induced glucose transport and antilipolysis in rat adipocytes. Studies with a selective inhibitor wortmannin. *J. Biol. Chem.* ***269***, 3568-3573.

Ouwens, D.M., van der Zon, G.C., and Maassen, J.A. (2001). Modulation of insulin-stimulated glycogen synthesis by Src Homology Phosphatase 2. *Mol.Cell Endocrinol.* ***175***, 131-140.

Parpal, S., Karlsson, M., Thorn, H., and Stralfors, P. (2001). Cholesterol depletion disrupts caveolae and insulin receptor signaling for metabolic control via insulin receptor substrate-1, but not for mitogen-activated protein kinase control. *J. Biol. Chem.* ***276***, 9670-9678.

Paz, K., Hemi, R., LeRoith, D., Karasik, A., Elhanany, E., Kanety, H., and Zick, Y. (1997). A molecular basis for insulin resistance. Elevated serine/threonine phosphorylation of IRS-1 and IRS-2 inhibits their binding to the juxtamembrane region of the insulin receptor and impairs their ability to undergo insulin-induced tyrosine phosphorylation. *J. Biol. Chem.* ***272***, 29911-29918.

Paz, K., Liu, Y.F., Shorer, H., Hemi, R., LeRoith, D., Quan, M., Kanety, H., Seger, R., and Zick, Y. (1999). Phosphorylation of insulin receptor substrate-1 (IRS-1) by protein kinase B positively regulates IRS-1 function. *J. Biol. Chem.* ***274***, 28816-28822.

Perz, M. and Torlinska, T. (2001). Insulin receptor--structural and functional characteristics. *Med.Sci.Monit. 7*, 169-177.

Pessin, J.E., Thurmond, D.C., Elmendorf, J.S., Coker, K.J., and Okada, S. (1999). Molecular basis of insulin-stimulated GLUT4 vesicle trafficking. Location! Location! Location! *J. Biol. Chem.* ***274***, 2593-2596.

Pitcher, J.A., Touhara, K., Payne, E.S., and Lefkowitz, R.J. (1995). Pleckstrin homology domain-mediated membrane association and activation of the beta-adrenergic receptor kinase requires coordinate interaction with G beta gamma subunits and lipid. *J. Biol.Chem.* ***270***, 11707-11710.

Prehoda, K.E., Lee, D.J., and Lim, W.A. (1999). Structure of the enabled/VASP homology 1 domain-peptide complex: a key component in the spatial control of actin assembly. *Cell* ***97***, 471-480.

Pronk, G.J., McGlade, J., Pelicci, G., Pawson, T., and Bos, J.L. (1993). Insulin-induced phosphorylation of the 46- and 52-kDa Shc proteins. *J. Biol.Chem.* ***268***, 5748-5753.

Qian, X., Vass, W.C., Papageorge, A.G., Anborgh, P.H., and Lowy, D.R. (1998). N terminus of Sos1 Ras exchange factor: critical roles for the Dbl and pleckstrin homology domains. *Mol.Cell Biol* ***18***, 771-778.

Quilliam, L.A., Huff, S.Y., Rabun, K.M., Wei, W., Park, W., Broek, D., and Der, C.J. (1994). Membrane-targeting potentiates guanine nucleotide exchange factor CDC25 and SOS1 activation of Ras transforming activity. *Proc.Natl.Acad.Sci.U.S.A.* ***91***, 8512-8516.

Quon, M.J., Butte, A.J., Zarnowski, M.J., Sesti, G., Cushman, S.W., and Taylor, S.I. (1994). Insulin receptor substrate 1 mediates the stimulatory effect of insulin on GLUT4 translocation in transfected rat adipose cells. *J. Biol. Chem.* ***269***, 27920-27924.

Quon, M.J., Chen, H., Ing, B.L., Liu, M.L., Zarnowski, M.J., Yonezawa, K., Kasuga, M., Cushman, S.W., and Taylor, S.I. (1995). Roles of 1-phosphatidylinositol 3-kinase and ras in regulating translocation of GLUT4 in transfected rat adipose cells. *Mol.Cell Biol* ***15***, 5403-5411.

Randhawa, V.K., Bilan, P.J., Khayat, Z.A., Daneman, N., Liu, Z., Ramlal, T., Volchuk, A., Peng, X.R., Coppola, T., Regazzi, R., Trimble, W.S., and Klip, A. (2000). VAMP2, but not VAMP3/cellubrevin, mediates insulin-dependent incorporation of GLUT4 into the plasma membrane of L6 myoblasts. Mol.Biol *Cell* ***11***, 2403-2417.

Razzini, G., Ingrosso, A., Brancaccio, A., Sciacchitano, S., Esposito, D.L., and Falasca, M. (2000). Different subcellular localization and phosphoinositides binding of insulin receptor substrate protein pleckstrin homology domains. *Mol.Endocrinol.* ***14***, 823-836.

Ricort, J.M., Tanti, J.F., Van Obberghen, E., and Le Marchand-Brustel, Y. (1996). Different effects of insulin and platelet-derived growth factor on phosphatidylinositol 3-kinase at the subcellular level in 3T3-L1 adipocytes. A

possible explanation for their specific effects on glucose transport. *Eur.J Biochem.* ***239***, 17-22.

Rose, D.W., Saltiel, A.R., Majumdar, M., Decker, S.J., and Olefsky, J.M. (1994) Insulin receptor substrate 1 is required for insulin-mediated mitogenic signal transduction. *Proc.Natl.Acad.Sci.U.S A.* ***91***, 797-801.

Rossman, K.L., Worthylake, D.K., Snyder, J.T., Siderovski, D.P., Campbell, S.L., and Sondek, J. (2002). A crystallographic view of interactions between Dbs and Cdc42: PH domain-assisted guanine nucleotide exchange. *EMBO J.* ***21***, 1315-1326.

Rozakis-Adcock, M., Fernley, R., Wade, J., Pawson, T., and Bowtell, D. (1993). The SH2 and SH3 domains of mammalian Grb2 couple the EGF receptor to the Ras activator mSos1. *Nature* ***363***, 83-85.

Saltiel, A.R. (2001). New perspectives into the molecular pathogenesis and treatment of type 2 diabetes. *Cell* ***104***, 517-529.

Saltiel, A.R. and Kahn, C.R. (2001). Insulin signaling and the regulation of glucose and lipid metabolism. *Nature* ***414***, 799-806.

Sawka-Verhelle, D., Tartare-Deckert, S., White, M.F., and Obberghen, E. (1996). Insulin receptor substrate-2 binds to the insulin receptor through phosphotyrosine-binding domain and through a newly identified domain comprising amino acids 591 - 786. *J. Biol. Chem.* ***271***, 5980-5983.

Sharma, P.M., Egawa, K., Gustafson, T.A., Martin, J.L., and Olefsky, J.M. (1997). Adenovirus-mediated overexpression of IRS-1 interacting domains abolishes

insulin-stimulated mitogenesis without affecting glucose transport in 3T3-L1 adipocytes. *Mol.Cell Biol. 17*, 7386-7397.

Sharma, P.M., Egawa, K., Huang, Y., Martin, J.L., Huvar, I., Boss, G.R., and Olefsky, J.M. (1998). Inhibition of phosphatidylinositol 3-kinase activity by adenovirus-mediated gene transfer and its effect on insulin action. *J. Biol. Chem. 273*, 18528-18537.

Shepherd, P.R., Withers, D.J., and Siddle, K. (1998). Phosphoinositide 3-kinase: the key switch mechanism in insulin signaling. *Biochem.J. 333*, 471-490.

Shpakov, A.O. and Pertseva, M.N. (2000). Structural and functional characterization of insulin receptor substrate proteins and the molecular mechanisms of their interaction with insulin superfamily tyrosine kinase receptors and effector proteins. *Membr.Cell Biol 13*, 455-484.

Simpson, F., Whitehead, J.P., and James, D.E. (2001). GLUT4--at the cross roads between membrane trafficking and signal transduction. *Traffic 2*, 2-11.

Smith, R.M., Harada, S., and Jarett, L. (1997). Insulin internalization and other signaling pathways in the pleiotropic effects of insulin. *Int.Rev.Cytol. 173*, 243-280.

Soisson, S.M., Nimnual, A.S., Uy, M., Bar-Sagi, D., and Kuriyan, J. (1998). Crystal structure of the Dbl and pleckstrin homology domains from the human Son of sevenless protein. *Cell 95*, 259-268.

Spiegelman, B.M. and Flier, J.S. (2001). Obesity and the regulation of energy balance. *Cell 104*, 531-543.

Stam, J.C., Sander, E.E., Michiels, F., van, L.F., Kain, H.T., van der Kammen RA, and Collard, J.G. (1997). Targeting of tiam1 to the plasma membrane requires the cooperative function of the N-terminal pleckstrin homology domain and an adjacent protein interaction domain. *J. Biol. Chem. 272*, 28447-28454.

Sun, X.J., Crimmins, D.L., Myers, M.G.J., Miralpeix, M., and White, M.F. (1993). Pleiotropic insulin signals are engaged by multisite phosphorylation of IRS-1. *Mol Cell Biol . 13*, 7418-7428.

Sun, X.J., Miralpeix, M., Myers, M.G.J., Glasheen, E.M., Backer, J.M., Kahn, C.R., and White, M.F. (1992). Expression and function of IRS-1 in insulin signal transmission. *J.Biol.Chem. 267*, 22662-22672.

Sun, X.J., Pons, S., Asano, T., Myers, M.G.J., Glasheen, E., and White, M.F. (1996). The Fyn tyrosine kinase binds Irs-1 and forms a distinct signaling complex during insulin stimulation. *J. Biol. Chem. 271* , 10583-10587.

Sun, X.J., Rothenberg, P., Kahn, C.R., Backer, J.M., Araki, E., Wilden, P.A., Cahill, D.A., Goldstein, B.J., and White, M.F. (1991). Structure of the insulin receptor substrate IRS-1 defines a unique signal transduction protein. *Nature 352*, 73-77.

Sun, X.J., Wang, L.M., Zhang, Y., Yenush, L., Myers, M.G.J., Glasheen, E., Lane, W.S., Pierce, J.H., and White, M.F. (1995). Role of IRS-2 in insulin and cytokine signaling. *Nature 377*, 173-177.

Takenawa, T. and Miki, H. (2001). WASP and WAVE family proteins: key molecules for rapid rearrangement of cortical actin filaments and cell movement. *J Cell Sci. 114*, 1801-1809.

Takeuchi, H., Matsuda, M., Yamamoto, T., Kanematsu, T., Kikkawa, U., Yagisawa, H., Watanabe, Y., and Hirata, M. (1998). PTB domain of insulin receptor substrate-1 binds inositol compounds. *Biochem.J 334*, 211-218.

Tamemoto, H., Kadowaki, T., Tobe, K., Yagi, T., Sakura, H., Hayakawa, T., Terauchi, Y., Ueki, K., Kaburagi, Y., and Satoh, S. (1994). Insulin resistance and growth retardation in mice lacking insulin receptor substrate-1. *Nature 372*, 182-186.

Tanaka, S., Ito, T., and Wands, J.R. (1996). Neoplastic transformation induced by insulin receptor substrate-1 overexpression requires an interaction with both Grb2 and Syp signaling molecules. *J. Biol. Chem. 271*, 14610-14616.

Tanti, J.F., Gremeaux, T., Van Obberghen, E., and Le Marchand-Brustel, Y. (1994). Serine/threonine phosphorylation of insulin receptor substrate 1 modulates insulin receptor signaling. *J. Biol. Chem. 269*, 6051-6057.

Touhara, K., Inglese, J., Pitcher, J.A., Shaw, G., and Lefkowitz, R.J. (1994). Binding of G protein beta gamma-subunits to pleckstrin homology domains. *J. Biol. Chem. 269*, 10217-10220.

Touhara, K., Koch, W.J., Hawes, B.E., and Lefkowitz, R.J. (1995). Mutational analysis of the pleckstrin homology domain of the beta- adrenergic receptor kinase. Differential effects on G beta gamma and phosphatidylinositol 4,5-bisphosphate binding. *J. Biol. Chem. 270*, 17000-17005.

Trahey, M. and McCormick, F. (1987). A cytoplasmic protein stimulates normal N-ras p21 GTPase, but does not affect oncogenic mutants. *Science 238*, 542-545.

Tsakiridis, T., Vranic, M., and Klip, A. (1994). Disassembly of the actin network inhibits insulin-dependent stimulation of glucose transport and prevents recruitment of glucose transporters to the plasma membrane. *J. Biol. Chem.* ***269***, 29934-29942.

Tsakiridis, T., Wang, Q., Taha, C., Grinstein, S., Downey, G., and Klip, A. (1997). Involvement of the actin network in insulin signaling. *Soc.Gen.Physiol.Ser.* ***52***, 257-271.

Tsukada, S., Simon, M.I., Witte, O.N., and Katz, A. (1994). Binding of beta gamma subunits of heterotrimeric G proteins to the PH domain of Bruton tyrosine kinase. *Proc.Natl.Acad.Sci.U.S A* ***91***, 11256-11260.

Ueyama, A., Yaworsky, K.L., Wang, Q., Ebina, Y., and Klip, A. (1999). GLUT-4myc ectopic expression in L6 myoblasts generates a GLUT-4-specific pool conferring insulin sensitivity. *Am.J Physiol.* ***277***, E572-E578

Vainshtein, I., Kovacina, K.S., and Roth, R.A. (2001). The Insulin Receptor Substrate (IRS)-1 Pleckstrin Homology Domain Functions in Downstream Signaling. *J. Biol. Chem.* ***276***, 8073-8078.

Valentinis, B., Romano, G., Peruzzi, F., Morrione, A., Prisco, M., Soddu, S., Cristofanelli, B., Sacchi, A., and Baserga, R. (1999) Growth and differentiation signals by the insulin-like growth factor 1 receptor in hemopoietic cells are mediated through different pathways. *J.Biol.Chem.* **274**, 12423-12430.

Valverde, A.M., Mur, C., Pons, S., Alvarez, A.M., White, M.F., Kahn, C.R., and Benito, M. (2001). Association of insulin receptor substrate 1 (IRS-1) y895 with Grb-2 mediates the insulin signaling involved in IRS-1-deficient brown adipocyte mitogenesis. *Mol.Cell Biol.* ***21***, 2269-2280.

Van der Geer, P. and Pawson, T. (1995). The PTB domain: a new protein module implicated in signal transduction. *Trends Biochem.Sci. 20*, 277-280.

Van Obberghen, E., Baron, V., Delahaye, L., Emanuelli, B., Filippa, N., Giorgetti-Peraldi, S., Lebrun, P., Mothe-Satney, I., Peraldi, P., Rocchi, S., Sawka-Verhelle, D., Tartare-Deckert, S., and Giudicelli, J. (2001). Surfing the insulin signaling web. *Eur.J.Clin.Invest. 31*, 966-977.

Vetter, I.R., Nowak, C., Nishimoto, T., Kuhlmann, J., and Wittinghofer, A. (1999). Structure of a Ran-binding domain complexed with Ran bound to a GTP analogue: implications for nuclear transport. *Nature 398*, 39-46.

Voliovitch, H., Schindler, D.G., Hadari, Y.R., Taylor, S.I., Accili, D., and Zick, Y. (1995). Tyrosine phosphorylation of insulin receptor substrate-1 in vivo depends upon the presence of its pleckstrin homology region. *J. Biol.Chem. 270*, 18083-18087.

Wang, D.S., Deng, T., and Shaw, G. (1997). Membrane binding and enzymatic activation of a Dbl homology domain require the neighboring pleckstrin homology domain. *Biochem Biophys Res Commun. 234*, 183-189.

Wang, D.S., Shaw, R., Winkelmann, J.C., and Shaw, G. (1994). Binding of PH domains of beta-adrenergic receptor kinase and beta-spectrin to WD40/beta-transducin repeat containing regions of the beta-subunit of trimeric G-proteins. *Biochem.Biophys.Res.Commun. 203*, 29-35.

Wang, L.M., Myers, M.G.J., Sun, X.J., Aaronson, S.A., White, M., and Pierce, J.H. (1993). IRS-1: essential for insulin- and IL-4-stimulated mitogenesis in hematopoietic cells. *Science 261*, 1591-1594.

Wang, Q., Bilan, P.J., Tsakiridis, T., Hinek, A., and Klip, A. (1998). Actin filaments participate in the relocalization of phosphatidylinositol3-kinase to glucose transporter-containing compartments and in the stimulation of glucose uptake in 3T3-L1 adipocytes. *Biochem.J **331***, 917-928.

Wang, Q., Somwar, R., Bilan, P.J., Liu, Z., Jin, J., Woodgett, J.R., and Klip, A. (1999). Protein kinase B/Akt participates in GLUT4 translocation by insulin in L6 myoblasts. *Mol.Cell Biol **19***, 4008-4018.

Watson, R.T., Shigematsu, S., Chiang, S.H., Mora, S., Kanzaki, M., Macara, I.G., Saltiel, A.R., and Pessin, J.E. (2001). Lipid raft microdomain compartmentalization of TC10 is required for insulin signaling and GLUT4 translocation. *J.Cell Biol **154***, 829-840.

White, M.F. (2002). IRS proteins and the common path to diabetes. *Am.J.Physiol.Endocrinol.Metab. **283***, E413-E422

White, M.F., Livingston, J.N., Backer, J.M., Lauris, V., Dull, T.J., Ullrich, A., and Kahn, C.R. (1988). Mutation of the insulin receptor at tyrosine 960 inhibits signal transmission but does not affect its tyrosine kinase activity. *Cell **54***, 641-649.

White, M.F. and Yenush, L. (1998). The IRS-signaling system: a network of docking proteins that mediate insulin and cytokine action. *Curr.Top.Microbiol.Immunol. **228***, 179-208.

Wiley, H.S. and Burke, P.M. (2001). Regulation of receptor tyrosine kinase signaling by endocytic trafficking. *Traffic. **2***, 12-18.

Withers, D.J., Gutierrez, J.S., Towery, H., Burks, D.J., Ren, J.M., Previs, S., Zhang, Y., Bernal, D., Pons, S., Shulman, G.I., Bonner-Weir, S., and White, M.F. (1998). Disruption of IRS-2 causes type 2 diabetes in mice. *Nature **391***, 900-904.

Wolf, G., Trub, T., Ottinger, E., Groninga, L., Lynch, A., White, M.F., Miyazaki, M., Lee, J., and Shoelson, S.E. (1995). PTB domains of IRS-1 and Shc have distinct but overlapping binding specificities. *J. Biol. Chem. **270***, 27407-27410.

Worthylake, D.K., Rossman, K.L., and Sondek, J. (2000). Crystal structure of Rac1 in complex with the guanine nucleotide exchange region of Tiam1. *Nature **408***, 682-688.

Wu, C., Butz, S., Ying, Y., and Anderson, R.G. (1997). Tyrosine kinase receptors concentrated in caveolae-like domains from neuronal plasma membrane. *J.Biol.Chem. **272***, 3554-3559.

Xiang, X., Yuan, M., Song, Y., Ruderman, N., Wen, R., and Luo, Z. (2002). 14-3-3 facilitates insulin-stimulated intracellular trafficking of insulin receptor substrate 1. *Mol.Endocrinol. **16***, 552-562.

Yamamoto, M., Toya, Y., Schwencke, C., Lisanti, M.P., Myers, M.G.J., and Ishikawa, Y. (1998). Caveolin is an activator of insulin receptor signaling. *J.Biol.Chem. **273***, 26962-26968.

Yamauchi, K. and Pessin, J.E. (1994a). Enhancement or inhibition of insulin signaling by insulin receptor substrate 1 is cell context dependent. *Mol.Cell Biol. **14***, 4427-4434.

Yamauchi, K. and Pessin, J.E. (1994b). Insulin receptor substrate-1 (IRS1) and Shc compete for a limited pool of Grb2 in mediating insulin downstream signaling. *J. Biol. Chem.* ***269***, 31107-31114.

Yamauchi, T., Tobe, K., Tamemoto, H., Ueki, K., Kaburagi, Y., Yamamoto-Honda, R., Takahashi, Y., Yoshizawa, F., Aizawa, S., Akanuma, Y., Sonenberg, N., Yazaki, Y., and Kadowaki, T. (1996). Insulin signaling and insulin actions in the muscles and livers of insulin-resistant, insulin receptor substrate 1-deficient mice. *Mol Cell Biol* ***16***, 3074-3084.

Yao, L., Janmey, P., Frigeri, L.G., Han, W., Fujita, J., Kawakami, Y., Apgar, J.R., and Kawakami, T. (1999). Pleckstrin homology domains interact with filamentous actin. *J. Biol. Chem.* ***274***, 19752-19761.

Yao, L., Kawakami, Y., and Kawakami, T. (1994). The pleckstrin homology domain of Bruton tyrosine kinase interacts with protein kinase C. *Proc.Natl.Acad.Sci.U.S A* ***91***, 9175-9179.

Yenush, L., Fernandez, R., Myers, M.G.J., Grammer, T.C., Sun, X.J., Blenis, J., Pierce, J.H., Schlessinger, J., and White, M.F. (1996a). The Drosophila insulin receptor activates multiple signaling pathways but requires insulin receptor substrate proteins for DNA synthesis. *Mol Cell Biol* ***16***, 2509-2517.

Yenush, L., Makati, K.J., Smith-Hall, J., Ishibashi, O., Myers, M.G.J., and White, M.F. (1996b). The pleckstrin homology domain is the principal link between the insulin receptor and IRS-1. *J. Biol.Chem.* ***271***, 24300-24306.

Yin, M.J., Yamamoto, Y., and Gaynor, R.B. (1998). The anti-inflammatory agents aspirin and salicylate inhibit the activity of I(kappa)B kinase-beta. *Nature* ***396***, 77-80.

Zacharias, D.A., Violin, J.D., Newton, A.C., and Tsien, R.Y. (2002). Partitioning of Lipid-Modified Monomeric GFPs into Membrane Microdomains of Live Cells. *Science* ***296***, 913-916.

Zhang, Z., Lee, C.H., Mandiyan, V., Borg, J.P., Margolis, B., Schlessinger, J., and Kuriyan, J. (1997). Sequence-specific recognition of the internalization motif of the Alzheimer's amyloid precursor protein by the X11 PTB domain. *EMBO J.* ***16***, 6141-6150.

Zhou, L., Chen, H., Xu, P., Cong, L.N., Sciacchitano, S., Li, Y., Graham, D., Jacobs, A.R., Taylor, S.I., and Quon, M.J. (1999). Action of insulin receptor substrate-3 (IRS-3) and IRS-4 to stimulate translocation of GLUT4 in rat adipose cells. *Mol.Endocrinol.* ***13***, 505-514.

Zhou, M.M., Ravichandran, K.S., Olejniczak, E.F., Petros, A.M., Meadows, R.P., Sattler, M., Harlan, J.E., Wade, W.S., Burakoff, S.J., and Fesik, S.W. (1995). Structure and ligand recognition of the phosphotyrosine binding domain of Shc. *Nature 378*, 584-592.